NASA CONTRACTOR REPORT 178392

CONTROL DESIGN CHALLENGES OF LARGE SPACE SYSTEMS AND SPACECRAFT CONTROL LABORATORY EXPERIMENT (SCOLE)

(NASA-CR-178392) CONTROL DESIGN CHALLENGES OF LARGE SPACE SYSTEMS AND SPACECRAFT CONTROL LABORATORY EXPERIMENT (SCOLE) Final Report (Control Research Corp.) 71 p
Avail: NTIS HC A04/MF A01 CSCL 22B G3/18

N88-11735
Unclas
0106532

JIGUAN GENE LIN

CONTROL RESEARCH CORPORATION
6 CHURCHILL LANE
LEXINGTON, MA 02173

CONTRACT NAS1-18185
OCTOBER 1987

National Aeronautics and
Space Administration

Langley Research Center
Hampton, Virginia 23665-5225

ACKNOWLEDGEMENT

This work was performed by the Control Research Corporation (CRC) under the contract NAS1-18185. The research was supported by NASA Langley Research Center (LaRC), Hampton, Virginia. The technical monitor was Dr. Suresh M. Joshi of LaRC.

The studies were conducted by the principal investigator, Dr. Jiguan Gene Lin (CRC). We wish to thank Dr. Joshi (LaRC) for his patience and assistance in the execution of this effort. We are also grateful to Mr. Larry Taylor of LaRC for his stimulating and penetrating technical discussions.

TABLE OF CONTENTS

1. INTRODUCTION

Supported by the Spacecraft Control Branch of NASA Langley Research Center under the Spacecraft Control Laboratory Experiment (SCOLE) program, the Control Research Corporation continued the investigation into the control design challenges of large space systems and Spacecraft Control Laboratory Experiment. This study concentrated on the second stage of a two-stage approach to active control of the flexible orbital configuration of SCOLE. The principal objective was to investigate if the structural vibrations excited by **time-optimal** line-of-sight pointing slew maneuvers of the **bang-bang type** could be quickly suppressed via **"modal-dashpot" design** of velocity output feedback control.

Structural vibrations in future large space systems such as space antennas, space platform, space station, or of deployed flexible payloads attached to the space Shuttle orbiter, and their interaction with on board controllers have become a major concern in the design and operation of such control systems as, say, for pointing and stabilization. The natural vibration frequencies of such systems are unconventionally low (tenths of 1 Hz in many cases) and closely spaced, many of which lie inside or nearby the bandwith of various traditional (rigid-body) control systems. In the past few years, many approaches were proposed for designing advanced control systems that would suppress vibrations in large flexible space structures, and various in-house laboratory experiments were also conducted, each being specifically set up for demonstrating some particular design techniques of interest. In 1983, the Spacecraft Control Branch at NASA Langley Research Center initiated the **Spacecraft Control Laboratory Experiment (SCOLE)** program and the **NASA/IEEE Design Challenge** [1] to promote direct comparison and realistic test of different approaches to control design against a common open-to-public laboratory article. As shown in Fig. 1-1, the article was intended to resemble a large space antenna attached to the Space Shuttle Orbiter by a long flexible mast, similar to the proposed space flight experiments and various space-based antenna systems, and to have a truly three-dimensional complex dynamics.

As stated in Ref. [1], the primary control task of the Experiment is **to rapidly slew or change the line-of-sight (LOS)** of an antenna attached to the space Shuttle orbiter, and **to settle or damp the structural vibrations** to the degree required for precision pointing of the antenna. The objective is to minimize the time required to slew and settle, until the antenna line-of-sight remains within a specified angle.

Research on a practical two-stage approach and some associated control design challenges in the context of SCOLE had been conducted earlier by Lin [2]-[5]. His initial efforts, also supported by the SCOLE program, were concentrated on "Stage 1" while the flexible-body dynamics of the configuration with a flexible mast beam was being actively developed at the Langley Research Center.

Among the most commonly held ideas for pointing/retargeting of large flexible space systems is the following intuitively appealing and rather practical two-stage approach: (**Stage 1**) slew the whole structure like a rigid body in a minimum time under the limited control moments and forces first, and then

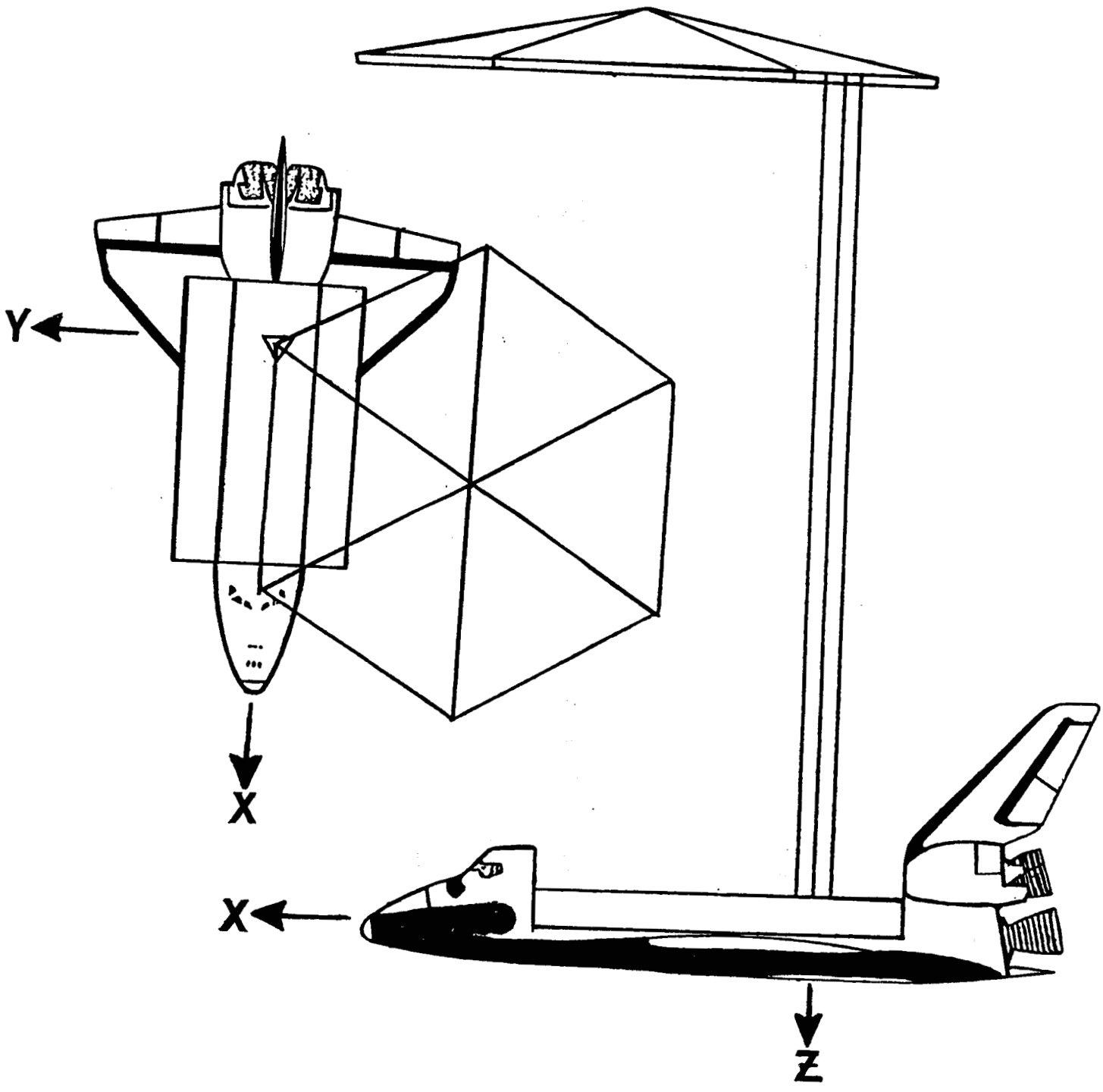

Fig. 1-1 Spacecraft Control Laboratory Experiment (SCOLE)--
the orbital Shuttle-Mast-Antenna configuration.

(**Stage 2**) damp out the excited structural vibrations afterwards. Such an approach undoubtedly will be a very relevant, and realistic as well, to study with SCOLE.*

To slew a spacecraft for a given angle in a **prespecified time**, there are many ways to command the slew actuators on board. The one that is easy to implement is a **bang-bang control**. That is, a constant force at its allowable maximum is applied in one direction half of the time and then in the opposite direction the other half. Such is the most convenient and common with reaction-jet thrusters, and most spacecraft including the space Shuttle use thrusters. As the structure considered for future space antennas and optics was becoming larger and more flexible, structural dynamicists suggested modifying the constant profile by a sine or versine function so as to smooth the switching. To explore further in their theorectical and experimental investigations, control engineers also started to apply Pontryagin's Maximum Principle of the optimal control theory [6] to develop open-loop profiles that would "minimize" excitation of the first few vibration modes.** Including more than a few modes generally will make it almost impossible, even with the aid of powerful digital computers, to carry out the complicated computations necessary for applying the optimal control theory. To implement any such slew profile other than the bang-bang type will also require that the thrusters be at least "throttleable" in fine steps, which is still beyond the current state of the art.

To slew SCOLE for the desired 20^0 under the specified limits on control moments and forces in a minimum time, instead of some arbitrarily fixed time, application of the well-known time-optimal bang-bang control theory [6]-[7] was considered the most appropriate for the Stage-1 design. The theory, however, is not directly applicable to SCOLE: due to the asymmetrical configuration and the moving coordinate frame that is fixed on the Shuttle body axes, all axes are tightly coupled through **nonzero products of inertia** as well as through **different moments of inertia**. After examining the major assumptions in the theory, Lin [2]-[3] was able to develop a useful practical design technique for time-minimized single-axis bang-bang slew maneauvers. This includes the possible "**bang-pause-bang control**" when some judicious slew rate limits are imposed on the slew design.

Analytical and numerical studies were then conducted on the implicit transcendental nonlinear expression initially provided by NASA Langley Research Center for SCOLE's line-of-sight error. A designer's choice of allowable initial alignment to take advantage of the low moment of inertia in the roll, as suggested by Taylor [1], was determined directly analytically. The slew angles to achieve the desired LOS pointing were thus determined. [4]-[5]

A computer program for SCOLE's complete 3-axis rigid-body dynamics was developed and used to simulate numerically the application of various time-

---

* The Space Shuttle, while in orbit, is under the single-axis "phase-plane" rigid-body attitude control of "Digital Auto-Pilot" (**DAP**). If the two-stage approach is applicable, then the current DAP can be used conveniently with various proposed flexible-structure flight experiments in space without having to make a major specific change in operation or design to suit each different experiment setup.

** Usually all but 2 to 3 modes of the structure were ignored.

minimized bang-bang type attitude slew maneuvers. The numerical simulation test results indicated that the single-axis bang-bang or bang-pause-bang slew maneuvers work fairly well for pointing the LOS of SCOLE under the specified conditions. In particular, applying a maximum allowable control moment (i.e., 10,000 lb-ft) on the Shuttle and a maximum allowable control force (i.e., 800 lb) on the Reflector, plus imposing 5 deg/sec slew rate limit on the design, yields **the best pointing accuracy** (0.097^{0}) with **minimized slew time** (3.733 sec) and **least sensitivity to nonzero products of inertia**. Such is a best design for LOS pointing slew maneuver for the SCOLE configuration so far as the Stage 1 is concerned.[5]

For designing vibration control systems (the Stage 2), a standard choice would be to apply the modern control and estimation theory, namely, the linear-quadratic-Gaussian (LQG) state-feedback control technique. The LQG technique has been well accepted because of its success in various other applications. **Control spillover** and **observation spillover**, however, have surfaced as major roadblocks to successful application of such a state-of-the-art state-feedback design technique to control vibrations in large flexible space structures. Current spacecraft and many other engineering systems on which the LQG technique has been very sucessful are of the rigid-body type that do not have as many closely spaced low-frequency vibration modes as there are in a future large flexible space system. Earlier, Balas [8] showed by an example and Herrick [9] followed by a hardware experiment that, because of control and observation spillover, even a simple flexible beam, which was initially stable in the open loop, **became unstable** when the "modern modal control" loops were closed.

On the other hand, dynamic properties of large flexible space structures can be enhanced by active augmentation of modal damping and stiffness through proper output-feedback control [10]-[24]. Lin [20]-[23] showed analytically that an appropriate output feedback control system, particularly when it is of the type of "modal dashpots" and/or "modal springs" [21], can even ensure **full-order closed-loop asymptotic stability** of a very general class of lightly damped large flexible space structures while improving their dynamic characteristics.

For Stage-2 design to damp the excited vibrations in the SCOLE configuration, one can consider using a modal-dashpot type of output feedback control system first. One may then consider using a **modal-dashpot augmented** LQG optimal state feedback control system, if the LOS stabilization performance is not enough to satisfy the specified stringent accuracy requirements.

Before proceeding to designing a vibration control system for SCOLE, many technical issues need to be addressed. For example, one needs to characterize SCOLE's vibration modes with respect to (i) the excitation by the rapid slew maneuvers, (ii) their contribution to the vibration (jittering) of SCOLE's line of sight, and (iii) the control authority of the control actuators. Which modes need to be controlled directly? Which modes only need some additional damping? Which are more likely to cause serious control spillover if not included as "modeled modes"? Those are among many technical questions one generally should look into before starting out a meaningful design for SCOLE's vibration control system.

2. MATHEMATICAL MODEL OF THE ORBITAL SCOLE CONFIGURATION

To assist our quantitative assessments of the vibratory impact of rapid bang-bang slew maneuvers on the flexible SCOLE configuration and the performance of proposed vibration control designs, we have developed a computer program to simulate various vibratory responses of the configuration. The computer simulation was based mainly on the modal data set **D3D585** provided by Dr. Suresh M. Joshi of NASA Langley Research Center as the flexible-body dynamics, and the nonlinear LOS error expression formulated by Mr. Larry Taylor [1]. We extended a portion of the expression by including a few more terms to take a better account of the effect of bending in the mast.

2.0 Outline of the Orbital Shuttle-Mast-Antenna Configuration

As shown in Fig. 1-1, the configuration of the SCOLE represents a large antenna attached to the Space Shuttle Orbiter by a flexible beam as the Mast. The configuration was chosen for its similarity to proposed space flight experiments and various space antenna systems.

The dynamics of the SCOLE configuration are described [1] by a distributed-parameter beam equations with rigid bodies in the three-dimensional space, each having mass and inertia at either end. One body represents the space Shuttle Orbiter, having the mass, inertia, and dimensions typical of the real one. The other body is a large antenna reflector. The equations of motion for the complete configuration are formed by incorporating the three-dimensional rigid-body equations into the partial differential equations of beam bending and torsion. The flexible mast is treated as a standard slender beam. The boundary conditions at the ends of the beam contain the forces and moments applied to the rigid Shuttle and reflector bodies. The mast is **not attached to the mass center** of the reflector, but rather significantly away in both x and y directions. The nonlinear kinematics of the two sizable bodies and the offset attachment of the reflector couple the three otherwise uncoupled beam equations. The reader is referred to Taylor and Balakrishnan's paper [1] for the details. The rigid-body part of the mathematical model was used by Lin earlier in his studies on the LOS pointing (i.e., the Stage 1) of the configuration. The studies on vibration control reported here were based on a most recent version of the flexible-body part available; see Section 2.1 below.

The line-of-sight (LOS) error of the SCOLE configuration is a highly nonlinear implicit expression. The line of sight is defined by a ray emited from the feed on the Shuttle which is reflected at the center of the Reflector. It is affected by the pointing error of the Shuttle, the offset attachment of the Reflector, and the misalignment due to the deflection and torsion of the Mast. The reader is again referred to Ref. [1] for the original formulation of the LOS error. An equivalent expression having a simple modification, which is more convenient than the original for both efficient numerical computations and in-depth analytical investigations, was used by Lin in his earlier rigid-body studies [3]-[5]. For the current flexible-body studies, the nonlinear LOS error expression also needs some more terms in order to have a better accounting for the bending of the mast beam; see Section 2.2 below.

2.1 Flexible-Body Dynamics

The bending and torsion characteristics of the SCOLE configuration were originally formulated in partial differential equations by Taylor and Balakrishnan [1]. Robertson [25] derived the corresponding equations of free motion taking into account the kinematic coupling resulted (i) from the offset attachment of the Reflector to the Mast and (ii) from the nonzero products of inertia of both the Shuttle and the Reflector. He then solved the equations in terms of trigonometric and hyperbolic functions and computed a set of natural frequencies and mode shapes. Such results are not readlily useful for control studies.

To facilitate the control analysis and design for SCOLE, Joshi [26] first derived a state-space model from Robertson's results; the data set was named "**BMDT3D**". Later, he improved Robertson's results, and also derived another state-space model, named "**D3D585**". Our computer simulation program was initially based on the data set BMDT3D, which contained only the first five flexible-body vibration modes. It was then updated when Dr. Joshi furnished us with the set D3D585 later.

The set D3D585 provides modal data in the state-space (A,B,C) form. It contains only the first 10 flexible-body modes but no rigid-body modes nor any nonlinear rigid-body dynamics. This set was quite appropriate for our purpose of assessing the vibratory impact on SCOLE. We found it more effecient and convenient, however, to compute the time transition of the states using the second-order modal equations directly, because of the decoupled nature of the former, than to do so using the first-order state equations. We thus converted the furnished data back to the following standard modal form:

$$\ddot{\eta}_i + \delta_i \dot{\eta}_i + \sigma_i \eta_i = \sum_{k=1}^{m} \phi_i^T b_{Fk} u_k \qquad i = 1,\ldots,N \tag{2-1}$$

$$y_j = \sum_{i=1}^{n} (c_{Vj}\phi_i \dot{\eta}_i + c_{Dj}\phi_i \eta_i) \qquad j = 1,\ldots,\ell \tag{2-2}$$

where
$$\delta_i = 2\zeta_i\omega_i, \qquad \sigma_i = \omega_i^2 \tag{2-3}$$

are, respectively, the damping and stiffness coefficients of the unit-mass linear oscillator representing the ith vibration mode; ω_i and ϕ_i denote the natural frequency and mode shape, respectively, of mode i; ζ_i denotes the inherent damping ratio of mode i, which had been assumed to be 0.3% for all flexible-body modes of SCOLE [1]. η_i and $\dot{\eta}_i$ denote the coordinate and velocity, respctively of the ith mode.

The kth force (torque) input is denoted by u_k, with column vector b_{Fk} representing the corresponding actuator influences on SCOLE. The jth measurement output is denoted by y_j, with row vectors C_{Vj} and C_{Dj} representing, respectively, the velocity and displacement sensor influences.

Putting (2-1) and (2-2) into a matrix form, we get

$$\ddot{\eta} + \Delta\dot{\eta} + \Sigma\eta = \Phi^T B_F u \tag{2-4}$$

$$y = C_V \Phi\dot{\eta} + C_D \Phi\eta \tag{2-5}$$

where

$$\Delta = \text{diag}\,[2\zeta_i\omega_i], \quad \Sigma = \text{diag}\left[\omega_i^2\right] \tag{2-6}$$

$$\Phi = [\phi_1, \cdots, \phi_n], \quad B_F = [b_{F1}, \cdots, b_{Fm}] \tag{2-7}$$

$$C_V = \begin{bmatrix} C_{V1} \\ \vdots \\ \vdots \\ C_{V\ell} \end{bmatrix} \qquad C_D = \begin{bmatrix} C_{D1} \\ \vdots \\ \vdots \\ C_{D\ell} \end{bmatrix}$$

$$\eta = \begin{bmatrix} \eta_1 \\ \vdots \\ \vdots \\ \eta_N \end{bmatrix} \qquad u = \begin{bmatrix} u_1 \\ \vdots \\ \vdots \\ u_m \end{bmatrix} \qquad y = \begin{bmatrix} y_1 \\ \vdots \\ \vdots \\ y_\ell \end{bmatrix} \tag{2-8}$$

In accordance with Robertson's formulation, we also assume that the bending and torsion in SCOLE are referred to the coordinate system defined on its initial undeformed configuration. Thus, before any deformation, the center of mass of the Shuttle is at the origin of the coordinates; the roll, pitch, and yaw axes (i.e., body x, y, z axes) of the Shuttle, align with the x, y, z coordinate axes* respectively; and, in particular, the straight mast beam coincides with the z coordinate axis. Note that, since the flexible mast was not treated as a cantilevered beam in Robertson's derivation, not only the mast may not be tangential to the z coordinate axis, but the center of mass of the Shuttle also may not remain at the origin, nor may the Shuttle body axes remain parallel to the coordinate axes, when a significant deformation of the mast occurs. The line of sight of the SCOLE configuration will thereby be significantly affected.

2.2 Line-of-Sight Error Expression with More Bending Terms

In order that the jittering of the line of sight (LOS) due to excited vibrations can be more accurately evaluated, we used almost the same nonlinear expression for the line-of-sight (LOS) error of the SCOLE configuration as originally given in Ref. [1]. Unlike the orginal, however, our improved version also takes into account the **z-axis dislocation of the Reflector due to bending of the mast**, and like the one Lin used earlier [4]-[5] the LOS vector R_{LOS} is not normalized. Note that the LOS error expression could be expanded in a Taylor series and a linearized version could be obtained by taking the first-order terms. A linearized version, though useful in linear-quadratic

* Robertson's y and z axes are opposite in sign to those defined by Taylor for SCOLE. We continue to adopt Taylor's definition for consistency with Lin's earlier studies [2]-[5] on the Stage 1.

optimal control designs, is not appropriate for our current use since the excited vibrations are sufficiently large in magnitude and the second- and higher-order terms of the series expansion may not be negligible at all.

The location of the center of the Reflector, represented by $\mathbf{R}_R$,is defined by the location of the joint where the Reflector is attached to the Mast; see Figure 2-2. Denote by $\mathbf{R}_J$ the location of the joint relative to the center of the Reflector, and by $\mathbf{R}_T$ the location of the same point (also the tip of the mast) with respect to the center of the Shuttle. Then the vector $\mathbf{R}_R$ is given by

$$\mathbf{R}_R = \mathbf{R}_T - T_1^T T_4 \mathbf{R}_J \tag{2-9}$$

$$\text{where} \quad \mathbf{R}_J = \begin{bmatrix} -18.75 \\ 32.5 \\ 0 \end{bmatrix} \tag{2-10}$$

The vector $\mathbf{R}_J$ is constant in magnitude because of the rigid reflector, but its **orientation with respect to the Shuttle is affected by the deflection** at the tip J. The product $T_1{}^T T_4$ of coordinate transformations T_1 and T_4 is to take care of the angular change. As in Ref. 1, T_1 denotes a direction-cosine transformation from the Shuttle to the Earth (inertial) coordinates, and T_4 one from the Reflector to the Earth coordinates.

A reasonable approximation for the tip location is given by

$$R_T \simeq \begin{bmatrix} \text{Bend}_x \\ \text{Bend}_y \\ -\sqrt{130^2 - \text{Bend}_x{}^2 - \text{Bend}_y{}^2} \end{bmatrix} \tag{2-11}$$

$$\text{where} \quad \text{Bend}_x = u_{xS} - u_{xR} \qquad \text{Bend}_y = u_{yS} - u_{yR}$$

u_{xS} and u_{yS} denote the deflections of the mast at the Shuttle end in the xz and yz planes, respectively; u_{xR} and u_{yR} are the corresponding deflections at the Reflector end.

Eqs. (2-9)-(2-11) constitute our additional modification to the LOS error expression. Note that the vector $\mathbf{R}_R$ originally given as (18.75, -32.5, -130) in Ref. [1] corresponds to the **undeformed case.** To see it, assume that ther

are no deflections at all. Then Bend_x and Bend_y are both zero, and T_4 is equal to T_1. Therefore, R_T = (0, 0, 130). Consequently, $R_R = R_T - R_J$ = (18.75, -32.5, 130).

In the analytical studies on the LOS error of SCOLE [4]-[5], we found it more convenient not to normalize the LOS vector $\mathbf{R}_{LOS}$ first, although the resulting error expression is the same since division by its norm is still made later at the end. The LOS error with such a trivial modification is given by

$$e_{LOS} = \pm \sin^{-1} \left[\, ||\mathbf{D}_T \times T_1 \mathbf{R}_{LOS}|| \, / \, ||\mathbf{R}_{LOS}|| \, \right] \tag{2-12}$$

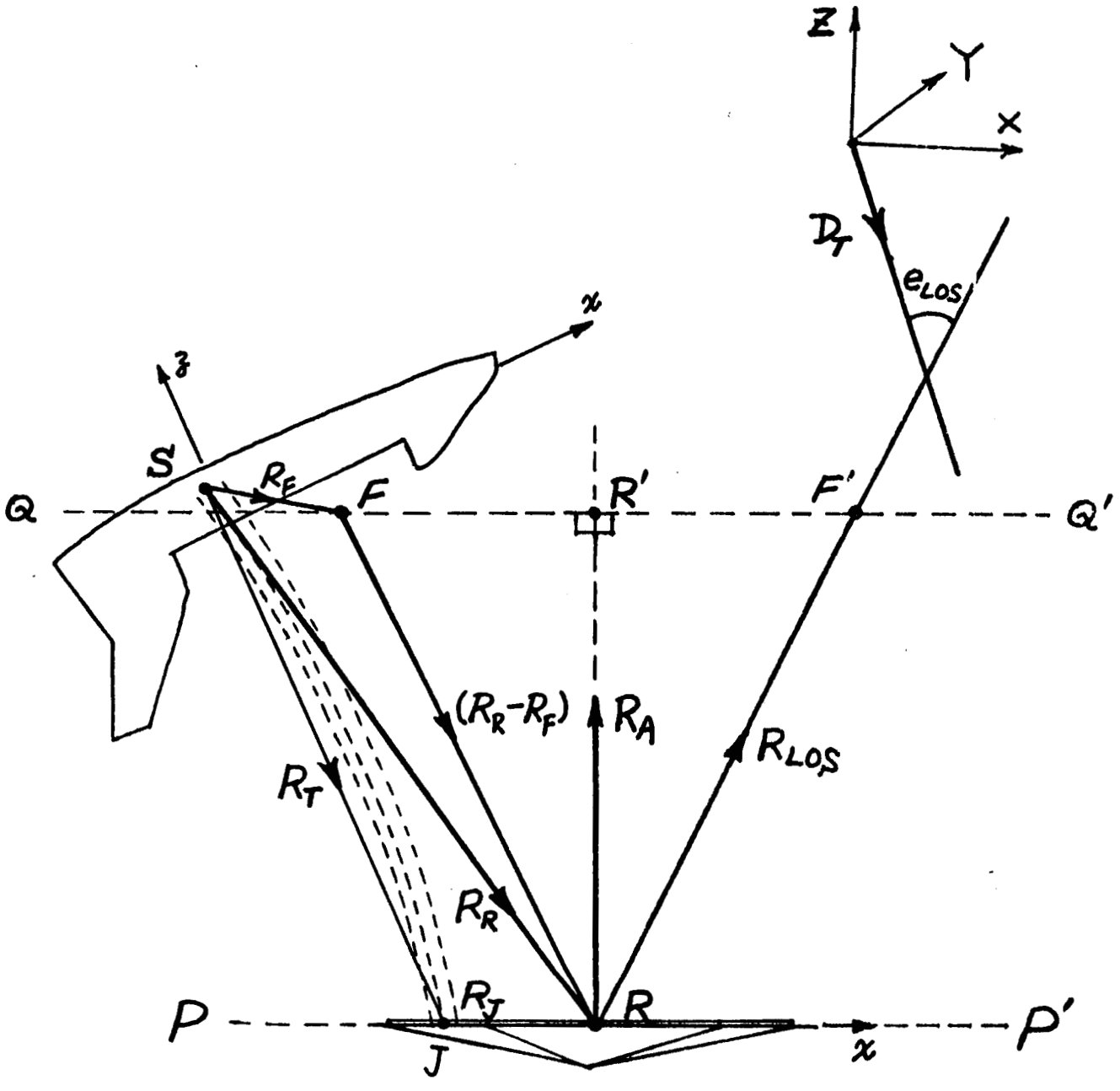

Fig. 2-2 Line-of-sight vectors $\mathbf{R}_R$ and $\mathbf{R}_{LOS}$, and Mast tip position vector $\mathbf{R}_T$.

with the unnormalized LOS vector being defined as

$$\mathbf{R}_{LOS} = RF' = \mathbf{R}_R - \mathbf{R}_F - 2[(\mathbf{R}_R - \mathbf{R}_F).\mathbf{R}_A]\mathbf{R}_A \qquad (2\text{-}13)$$

Where as defined in [1], $\mathbf{R}_F$ is the vector representing the feed location (3.75, 0, 0). $\mathbf{R}_A$ is a unit vector in the direction of the Reflection axis in the Shuttle body coordinates, i.e.,

$$\mathbf{R}_A = T_1^T \, T_4 \begin{bmatrix} 0 \\ 0 \\ 1 \end{bmatrix}.$$

For the target direction specified in [1] as D_T = (0, 0, 1), Expression (2-12) reduces to

$$e_{LOS} = \pm \sin^{-1}\left[\sqrt{(T_{1r1} \, \mathbf{R}_{LOS})^2 + (T_{1r2} \, \mathbf{R}_{LOS})^2} \; / \; ||\mathbf{R}_{LOS}||\right] \qquad (2\text{-}14)$$

where T_{1r1} and T_{1r2} denote respectively the first and the second rows of matrix T_1.

3. VIBRATORY RESPONSES TO BANG-BANG TYPE RAPID SLEW MANEUVERS

Several LOS pointing slew maneuvers of the bang-bang type were applied to our computer simulation of the SCOLE flexible-body dynamics. The resulting responses range from excessive to minimal, depending on the magnitude of the applied force at the Reflector. Note, however, that all these slew maneuvers were designed to provide minimized slew time under the increasingly tight limit imposed on the respective applied force.

The slew maneuver that excited the **most violent vibrations** in SCOLE was chosen for studying the control design and for generating in-depth insights into the vibration control challenges. On the other hand, the least violent one deserves further exploration in the future, since it may potentially require a smaller total time for both slew and stabilization.

In assessing the impact of structural vibrations on SCOLE, we view the slew maneuvers as **time-dependent disturbances** instead, and only the vibratory portion of the time-domain responses are of real interest. Therefore, it is reasonable that we concentrate only on the flexible-body and temporarily ignore any rigid-body dynamics in this study. This assumption is equivalent to the absence of rigid-body dynamics. It is also reasonable to assume that, before being subject to such disturbances, SCOLE was initially at rest and had no deformation nor LOS error. The former assumption is equivalent to setting to zero the initial conditions on the normal coordinates and velocities of all modes, and the latter equivalent to aligning the undeformed SCOLE configuration with the attitude (ϕ_1,θ_1,ψ_1) that corresponds to zero LOS error. Such roll-pitch-yaw Euler angles, calculated and used by Lin earlier [4]-[5], are listed below for reference:

$$\phi_1 = -14.03624347^\circ; \qquad \theta_1 = -6.38707294^\circ; \qquad \psi_1 = 0^\circ.$$

3.1 Excitation by the Rapid Time-Minimized Bang-Pause-Bang Slew Maneuver

We first examined, through numerical simulation, the SCOLE flexible-body dynamics under the excitation of the **rapid time-minimized** roll-axis **bang-pause-bang (BPB)** slew maneuver that was considered a best candidate for pointing the line of sight of the SCOLE as a rigid body [4]-[5]. Among many other single-axis LOS pointing slew maneuvers of the bang-bang type previously studied, this BPB maneuver was judged to be the best compromise in terms LOS **pointing accuracy** achievable, **slew time** required, and **performance robustness** to nonzero products of inertia. It was designed to slew the SCOLE configuration about the negative roll (i.e., -x) axis for about 20° to correct the initial 20° LOS error specified in [1]. This slew maneuver requires that the maximum allowable moment (10,000 lb-ft) be applied to the Shuttle about the negative roll axis and simultaneously the maximum allowable force (800 lb) at the Reflector center along the negative y axis, both for only 0.867 sec.; then, after a long pause of 3.158 sec., these maximum moment and force be applied again for only 0.867 sec. but in the opposite directions (i.e., positive roll and y axes, respectively).

Such a BPB slew maneuver was applied to our computer simulation of the SCOLE flexible-body dynamics. The simulation results are summarized by the plots in Fig. 3-1a, which show that such a maneuever would cause excessive

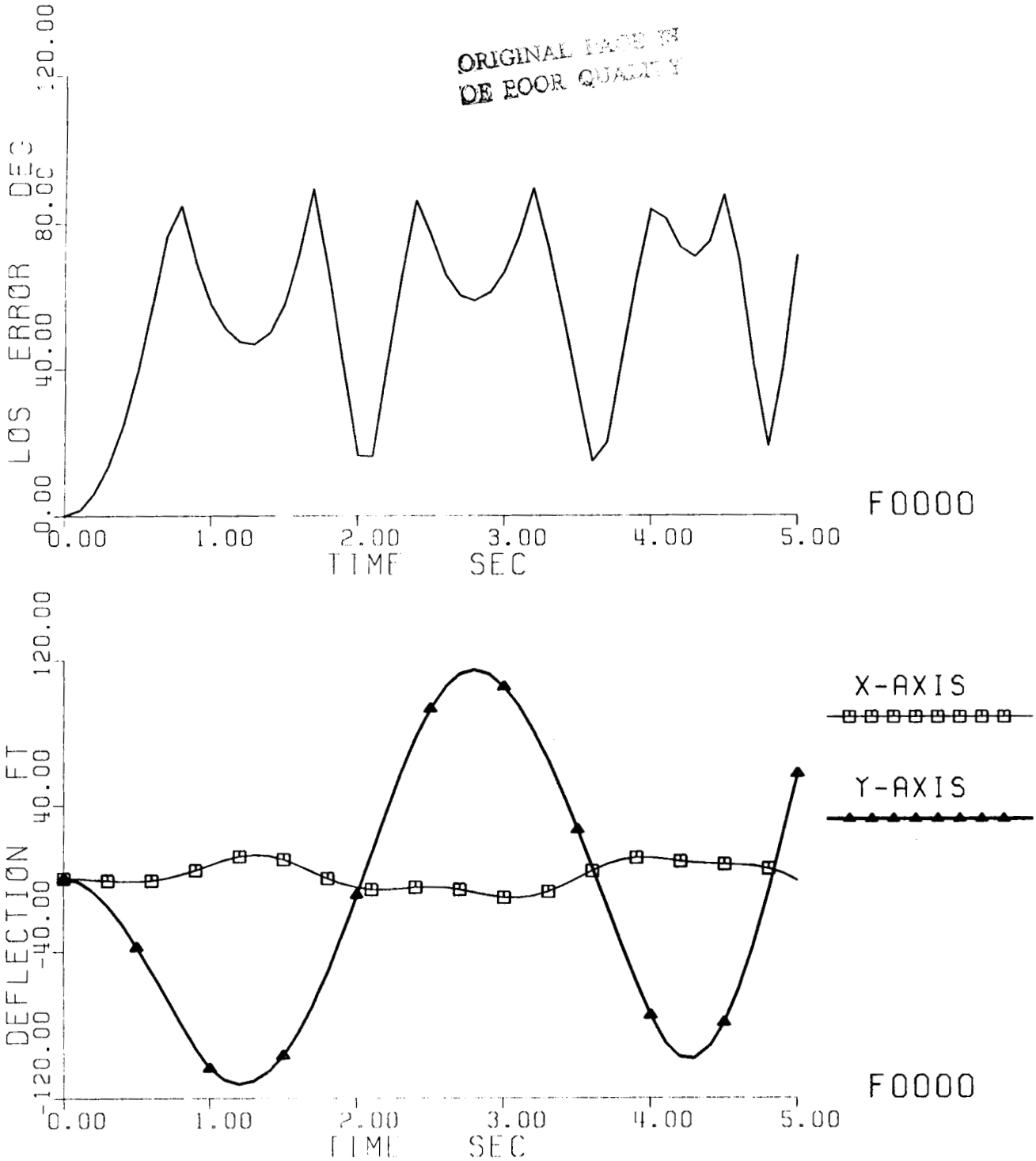

Fig. 3-1 Vibratory responses to Rapid Time-minimized Bang-Pause-Bang Slew;
a. Line-of-sight error and Mast tip deflection.

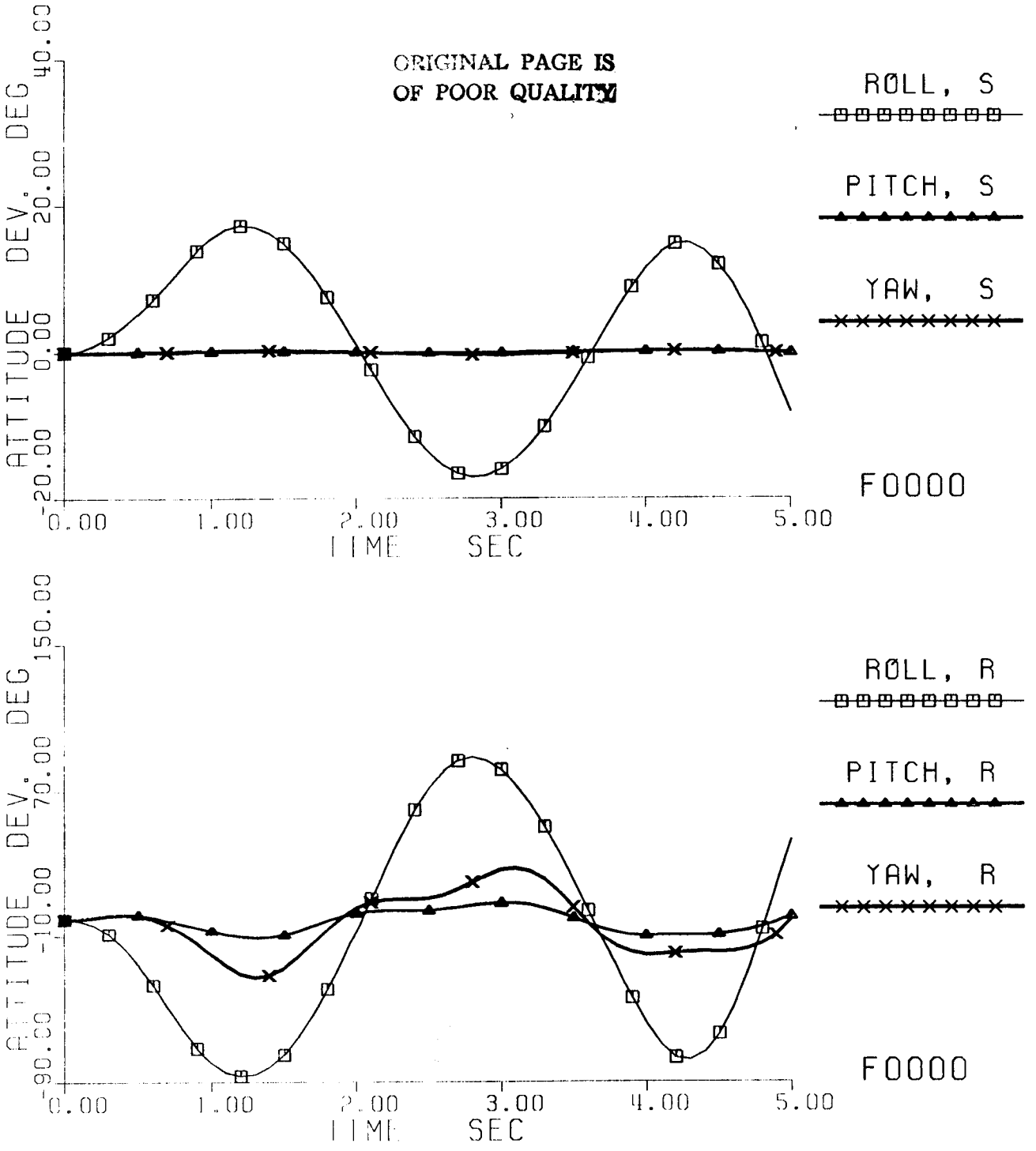

Fig. 3-1 Vibratory responses to Rapid Time-minimized Bang-Pause-Bang Slew;
b. Attitude deviations at the Shuttle (S) and the Reflector (R) ends.

vibrations in SCOLE! Observe that: the line of sight vibrated with error between 89.8° (or 133.3° if not taking on the principal value of the arcsine in Expression (2-14)) and 14.7°; the tip of the mast vibrated in the yz-plane between +114 ft and -113 ft.

Fig. 3-1b show the deviations in Euler attitude angles of the Shuttle (S) and the Reflector (R) from their "nominal" alignment of zero LOS error. These deviations correspond to the bending slopes and the torsion at the respective end of the mast. Observe that the Shuttle rolled to the right and the left between +17.16° and -17.06°, while the Reflector rolled to the left and right between -86.96° and +88.35°. There were virtually no pitch and yaw motions of the Shuttle, but the Reflector pitched between -10.63° and 8.75° and yawed betweeen -32.27° and +27.97°.

In general, some significant excitation of the vibration modes of a flexible space system, such as the orbital SCOLE configuration, should be expected when large moments and forces were used to their limits in a bang-bang manner to minimize the slew time. The appalling magnitude of the vibratory impact, however, was indeed a surprise.

Such excessive vibrations certainly post serious challenges to the Stage-2 design, i.e., the control design for suppressing such vibrations after the excitation. Can such large-magnitude vibrations be brought down to some tolerable level in about the same length of time (say, 5 sec.) as the slew maneuver? How to design such a fast effective vibration controller? We shall continue to address such design challenges in Section 4.

3.2 Excitation by Other Rapid Time-Minimized Bang-Bang Slew Maneuvers

Are all slew maneuvers of bang-bang type so terrible to flexible space systems? Why are the excited vibrations in SCOLE so large in magnitude? Even when one can design a powerful fast vibration controller capable of damping out such vibrations, one still cannot stop thinking of these and other puzzling questions. To investigate further, we conducted the following numerical experiments on our computer simulation of SCOLE flexible-body dynamics. All were the same as before, except that a different bang-bang slew maneuver was applied.

3.2.1 **Experiment F10 -- No force on Reflector.** First we tried to use only the 10,000 lb-ft moment on the Shuttle. The same roll-axis bang-bang slew maneuver using only such a moment for accomplishing the same 20° pointing task in the minimum time as was previously designed and evaluated on the rigidized configuration in [4]-[5] was tried. This maneuver requires that the maximum moment be applied first about the negative roll axis for 6.307 sec, and then switched to the opposite directions (i.e., positive roll axis) for another 6.307 sec. It was truly a **bang-bang** (BB) control.

The simulation results, as shown by plots in Fig. 3-2, clearly show that the vibratory impact was greatly reduced. The LOS error was only 6.25° at most, and the mast tip vibrated only between +5.06 ft and -5.18 ft.

Of course, the (minimized) slew time is much longer; it is a main reason why this maneuver has been rejected earlier [4]-[5] as a Stage 1 design for

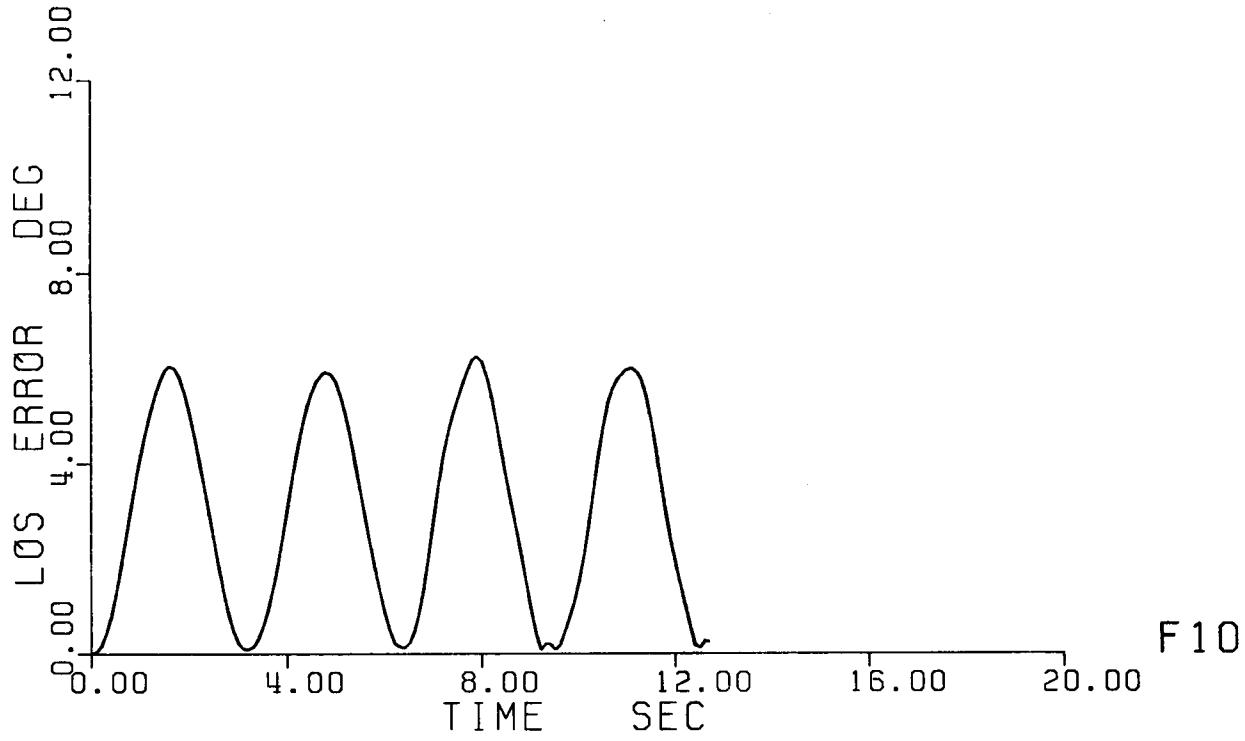

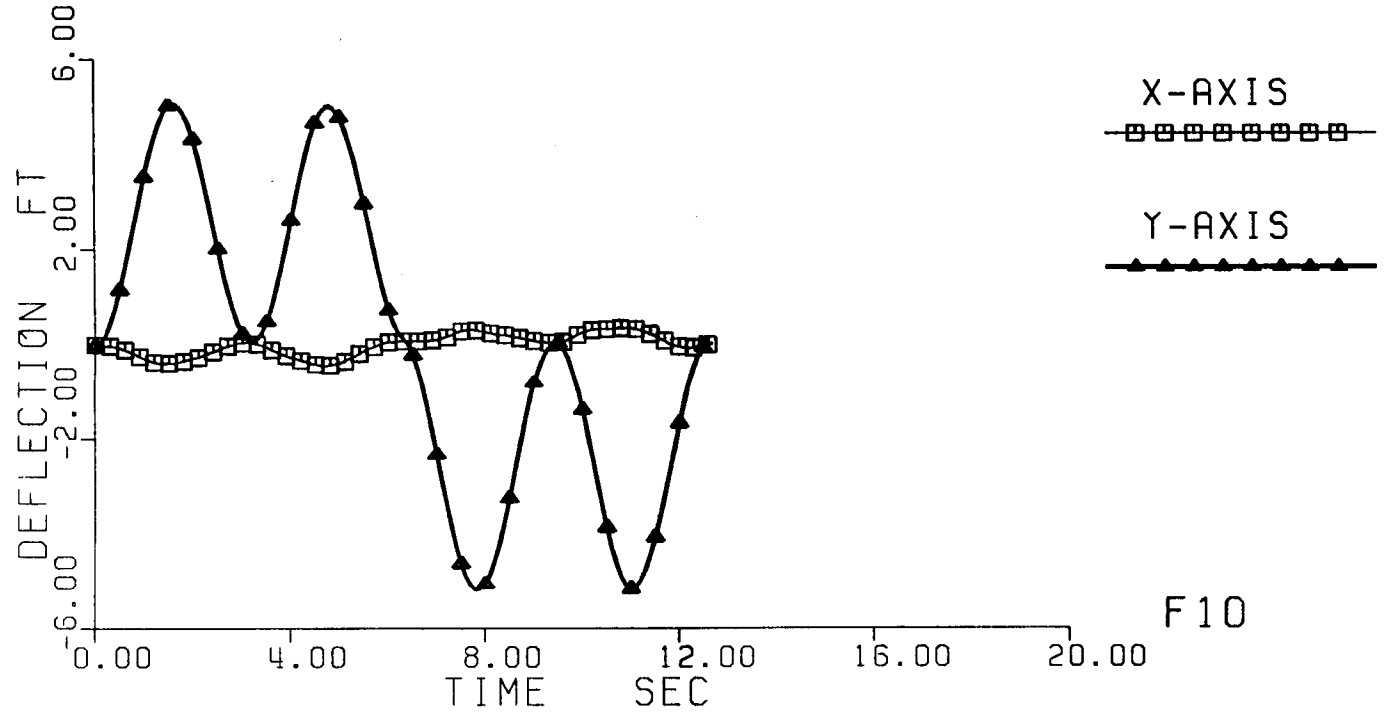

Fig. 3-2 Vibratory responses to Rapid Time-minimized Bang-Bang Slew: 0 lb;
a. Line-of-sight error and Mast tip deflection.

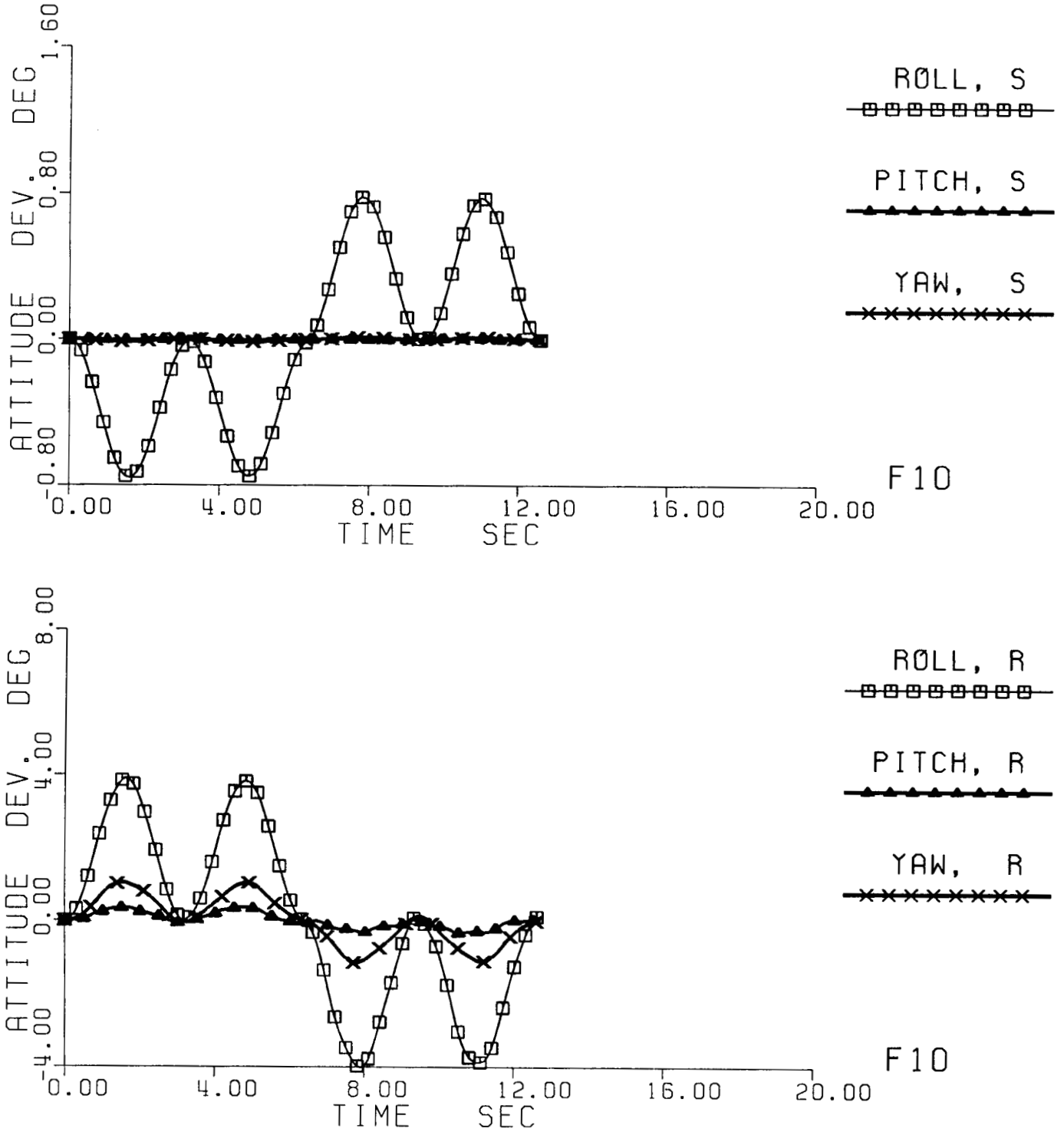

Fig. 3-2 Vibratory responses to Rapid Time-minimized Bang-Bang Slew: 0 lb;
b. Attitude deviations at the Shuttle (S) and the Reflector (R) ends.

SCOLE. This simulation is useful only when its results are compared with the foregoing case of using additional 800 lb force on the Reflector: it serves as an opposite extreme, since no force was applied to the Reflector at all.

By a careful inspection of the time histories of the tip deflection in both cases (see Figs. 3-1b and 3-2b), we can make the following interesting observations. While the moment was being applied to the Shuttle about the negative roll axis without any force on the Reflector, the beam bent backwards and the Reflector lagged behind*. On the contrary, the addition of the maximum force on the Reflector reversed the situation, even though the additional force had exactly the same purpose of rolling the configuration to the same side as the moment on the Shuttle! The Reflector then became leading instead of lagging.

3.2.2 **Experiment F180 -- 80 lb Force on Reflector.** The leading of the Reflector might be responsible for the huge increase in LOS error, as implied by the above observations. It is therefore reasonable that reducing the applied force might reduce the lead and hence reduce the LOS error. A second experiment was thus conducted with an 80 lb maximum force, which is only one tenth of the original allowable maximum.

A new roll-axis slew maneuver was designed, in the same way as the first BPB slew maneuver; but only 80 lb, instead of 800 lb, force was to be used in conjunction with the same 10,000 lb-ft moment to accomplish the same 20° LOS pointing in a minimized time. It turned out to be a **bang-bang** maneuver instead, since the slew rate would not reach the imposed 5 deg/sec limit. In almost the same way as in the case of 800 lb, the slew maneuver requires that both the moment and the (tighter-limited) force be applied with respect to the corresponding negative axes for 4.416 sec, and then reversed to the corresponding positive axes for another 4.416 sec, but with no pause in between.

The simulation results, as summaried by plots in Fig. 3-3, confirmed what we thought. The lead by the Reflector is now **greatly reduced**, and so are the LOS error and the mast bending, compared to the case of 800 lb (Fig. 3-1). The LOS error was only 24.7° at the highest peak of its time history; the tip deflected only between +20.59 ft and -10.83 ft; and the Reflector rolled only between +15.98° and -8.31°.

These results have clearly shown that the 800 lb force was directly responsible for the excessive vibrations and the unreasonable LOS error.

Next, compare these results with those of Experiment F10 (Fig. 3-2). A peak LOS error of 24.7° is fairly large compared to only 6.25° of Experiment F10; so is a maximum deflection of 20.59 ft compared to only 5.18 ft of F10. Does this mean that no force should be applied to the Reflector at all? No, we did not think so! Instead, we reasoned that if one could **reduce the lead** slightly further, one could further reduce both the LOS error and the tip deflection. So a third experiment with a slightly smaller force was performed.

---

* Note that when a negative moment is applied to the Shuttle, a positive deflection indicates the lagging of both the mast tip and the Reflector.

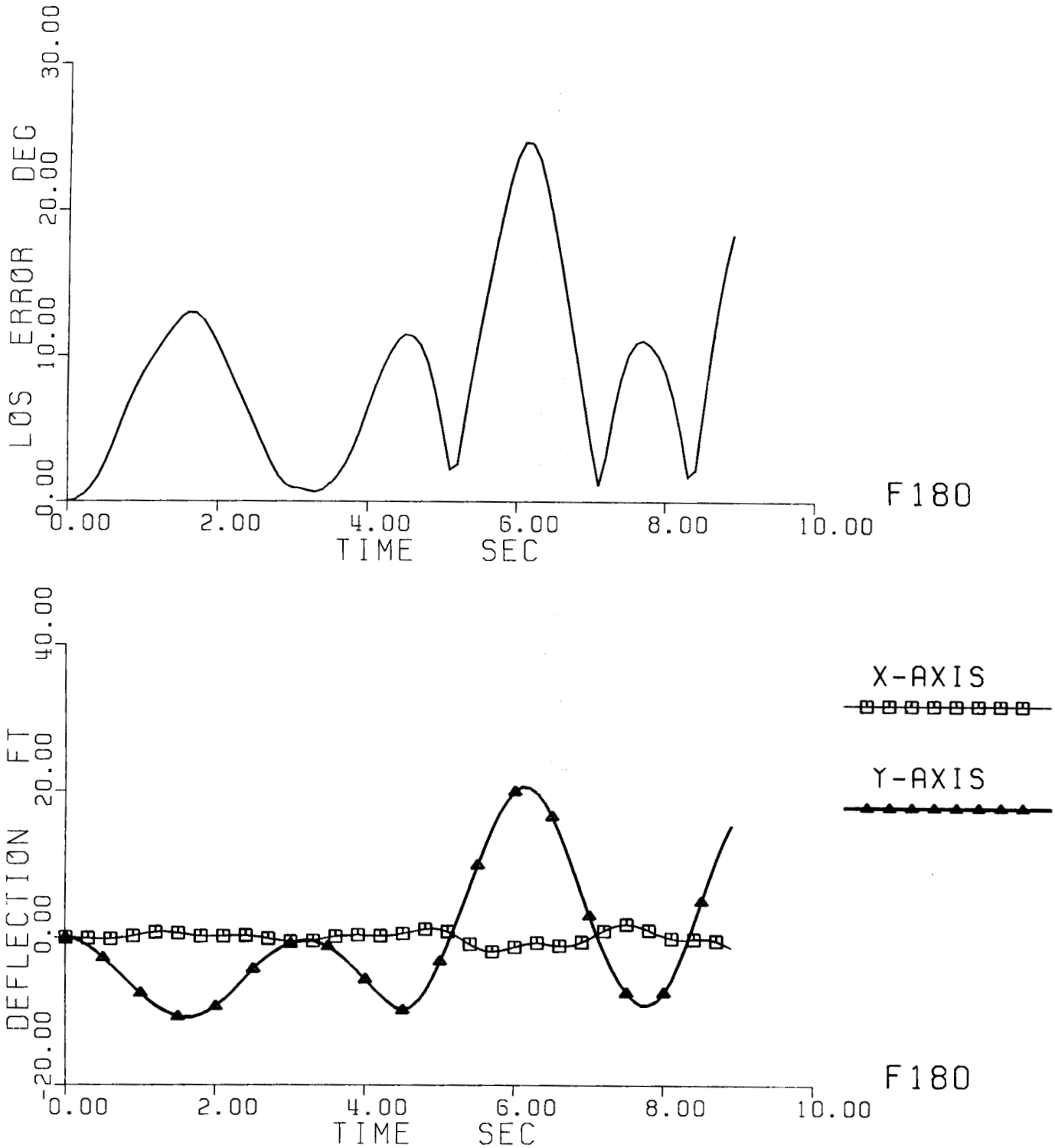

Fig. 3-3 Vibratory responses to Rapid Time-minimized Bang-Bang Slew: 80 lb; a. Line-of-sight error and Mast tip deflection.

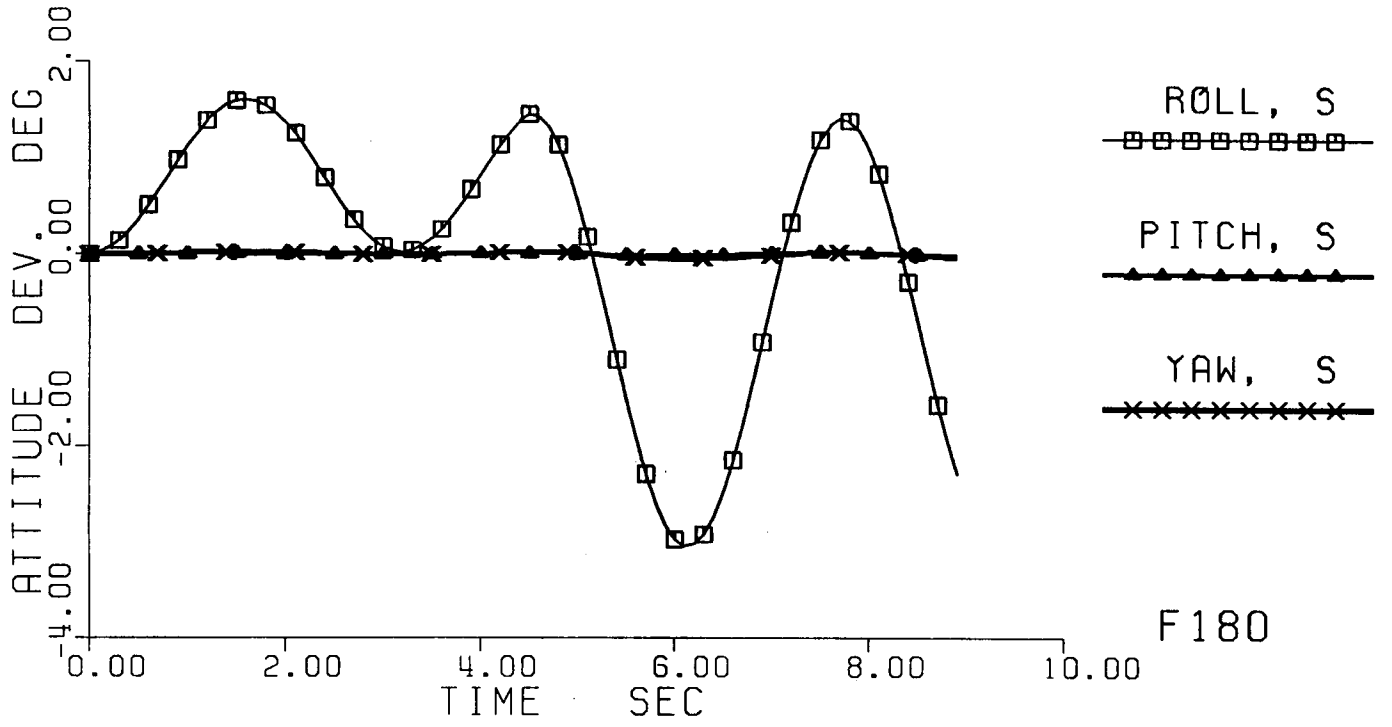

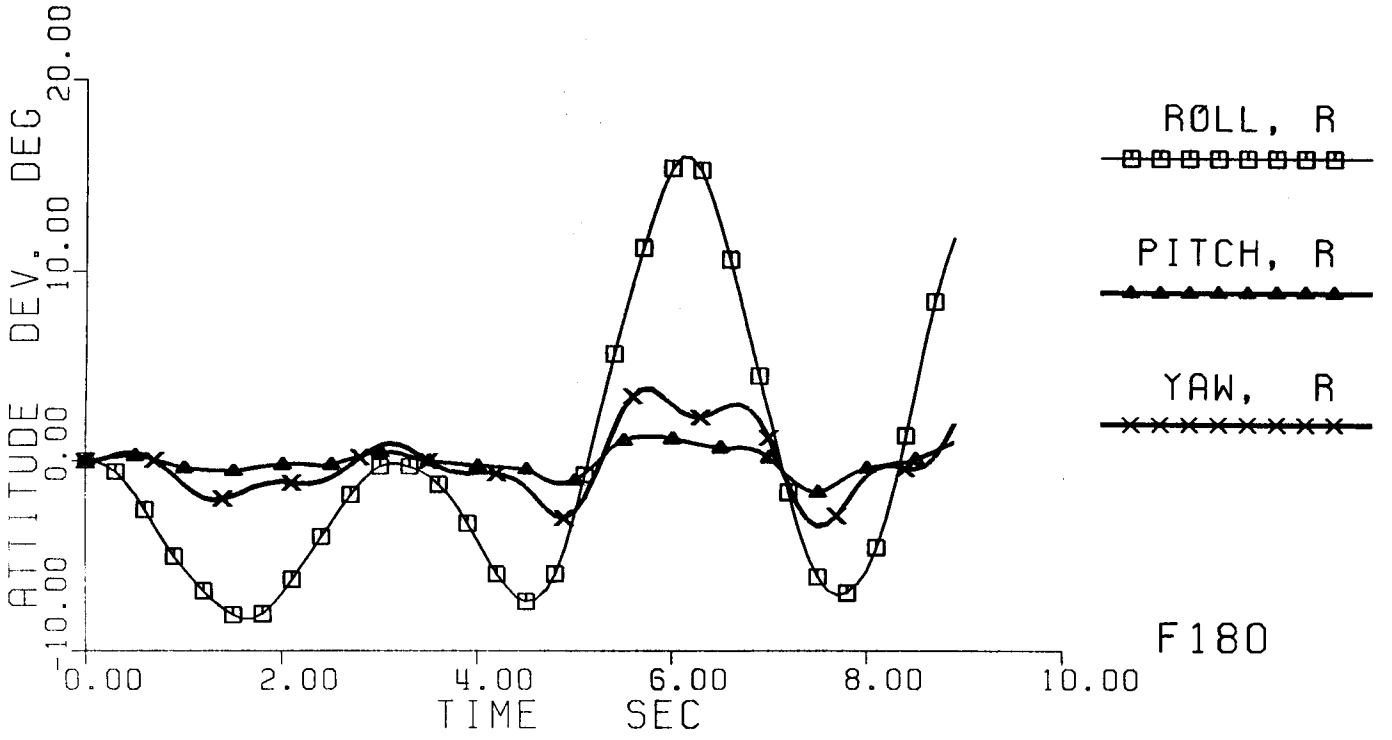

Fig. 3-3 Vibratory responses to Rapid Time-minimized Bang-Bang Slew: 80 lb; b. Attitude deviations at the Shuttle (S) and the Reflector (R) ends.

3.2.3 **Experiment F125 -- 25 lb Force on Reflector.** Since the Shuttle-attached SCOLE configuration was chosen because of its similarity to proposed space flight experiments [27]-[29], we thought it would also be more realistic to consider a force of about the same level as the vernier RCS thrusters on-board the Shuttle Orbiter. Since the existing vernier thrusters generate 24 to 24.5 lb thrust each [30], we simply selected 25 lb for the third experiment.

Again a new roll-axis slew maneuver was designed in the same way as before for accomplishing the same 20° LOS pointing in the minimum time. It certainly is a **bang-bang** maneuver, like the case with 80 lb force. This BB slew maneuver requires that both the 10,000 lb-ft moment and the 25 lb force be applied with respect to the negative roll and y axes, and then switched to the positive axes, as before, for 5.479 sec each time.

The results, as shown in Fig. 3-4 by plots, are very pleasing, indeed. The largest LOS error was less than 0.51°; the tip deflected only between +0.25 and -0.3 ft; and the Reflector rolled only between +0.16° and -0.3° ! All are **one order of magnitude smaller** than those from applying no force on the Reflector! Of course, the time required for completing the 20° slew of the line-of-sight is also shorter. In summary, for a BB slew maneuver of the flexible SCOLE configuration, **using a force of 25 lb on the Reflector in addition to a 10,000 lb-ft moment on the Shuttle is in all aspects superior** to using no additional force there.

The force of 25 lb is simply a rather arbitrary trial value. One could continue to search for an optimal value that would result in still smaller tip deflection, but we did not do so because we felt that our original purpose had already been served very well.

If LOS error were the only concern and time were not so important, then one should immediately stop studying the use of 800 lb force on the Reflector. On the other hand, since time is at least equally important for SCOLE, it is not clear at all that 25 lb might be preferred outright to 800 lb: the minimum time required for the same 20° slew is 10.959 sec for the case of 25 lb but only 4.892 sec for the case of 800 lb, that is, more than twice longer. Moreover, in both cases, some active vibration controllers are still needed to damp out the excited vibrations; and hence some additional time is required in order that the required LOS accuracy of 0.02° can be met.

To damp out excessive vibrations, such as excited by the BPB roll-axis maneuver using both an 800 lb force and a 10,000 lb-ft moment, can be serious challenges to the Stage-2 control design. Insight and techniques generated from dealing with such challeanges certainly will be useful in designing effective vibration controllers for the case of using a smaller force, such as 25 or 80 lb.

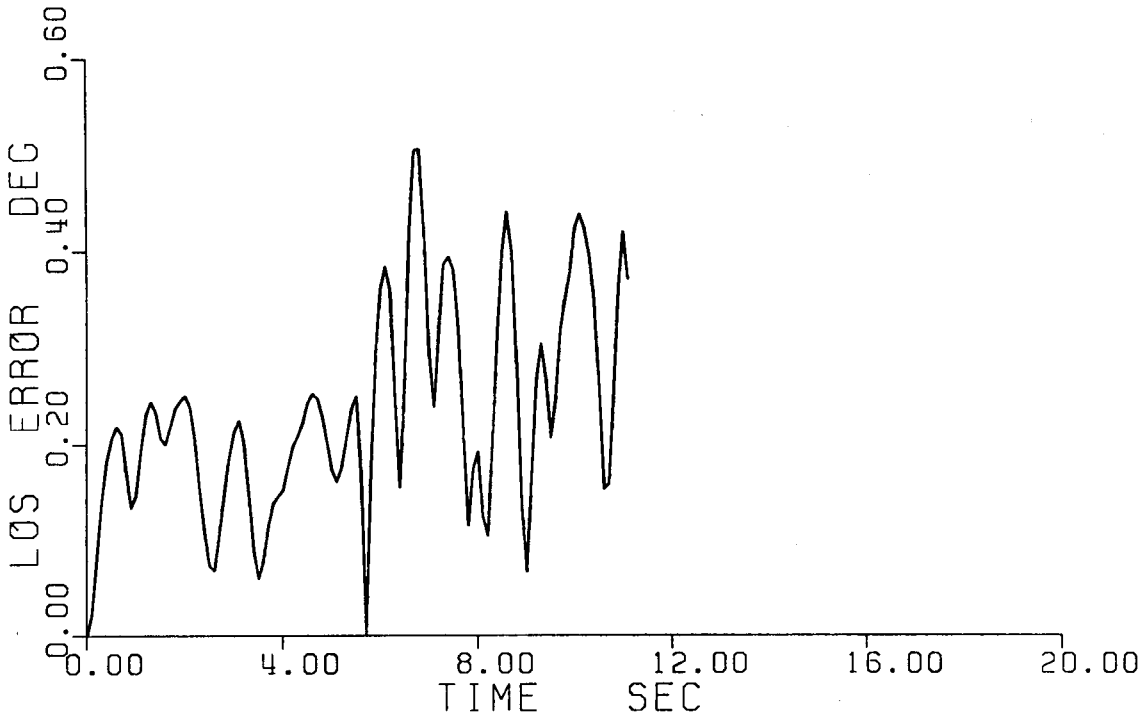

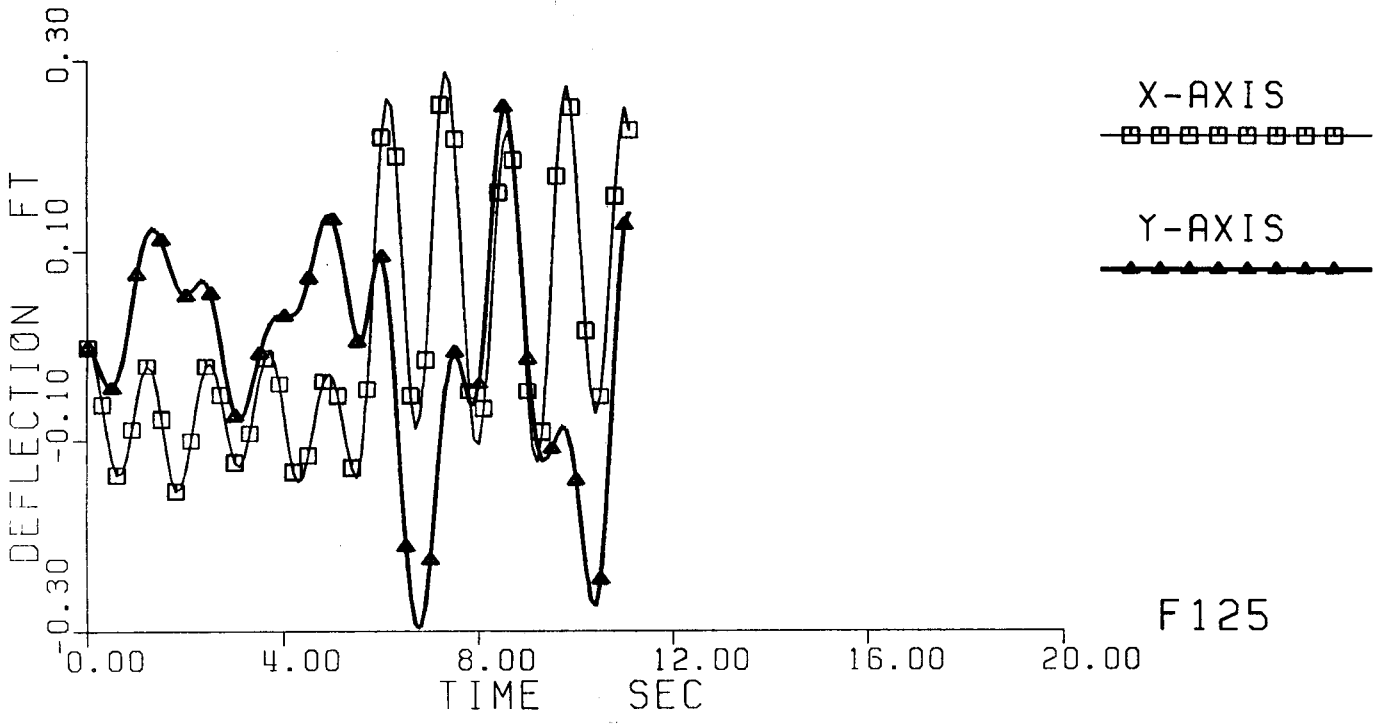

Fig. 3-4 Vibratory responses to Rapid Time-minimized Bang-Bang Slew: 25 lb; a. Line-of-sight error and Mast tip deflection.

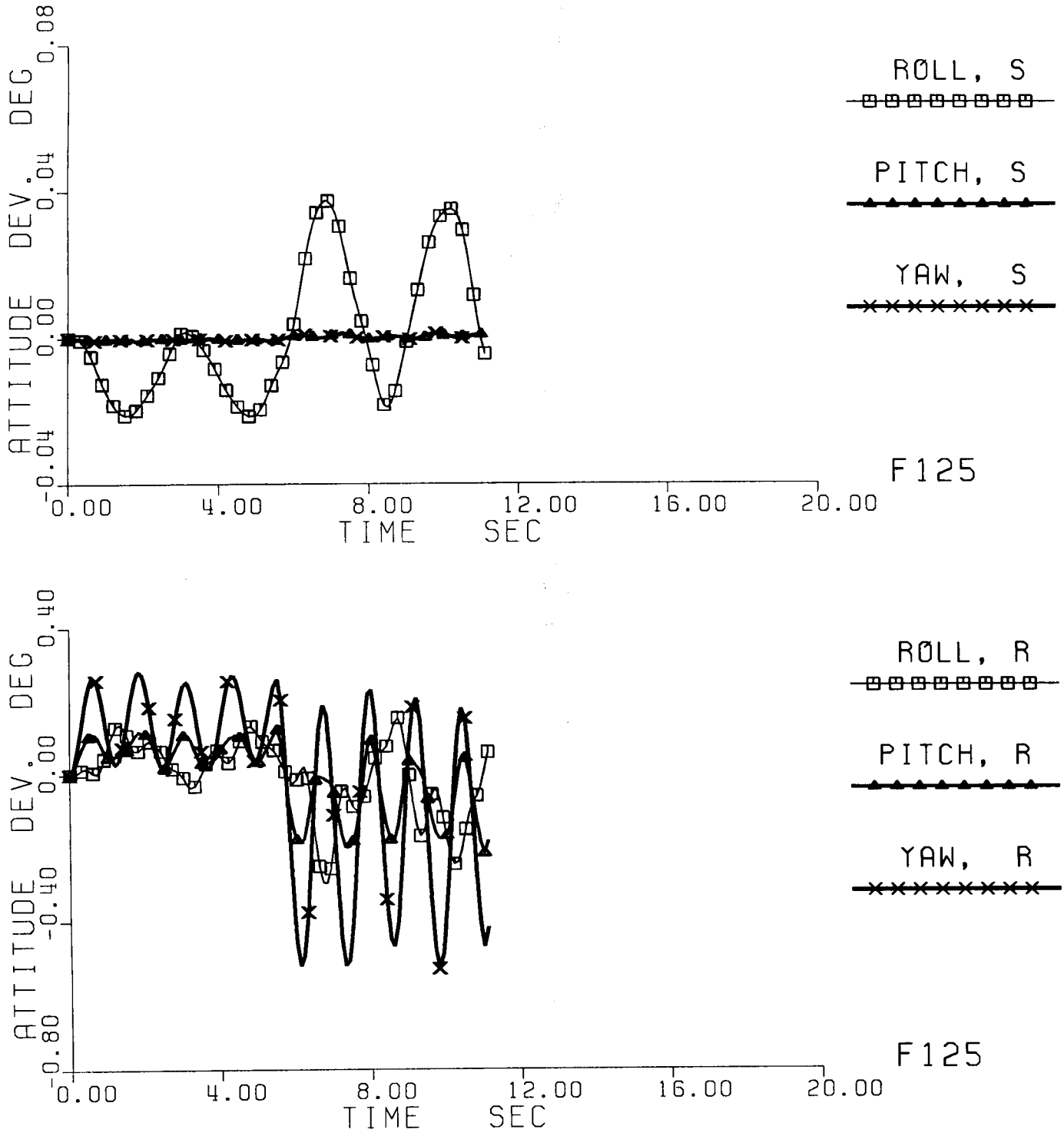

Fig. 3-4 Vibratory responses to Rapid Time-minimized Bang-Bang Slew: 25 lb; b. Attitude deviations at the Shuttle (S) and the Reflector (R) ends.

4. ACTIVE VIBRATION CONTROL FOR SCOLE

4.1 Direct Velocity-Output Feedback Control

Let y_V denote the velocity-sensor outputs. Then from the system Eqs. (2-4)-(2-5), we have

$$y_V = C_V \Phi \dot{\eta} \tag{4-1a}$$

The general form of direct velocity-output feedback control is

$$u = - G y_V \tag{4-1b}$$

where G denotes a matrix of constant feedback gains. Substituting (4-1) in (2-4) results in the following closed-loop system

$$\ddot{\eta} + (\Delta + \Phi^T B_F G C_V \Phi)\, \dot{\eta} + \Sigma \eta = 0 \tag{4-2}$$

The modal stiffness matrix Σ of SCOLE flexible-body dynamics is positive definite, since no zero-frequency rigid modes were included in dataset D3D585. By applying the classical Kevin-Tait-Chetaev theorem, its extensions, or Liapunov's second method, one can show (see, e.g. [17]-[23]) that the closed-loop system (4-2) is:

(i) stable (in the sense of Liapunov) if the augmented damping matrix

$(\Delta + \Phi^T B_F G C_V \Phi)$ is symmetric and nonnegative definite, and

(ii) asymptotically stable if the augmented damping matrix is positive definite.

When the velocity sensors are, as generally assumed, co-located with the sensors, i.e., $C_V = B_F^T$, the additional damping matrix $(\Phi^T B_F G C_V \Phi)$ is always nonnegative definite*, whether the gain matrix G is positive or merely non-negative definite. In other words, direct velocity-output feedback control at least will never destabilize the system, even when no inherent damping exists (i.e., $\Delta = 0$).

For most practical cases where there are less actuators than vibration modes and there are virtually no inherent damping (i.e., Δ is small and some of its diagonal elements are virtually zero), the existing theory cannot help determine whether a closed-loop system is asymptotically stable or not, though numerical results can [17].

The theory is not enough to help design the feedback gains, either. Usually designers simply restrict the gain G to be diagonal matrix, and therefore, make each co-located pair of actuator and sensor act like no more than a (passive) dashpot. Having no systematic method to help calculate the required or desirable values for the feedback gains, some designer even set the diagonal elements rather arbitrarily to some trial positive numbers. A practical ques-

---

* Only in a rare special case, which is rather unrealistic to truly flexible large space systems, where there are as many independent actuators (and co-located independent sensors) as there are vibration modes and the influence matrix B_F is nonsingular, will a positive definite gain matarix G quarantee that the product $\Phi^T B_F C_V \Phi$ is also positive definite.

tion is: how to design the gains so as to add more damping selectively to some specific modes than others? How not to restrict the resulting design to be strictly local feedback? How to design the direct velocity-output feedback as a really multi-variable control system? A systematic design method is needed.

4.2 Concept of Modal Dashpots

The diagonal form of feedback gain matrices spreads the control effort thin over all the vibration modes. One cannot design the diagonal form for adding desirable amounts of damping respectively to certain selected vibration modes. On the other hand, when one wishes to add a certain amount of damping to each mode, one might consider computing the gain matrix G as the general solution of the following NxN matrix equation

$$\Phi^T B_F \; G \; C_V \Phi = \Delta^* \tag{4-3}$$

without restricting it to be diagonal, where Δ^* denotes the matrix of desired additional modal damping. Expressed in terms of additional damping ratio ζ_i^* desired of each mode, the matrix Δ^* may take on the same simple form as Eqs. (2-6), (2-3), i.e.,

$$\Delta^* = \text{diag}\left[\delta_i^* \right] \tag{4-4a}$$

and

$$\delta_i^* = 2\zeta_i^* \omega_i \quad i = 1, \ldots, N \tag{4-4b}$$

Note that for a realistic flexible space structure there are much more vibration modes than there are locations for placing actuators or sensors (i.e., $N>>\ell$ and $N>>m$). Thus, if one wishes to augment some indeterminate amount of active damping to all the modes, then one may try to obtain an **approximate solution** of Eq.(4-3), such as of the least squared error like the following

$$G^P = (\Phi^T B_F)^P \; \Delta^* \; (C_V \Phi)^P \tag{4-5}$$

where A^P denotes the Moore-Penrose pseudo-inverse. No conditions on the matrix $\Phi^T B_F$ or $C_V \Phi$ need to be satisfied, and the pseudo-inverses can be calculated numerically using the **singular value decomposition** [31]-[32].

Solutions of the form (4-5) have three major practical drawbacks. First, the number N of vibration modes in a realistic flexible structures is enormously large, making it impractical, if not impossible, to calculate the pseudo-inverses of the **extremely large** matrices $\Phi^T B_F$ and $C_V \Phi$. Secondly, one still cannot really focus a specific subset of the modes, since the solution G^P is merely a least-square approximation, with **errors spread all over the modes.** Thirdly, also because of approximation errors, the resulting product

$$\Phi^T B_F \; G^P \; C_V \Phi$$

might not be symmetric, and hence stability might not be guaranteed.

In practice, one needs to concentrate on a relatively small number of important modes. In many cases, one cannot care less for those modes which are less important when one cannot even get what is required for suppressing

the more important ones. Thus, assume that some n modes (n<<N) are the most important, and a reduced-order dynamic model is formed by selecting only those n modes. Call those modes modeled modes and the rest unmodeled modes. Partition the matrices η, Φ, Δ, and Σ accordingly into the **modeled (M)** and the **unmodeled (U)** parts, i.e.,

$$\eta = \begin{bmatrix} \eta_M \\ \eta_U \end{bmatrix} \qquad \Phi = [\Phi_M, \Phi_U] \qquad \Delta = \text{black-diag}[\Delta_M, \Delta_U] \qquad \Sigma = \text{black-diag}[\Sigma_M, \Sigma_U] \tag{4-6}$$

Then, the closed-loop equation for the **reduced-order model** is

$$\ddot{\eta}_M + (\Delta_M^T + \Phi_M^T B_F G C_V \Phi_M)\,\dot{\eta} + \Sigma_M \eta_M = 0 \tag{4-7}$$

Now, let a reduced matrix Δ_M^* be given that corresponds to the desired additional damping for the n modeled modes. Then the design is reduced to solving the following much smaller nxn matrix equation, instead of the NxN Eq. (4-3), for the gain matrix G:

$$\Phi_M^T B_F \; G \; C_V \Phi_M = \Delta_M^* \tag{4-8}$$

As before, a solution in the same general form as (4-5) can be obtained numerically by computing the pseudo-inverses of influence matrices $(\Phi_M{}^T B_F)$ and $(C_V \Phi_M)$. It is still an approximate solution unless some rank conditions are satisfied by the influence matrices.

Of the particular interest is when the control influence matrix $(\Phi_M{}^T B_F)$ has the **full row rank** and the observation influence matrix $(C_V \Phi_M)$ has the **full column rank.** In other words,

$$\text{rank}(\Phi_M^T B_F) = \text{row}(\Phi_M^T B_F) = n \tag{4-9a}$$

$$\text{rank}(C_V \Phi_M) = \text{column}(C_V \Phi_M) = n \tag{4-9b}$$

Such a special case requires that $n \leq \ell$ and $n \leq m$, i.e., the number of modeled modes do not exceed both the number of actuators and the number of sensors to be used in the feedback control. Under the full-rank conditions (4-9), the pseudo-inverses are also **generalized inverses.** That is,

$$(\Phi_M^T B_F)^P = (\Phi_M^T B_F)^R = \text{right generalized inverse of } \Phi_M^T B_F$$

$$= (\Phi_M^T B_F)^T \left[(\Phi_M^T B_F)(\Phi_M^T B_F)^T \right]^{-1} \tag{4-10}$$

$$(C_V \Phi_M)^P = (C_V \Phi_M)^L = \text{left generalized inverse of } C_V \Phi_M$$

$$= \left[(C_V \Phi_M)^T (C_V \Phi_M) \right]^{-1} (C_V \Phi_M)^T \tag{4-11}$$

The gain matrix G^* computed therewith solves Eq. (4-8) exactly†. The closed-form expression is given by

$$G^* = (\Phi_M^T B_F)^R \, \Delta_M^* \, (C_V \Phi_M)^L \tag{4-12}$$

Consequently, the reduced-order closed-loop system equation (4-7) thereby simplifies to

$$\ddot{\eta}_M + (\Delta_M + \Delta_M^*) \, \dot{\eta}_M + \Sigma_M \eta_M = 0 \tag{4-13}$$

The desired damping Δ_M^* is thus added to the reduced-order model exactly as specified. For stability, the matrix Δ_M^* of additional damping only needs to be nonnegative definite; it need not be diagonal.

When Δ_M^* is chosen to be a diagonal matrix, as it is often convenient and reasonable to do in practice, the resulting velocity-output feedback control will perform like a **separate "dashpot" attached to each mode** of the reduced-order model. Specifically, let

$$\Delta_M^* = \text{diag} \left[\delta_{Mi}^* \right] \tag{4-14}$$

Then (4-13) can be rewritten in the component form like (2-1) as follows:

$$\ddot{\eta}_{Mi} + (\delta_{Mi} + \delta_{Mi}^*) \, \dot{\eta}_{Mi} + \omega_{Mi}^2 \, \eta_{Mi} = 0 \tag{4-15}$$

where η_{Mi} denotes the normal coordinate of the ith modeled mode. Eq. (4-15) obviously means that the ith modeled mode, like an **independent linear oscillator**, is augmented with an additional dashpot whose damping coefficient is δ_{Mi}^*. This is why Canavin called such s design a "decoupled controller", or "modal dashpots" [11].

The diagonal elements δ_{Mi}^* should be nonnegative to make a practical sense. Like (4-4), it can be given in terms of damping ratios ζ_{Mi}^* and natural frequencies ω_{Mi} as

$$\delta_{Mi}^* = 2 \, \zeta_{Mi}^* \, \omega_{Mi} \tag{4-16}$$

---

† Given whatever values to the matrices, it is mathematically an exact solution so far as the equation (4-8) is concerned. Of course, it may not be an exact solution so far as the system (4-2) or even (4-7) is concerned, when any matrix, for example the modal matrix Φ as usual, contains some modeling or computational errors. Small errors in Φ may invalidate stability results of general feedback gains but not the modal-dashpot type [20]-[23].

4.3 Improvement on the Design Method

One can design very effective vibration controllers by the method of modal dashpots, as demonstrated by our applications to SCOLE. The interesting simple formula (4-10)-(4-12), however, **does not by itself complete the design method for an effective control of structural vibrations.** In fact, when the concept of modal dashpots was initially formulated by Canavin [10]-[12] as "decoupled controller", it was accompanied by two major technical drawbacks that almost rendered itself practically useless. Later, through various numerical evaluations and theoretical analyses, Lin and his associates [20]-[24] identified the underlying causes of these problems, and greatly enhanced the utility of this concept. In the course of applying it to the challenging SCOLE vibration control design problem, we also made some additional improvement on this design method.

A first initial technical drawback was the high-gain low-damping problem. After he applied it to a representative large space structure (of which 37 vibration modes were considered), Canavin concluded that "the decoupled controller may be of limited utility due to the high gains produced by this approach "[11]. The feedback gains were mostly in the orders of 10^{10} to 10^{12}, while only additional 10% of critical damping was designed for each of the 12 modes he had selected to be "controlled" (i.e., modeled) modes.

Aubrun [13] proposed the approach of low-authority control (LAC) by limiting to 10% modal damping and by using sufficiently small gains so that the amount of active damping achievable is predictable. Since then, direct velocity-output feed back control has been commonly thought to be of only low authority, low performance, and secondary importance. However, the vibration controllers of Aubrun's design should be of low authority, not because of direct velocity-output feedback, but rather because of the applicability of Jocobi's root perturbation formula on which he based his theory. **For his use of the perturbation formula to remain valid,** the control authority (and specifically the feedback gains) must be sufficiently low so that the closed-loop eigenvalues and eigenvectors would be resulted from only infinitesimal perturbations, i.e., **only very small increase in damping ratios.**

A second initial technical drawback of the basic design method was severe interactions between modeled and unmodeled modes. When the method was applied to another representative large space structure (i.e., ACOSS model 2 [33]), the interactions were so severe that the desired damping performance on the modeled modes was degraded very badly, although the closed-loop system remained stable [24].

The following common causes were discovered.

(1) Some modeled modes had too small control influences ($\phi_{Mi}{}^T B_F$) or too small observation influences ($C_V \phi_{Mi}$). This made the generalized inverses $(\Phi_M{}^T B_F)^R$ or $(C_V \Phi_M)^L$, and hence the resulting gain matrix, unnecessarily large. Theoe low-influence modes should he deleted from the reduced-order model, or else some actuators or sensors should be relocated to improve their influences on these modes.

(2) Some of the rows in matrix $\Phi_M{}^T B_F$ had too small degree of independence from the others, or some columns of $C_V \Phi_M$ had the similar situation. This also

made the generalized inverses, and the gain matrix, unnecessarily large in magnitude. Like (1) above, these modes should be excluded, or the location of some actuators or sensors be improved.

(3) Some low-frequency unmodeled modes had too large control influences ($\phi_{Uj}{}^{T}B_F$) or observation influences ($C_V\phi_{Uj}$) compared to those of the modeled modes. This made excessive spillover. These modes should be added to the reduced-order model; otherwise, some actuatore or sensors should be relocated, or their influences be properly synthesized [35]-[36].

(3) Some of the desired additional damping coefficeints ($\delta_{Mi}{}^{*}$) were too large for some modeled modes, even all were set equal to the same small design value (say, $\zeta_{Mi}{}^{*} \equiv 0.1$). This made some part of the gain matrix unnecessarily large, and hence increased interactions with some unmodeled modes.

Open-loop responses of individual modeled modes should be analyzed and the need for additional damping realistically guesstimated with respect to the control/observation influences on each modeled mode. For properly designed modal dashpots, e.g., our design for SCOLE, the additional damping could be as high as 67% for some modes or as low as 3% for some others, depending on the ability of the actuators as well as on the individual open-loop responses.

We have begun to develop the concept of modal dashpots into a useful systematic design method for direct output feedback vibration control. Although the closed-form formula has reduced the design of modal dashpots to simple cranking of numbers, yet to make it really work for effective control of large excited structural vibrations in flexible space systems, such as the SCOLE configuration, many careful pre-design steps have to be taken.

The design method was initially formulated by Canavin without explicit consideration of limitations on the requirement for control forces and torques. Now, the explicit limits must be considered when applying the method to SCOLE. Also, some saturation "circuitry" must be imposed on the feedback control so that the magnitude of the forces or moments generated by the modal dashpots would automatically be limited to 800 lb and 10,000 lb-ft, respectively. Saturation may not destroy stability when actuators are co-located with sensors [37], but would somehow limit the performance of the feedback controller.

5. DESIGN OF MODAL DASHPOTS FOR SCOLE

The vibrations in the SCOLE configuration excited by the rapid time-minimized BPB LOS pointing slew maneuver, as reported in Section 3.1, posted three serious vibration control design challenges:

(1) The excited vibrations were excessively and unrealistically large in magnitude: the line of sight once had an error of 89.9° (or beyond) and the 130-ft mast once had a tip deflection of 114 ft.

(2) The allowable time was extremely short: it should be minimized, so only an equally short time (specifically, only 5 sec, which was approximately equal to the maneuver time) was allowed.

(3) The available control forces and moments were limited: the 800 lb and 10,000 lb-ft limits were imposed the same way as on slew maneuvers.

In order to design effective modal dashpots for suppressing such excessively large vibrations in SCOLE in a very short time, we conducted careful pre-design analyses on the vibration modes and their influences by the actuators and sensors. The candidates for modeled modes were selected, and then divided into two groups according to the actuator influences. The design of the modal dashpots was therefore divided into two parts accordingly.

5.1 Analysis on Vibration Modes

Initially, two different numerical analyses of SCOLE vibration modes were made, each with a different standard measure of importance. The results were inconsistent. Then a third measure was developed and used; the results were finally fair and satisfactory.

5.1.1 Measure 1: LOS Error due to Initial Modal Displacement

"LOS error contribution" is a common measure used by many structural dynamicists for determining if a vibration mode is "critical" or not, i.e., if it needs active control or not. It was used by Draper Laboratory [33]-[34], and accepted by other **ACOSS*** and **VCOSS**** contractors [38]-[45] as the standard approach, in the modal analysis of both Model No. 1 (namely, the Tetrahedron) [34] and Model No. 2 [33] of representative large flexible precision space structures. The standard approach is to express the LOS error as a linear function of physical coordinates under the assumption that all the displacements are sufficiently small. When the physical coordinates are transformed into the normal coordinates of the structure, the LOS error become a linear function of the normal coordinates. The "critical modes" are then determined by comparing the modal coefficients of the LOS error.

Such a measure is not directly applicable to rapid pointing of the SCOLE configuration nor, in general, to large space structures that are subject to rapid slew or retargeting maneuvers. First, the displacements (deflections and torsions, for example) generally are large, hence the linearization of the LOS error is not valid. Thus, for SCOLE, we used the original nonlinear expression

---

* **Active Control of Space Structures**, a DARPA technology program.

** **Vibration Control of Space Structures**, sponsored by Air Force Wright Aeronautical Laboratories.

without linearization. Secondly, the LOS error is a dynamic vibratory response, instead of being simply a static displacement of the line-of-sight. Thus, instead of comparing only the LOS error coefficients, we compared the time histories of the LOS error the individual modes would separately cause if they were intially excited alone.

For this analysis, the SCOLE configuration was assumed to be initially at rest with no LOS error*, and only one mode was excited each time because of a unit initial displacement in its normal coordinate. Specifically, for the ith time history, the initial condition was assumed to be:

$$\eta_i = 1, \text{ and } \eta_j = 0 \text{ for all } j \neq i \; ; \quad \dot{\eta}_j = 0 \text{ for all } j.$$

For each such initial modal displacement, the time history of the resulting LOS error was calculated separately using our computer simulation program.

The results of 10 separate cases (one for each mode) are shown together by the overlapped plots in Fig. 5-1, where each curve represents a **completely separate** time history of LOS error. Listed below are the highest peak value of each time-history curve.

Mode:	1	2	3	4	5	6	7	8	9	10
Peak:	.37	.53	.54	.93	1.3	.14	.51	.002	.18	.03

The relative importance of the 10 modes is thus given in the descending order as follows.

Mode: 5, 4, 3, 2, 7, 1, 9, 6, 10, 8.

5.1.2 **Measure 2: Modal Response to the Rapid Pointing Maneuver**

By intuition, a vibration mode is more in need of active control than others when its magnitude of excited vibration is larger. Thus, a second measure of importance for the SCOLE configuration naturally is the vibratory response of each mode to the rapid pointing maneuver. For this analysis, the configuration was assumed, as before (in Section 3.1), to be initially at rest without any LOS error or any nonzero initial conditions, and the same BPB slew maneuver was the source of excitation. The time history of the resulting modal response $\eta_i(t)$ was calculated for each mode separately.

The results are shown by the plots in Fig. 5-2, with each curve representing an individual mode. Listed below are the highest peak value of the curves.

Mode:	1	2	3	4	5	6	7	8	9	10
Peak:	21.6	603	41.2	13.7	0.49	0.48	0.28	.058	.041	.001

Accordingly, the relative importance of the 10 modes is thus given by the following descending order:

Mode: 2, 3, 1, 4, 5, 6, 7, ...

---

* As stated in the beginning of Section 3, we assumed that, before any of its vibration mode was subject to excitation, SCOLE was initially at rest and had no deformation nor LOS error. Specifically, the undeformed configuration was assumed to have been aligned with the attitude angles of zero LOS error. Therefore, if all the normal coordinates and velocities were zero, the LOS error would remain zero.

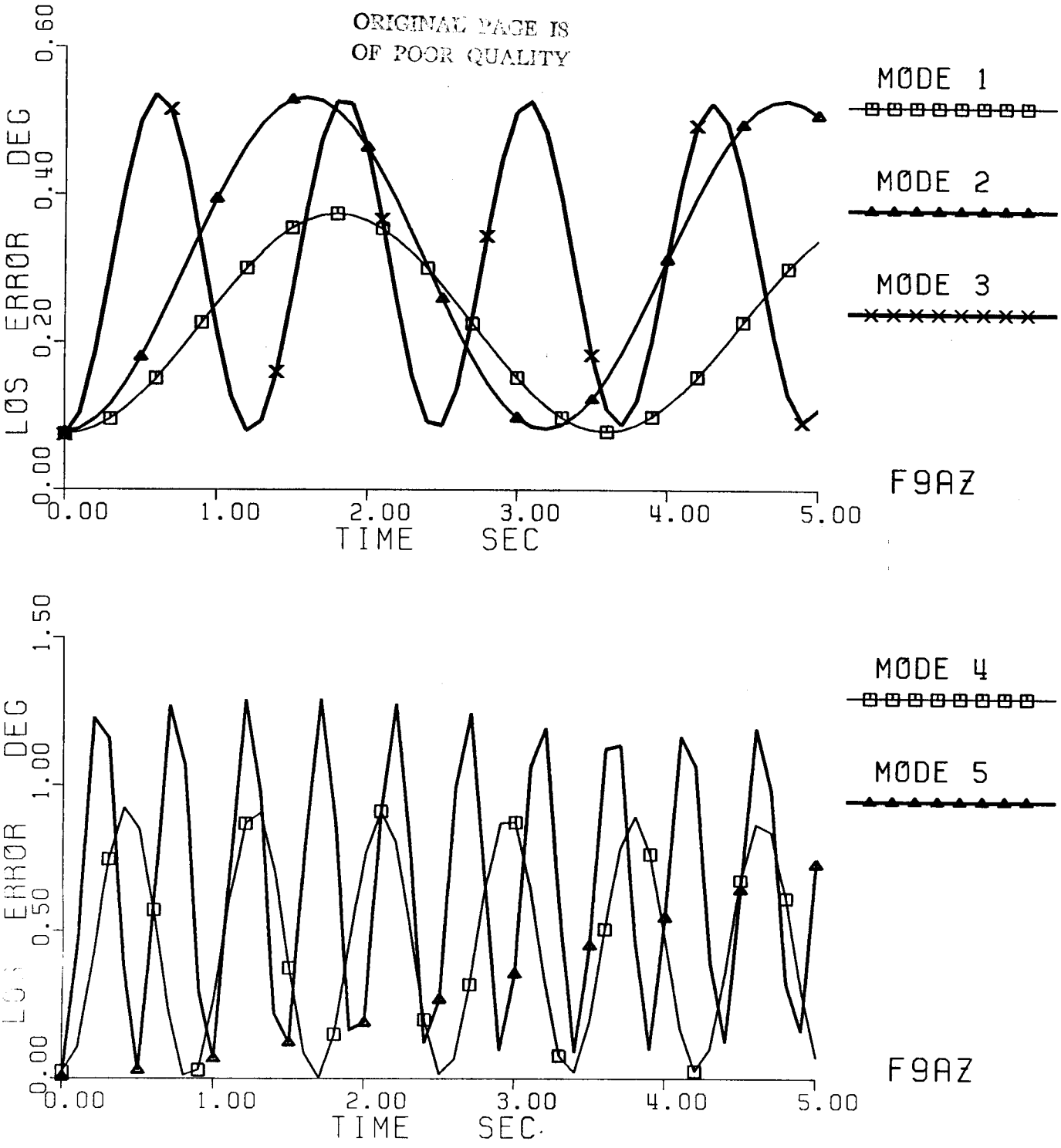

Fig. 5-1a Line-of-sight error due to unit initial modal displacement in Modes 1, 2, 3, 4, and 5, respectively. The separate time histories are plotted together for easy comparison and use with Measure 1.

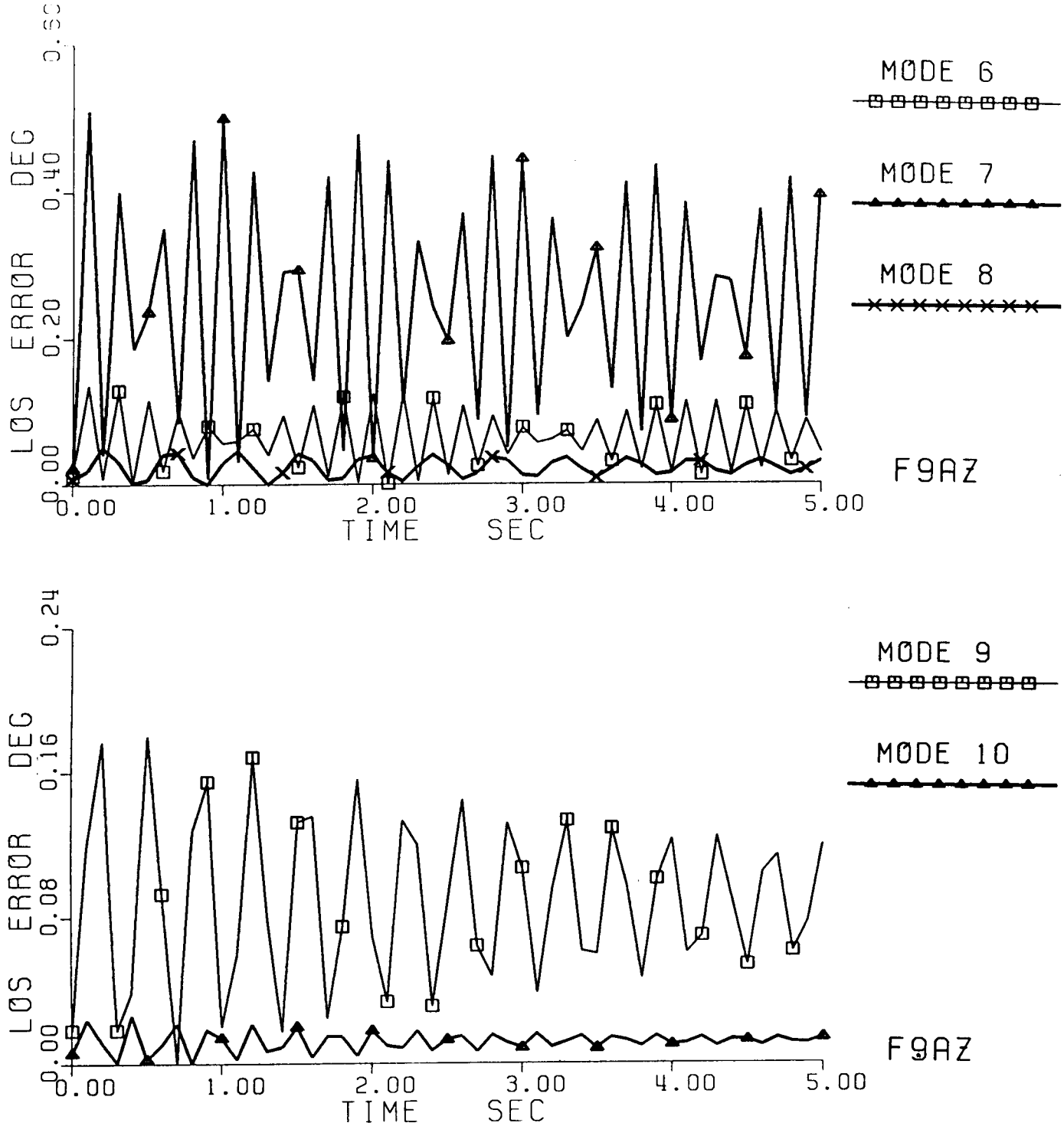

Fig. 5-1b Line-of-sight error due to an initial modal displacement in Modes 6, 7, 8, 9, and 10, respectively. The separate time histories are plotted together for easy comparison and use with Measure 1.

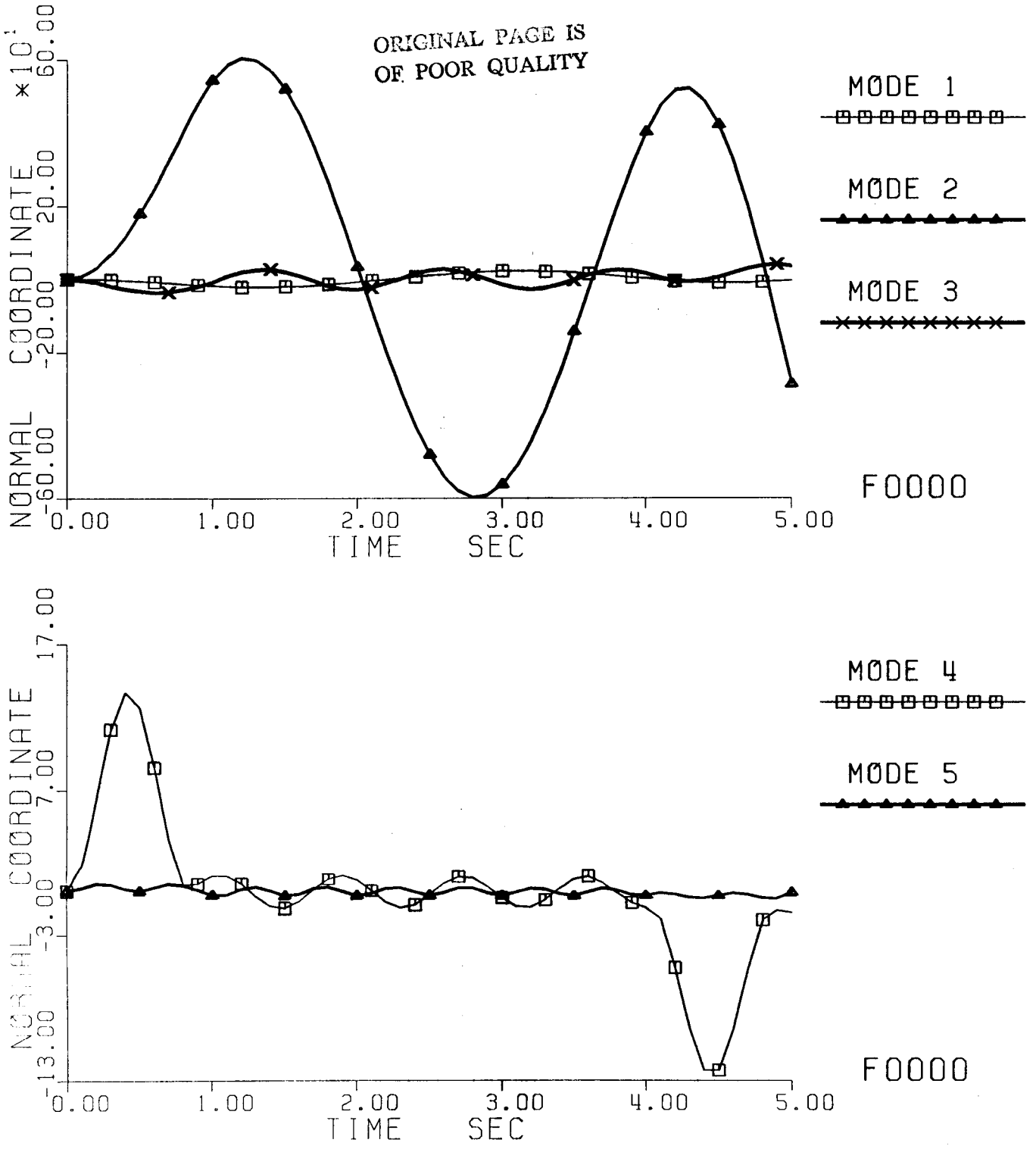

Fig. 5-2a Normal coordinates of Modes 1, 2, 3, 4, and 5, respectively. The cause of excitation was the rapid time-minimized bang-pause-bang pointing slew maneuver. These time histories are plotted together for easy comparison and use with Measure 2.

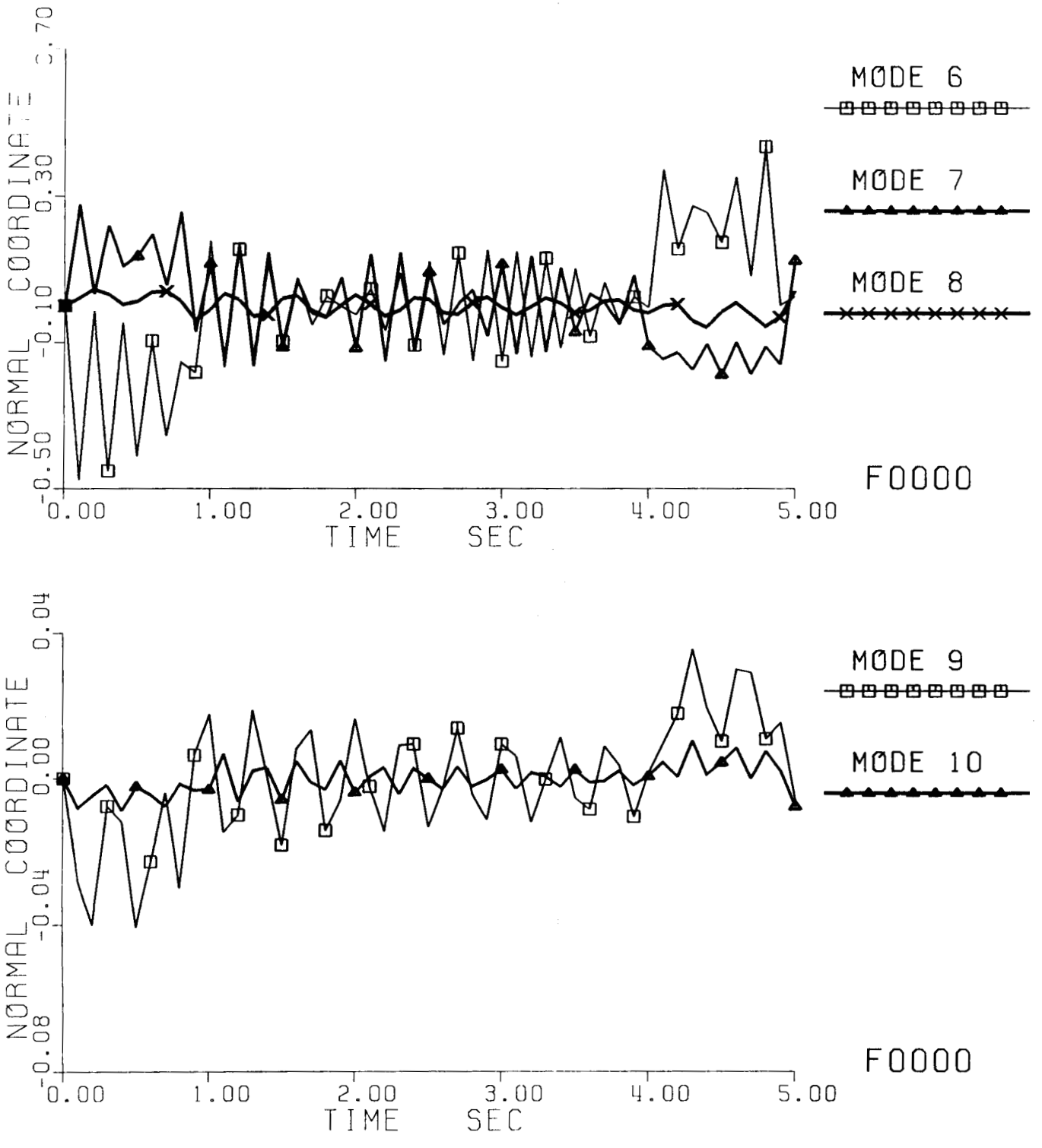

Fig. 5-2b Normal coordinates of Modes 6, 7, 8, 9, and 10, respectively. The cause of excitation was the rapid time-minimized bang-pause-bang pointing slew maneuver. These time histories are plotted together for easy comparison and use with Measure 2.

5.1.3 **Measure 3: LOS Error Solely due to Each Mode Excited by the Maneuver**

To measure by the LOS error a vibration mode could cause, or to measure by the extent to which a vibration mode could be excited, seems to be a rather reasonable technique by itself, but the resulting rankings were inconsistent and rather confusing. For example, Mode 5 is the most important one by Measure 1 but only the fifth by Measure 2. Moreover, Mode 5 could even be ignored because of its insignificant Measure-2 value (about two orders of magnitude smaller than the fourth). Similarly, Mode 1 ranks number 3 by Measure 2 but only number 6 by Measure 1. It was hard to determine rationally which modes would really need active control. A third measure was then developed.

For this analysis, the LOS error caused by a single mode alone was calculated **separately,** like for Measure 1, but the mode causing the error was excited by the very maneuver of concern, instead of initial conditions. All the initial conditions were assumed to be zero. On the other hand, the excitation of the vibration modes was exactly the same as for Measure 2, but the resulting LOS error, instead of the modal response, was taken as the measure.

This measure is a **sound rational combination of the cause (slew excitation) and the effect (LOS error) with respect to each vibration mode.** It can appropriately indicate for each mode individually the extent to which a single mode could be excited, and the degree of LOS error this mode alone could cause if it alone were so excited and, hypothetically, no other modes were present at all.

The 10 separate numerical results are shown together by the plots in Fig. 5-3. Each curve represents the LOS error caused **solely by a single mode** while the mode was being excited by the rapid slew maneuver. The table below lists the highest peak value of the each curve.

Mode:	1	2	3	4	5	6	7	8	9	10
Peak:	3.26	88.6	9.57	6.53	0.33	.036	.077	.002	.004	.0002

The relative importance of the 10 modes is thus given by the following descending order:

Mode: 2, 3, 4, 1, 5, 7, 6,...

An inspection of this ranking and the peak values will show that a significant break between the fourth- and fifth-ranked modes (i.e., modes 1 and 5, respectively). We thus selected the four top-ranked modes, i.e., modes 2, 3, 1, and 4, as the **primary candidates** for modeled modes.

Mode 5 is marginally important compared to other modes, but is the fifth in the rank and has a much higher value than the remainder. We therefore considered it to be a **secondary candidate** for modeled modes.

Mode 1 could have been ranked higher than Mode 4 if the time average were used instead. This would make no significant difference, however, since both were among the top four modes anyway, and these four had all been selected to be primary candidates for modeled modes.

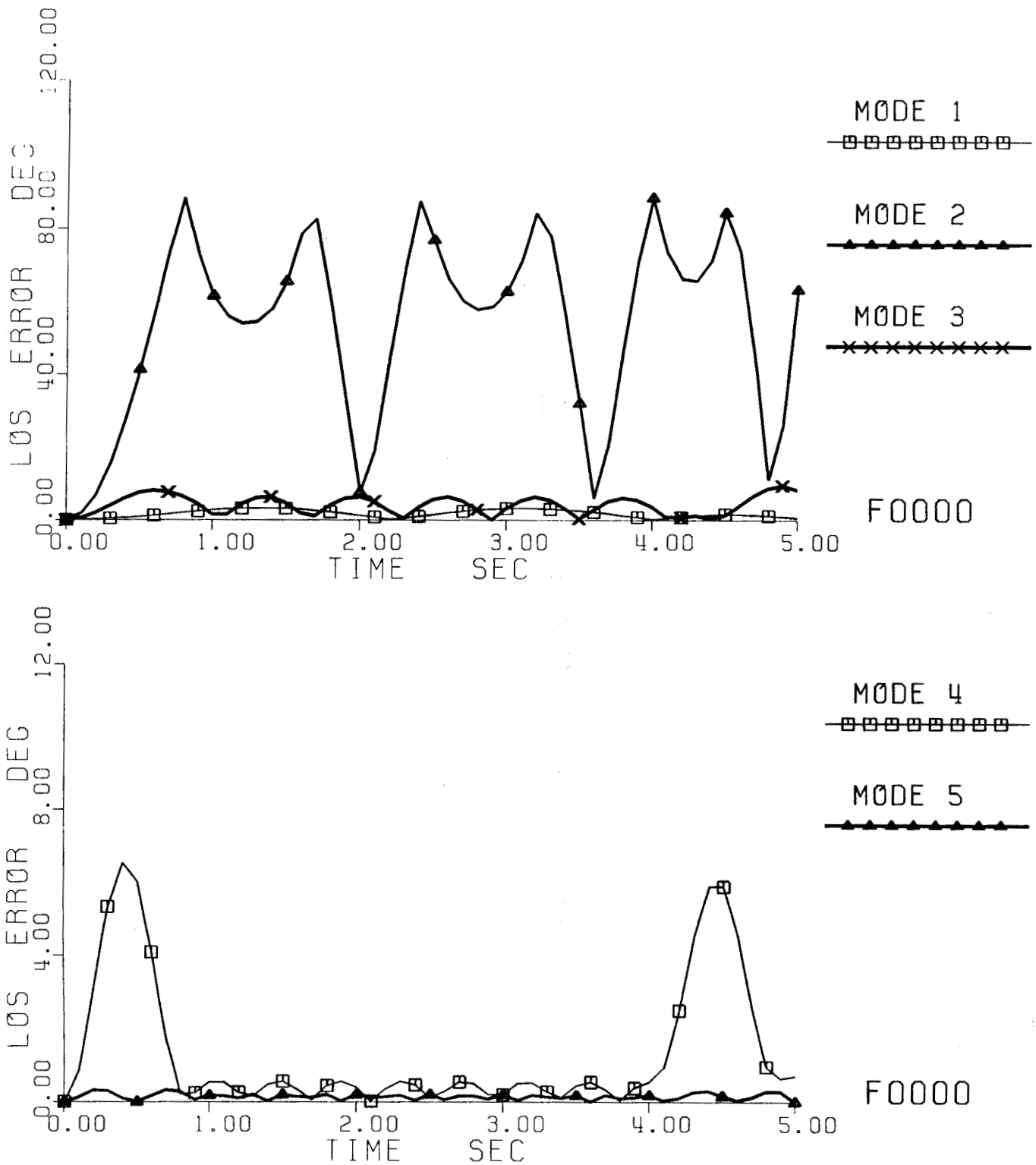

Fig. 5-3 Line-of-sight error caused by a single mode alone while the mode was being excited by the pointing maneuver. The separate time histories are plotted together for easy comparison and use with Measure 3.

a. Modes 1, 2, 3, 4, and 5.

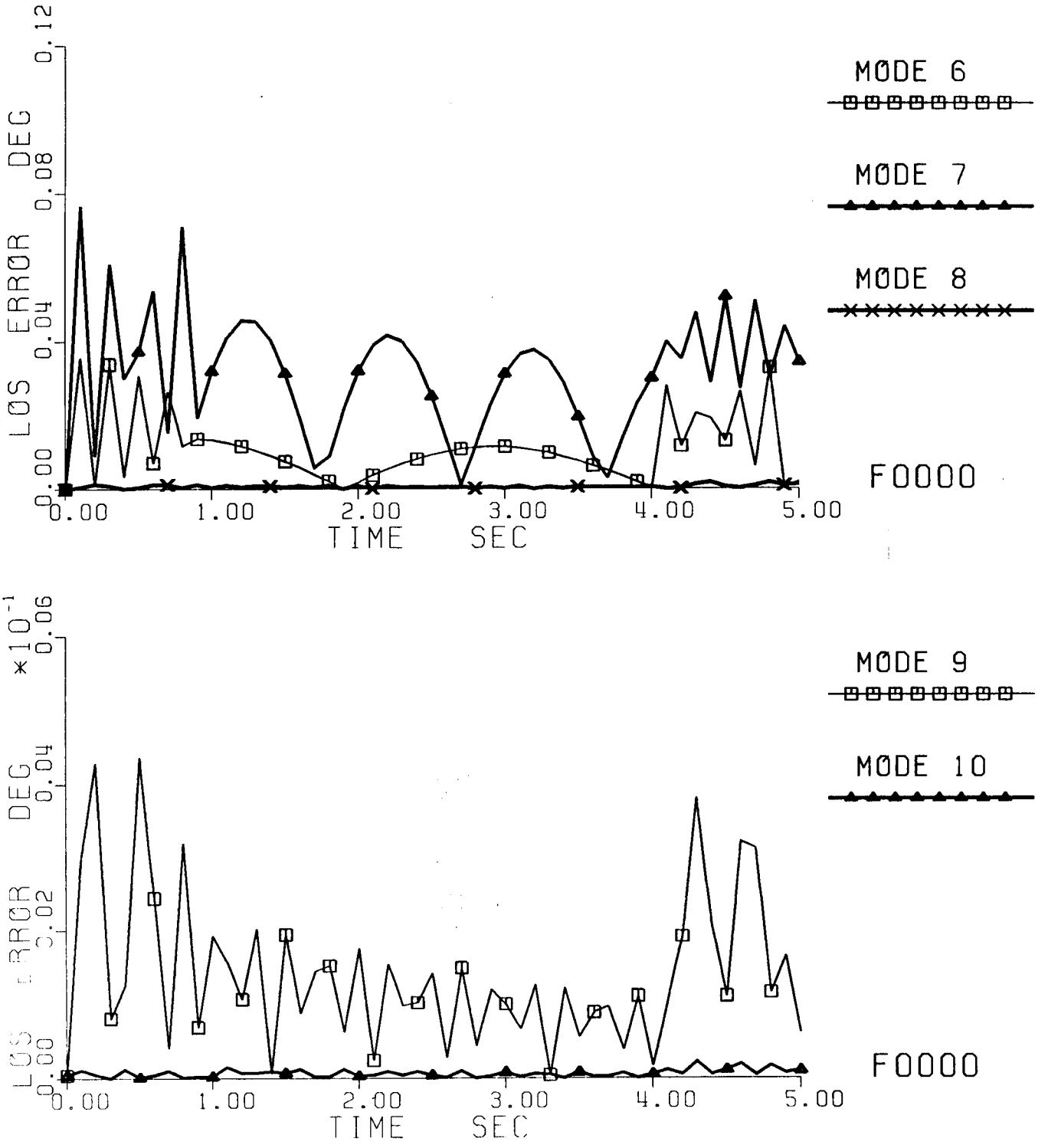

Fig. 5-3 Line-of-sight error caused by a single mode alone while the mode was being excited by the pointing maneuver. The separate time histories are plotted together for easy comparison and use with Measure 3.

b. Modes 6, 7, 8, 9, and 10.

5.2 Analysis on Modal Control Influences of Actuators

We recently discovered that the high-gain problem Canavin encountered in his first modal dashpot design [11] would not have existed if he had paid attention to the ill conditioning of the coefficient matrix $\Phi_M{}^T B_F$ he used in his numerical example. Among the 12 "controlled modes" he selected to form his reduced-order design model, several have very little control influences from the 32 actuators he used on the structure*. It is intuitively apparent that actuators having smaller influences on a given mode are less effective in controlling the mode, and thus require to be compensated with larger gains. Mathematically speaking, when the smallest "singular value" of the coefficient matrix $\Phi_M{}^T B_F$ is one order of magnitude smaller, the largest singular value of the resulting gain matrix G* as a solution of Eq. (4-7) generally is two orders of magnitude larger. This means that **not all his "controlled" modes should be included** in the modal-dashpot design without any discrimination against excessively small control influences by the actuators. In other words, all the available actuators need **not be lumped together to control all his "controlled" modes through one large feedback gain matrix.**

To make an effective design for the SCOLE configuration, we analyzed the control influences of the actuators first and match those modes in need of active control with the right actuators.

For evaluating and comparing their modal influences properly, we grouped the actuators according to their location on the SCOLE configuration as well as their type. As a result, the actuators** were divided into the following four different groups:

Group 1: Actuators 1 to 3, for applying moments on the Shuttle about its body x, y, and z axes, respectively;

Group 2: Actuators 4 to 6, for applying moments on the Reflector about its body x, y, and z axes, respectively;

Group 3: Actuators 7 and 8, for applying forces at the Reflector mass center in the x and y directions, respectively;

Group 4: Actuators 9 to 12, for applying forces at two specific points on the Mast beam in the x and y directions, respectively.

The control influences on each mode, say mode i, from all the actuators in a specific group can be summarized by calculating their RMS (Root-Mean-Square) value

$$\sqrt{\left[(\phi_i^T b_{F1})^2 + (\phi_i^T b_{F2})^2 \ \ldots \ + (\phi_i^T b_{Fk})^2\right]/k}$$

over the group. Listed in Table 5-1 are these RMS values in the descending order.

---

* The antenna-like structure consisted of a large dish in the forward section and a gimbaled equipment section to the aft. It had 32 member dampers (as the co-located actuators and rate sensors). Its finite-element model has 35 degrees of freedom.

Table 5-1 RMS Actuator Influences on first 10 Modes

Mode	Group 1 Act. 1 - 3	Mode	Group 2 Act. 4 - 6	Mode	Group 3 Act. 7 - 8	Mode	Group 4 Act. 9 - 12
2	0.30019961E-02	5	0.36487188E-01	2	0.14311218E+01	2	0.10711402E+00
4	0.41220308E-03	4	0.25172627E-01	1	0.14061384E+01	1	0.10338868E+00
1	0.40146321E-03	3	0.15999462E-01	3	0.81986851E+00	3	0.10171293E+00
3	0.19184369E-03	2	0.15595800E-01	4	0.39743480E+00	4	0.69439910E-01
5	0.11186474E-03	7	0.14711439E-01	7	0.30395976E+00	9	0.68373762E-01
6	0.69881789E-04	1	0.13037169E-01	9	0.25503686E+00	8	0.67025743E-01
7	0.36829457E-04	9	0.57048416E-02	6	0.21852742E+00	5	0.63191518E-01
8	0.26261532E-04	6	0.34139471E-02	8	0.14623879E+00	10	0.46103600E-01
9	0.15072107E-04	8	0.12352261E-02	10	0.10801539E+00	6	0.39935779E-01
10	0.13497747E-04	10	0.63637015E-03	5	0.74399590E-01	7	0.32263912E-01

Table 5-2 RMS Sensor Influences on first 10 Modes

Mode	Group 1 Sen. 1 - 3	Mode	Group 2 Sen. 4 - 6	Mode	Group 3 Sen. 7 - 8	Mode	Group 4 Sen. 9 - 12
2	0.28690067E-03	5	0.34890966E-02	2	0.13466856E+00	2	0.10711402E+00
4	0.39390128E-04	3	0.32387748E-02	1	0.12736945E+00	1	0.10338868E+00
1	0.39113598E-04	4	0.24055073E-02	3	0.12407852E+00	3	0.10171293E+00
3	0.18940789E-04	2	0.15346858E-02	4	0.38158901E-01	4	0.69439910E-01
5	0.10689848E-04	7	0.14879148E-02	7	0.36793593E-01	9	0.68373762E-01
6	0.66779044E-05	1	0.13531352E-02	9	0.30879460E-01	8	0.67025743E-01
7	0.35194691E-05	9	0.67911280E-03	6	0.20832075E-01	5	0.63191518E-01
8	0.25095521E-05	6	0.32624099E-03	8	0.14005536E-01	10	0.46103600E-01
9	0.14402938E-05	8	0.11804001E-03	10	0.10299906E-01	6	0.39935779E-01
10	0.12898448E-05	10	0.60812166E-04	5	0.90737212E-02	7	0.32263912E-01

Observe that Actuators 1 to 3 (Group 1) have an RMS value for Mode 2 that is one order of magnitude higher than all other modes, and hence are most effective in controlling Mode 2 than controlling other modes. Observe also that Mode 2 ranked the highest in RMS value with respect to Group-3 actuators 7 and 8. In addition, this RMS value is two orders of magnitude higher than that with Actuators 1 to 3. Consequently, Actuators 7 and 8 should be more effective for controlling mode 2 and require much smaller feedback gains. Note that Actuators 9 to 12 (Group 4) are less effective than Actuators 7 and 8 in controlling Mode 2.

With a similar argument, Actuators 7 and 8 are also most effective in controlling Mode 1. Therefore, **Modes 1 and 2** and no more others should be selected as the "modeled modes" in the design of the modal dashpots using **Actuators 7 and 8.**

Since Mode 3 is a torsion mode and is more appropriate to be controlled by moments than forces. The RMS values clearly suggest that Actuators 4 to 6 (Group 3) will be more effective than Actuators 1 to 3 for controlling Mode 3. Although among the four groups, Actuators 9 to 12 did have the highest RMS values of control influences on Mode 3, we did not expect the proof-mass actu-

ators (9 to 12) to be capable of suppressing large torsional vibrations of any mode in such a very short time.

The RMS control influence on Mode 4 is larger from Actuators 4 to 6 than from Actuators 1 to 3. Consequently, both **Modes 3 and 4** should be selected as the "modeled modes" in the design of modal dashpots using **Actuators 4 to 6.**

All the four primary condidates have been selected as the "modeled modes" for the appropriate matching groups of actuators. A review of Table 5-1 will show that Mode 5, the secondary candidate, has a higher RMS value of control influences from the same Group 2 of actuators than both Modes 3 and 4. According to a previous study by Lin and Jasper [24], such a situation would result in large spillover of Mode 5, severe dynamic interactions of modeled modes with unmodeled modes, and significant degradation of damping performance if Mode 5 were not **also modeled with Modes 3 and 4** for control by **Actuators 4 to 6.**

To summarize, this analysis shows applying moments and forces at the Reflector end of the Mast beam will be more effective in controlling the excited vibrations in SCOLE (and particularly Modes 1 to 5) than at the Shuttle end or at the intermediate points of the flexible mast. Instead of lumping up all candidate modes (1 to 5) to be controlled by Actuators 4 to 8 together, the designer for modal dashpots should match these modes with their most effective or most appropriate actuators. Specifically, Modes 1 and 2 should be controlled by Actuators 7 and 8 and Modes 3 to 5 by Actuators 4 to 6.

There is no need to include more modes to each group since there are enough actuators to be distributed among all the 5 most important modes of the SCOLE flexible-body dynamics. Including more modes may not always help: it might simply increase the magnitude of the feedback gains without any real benefit, particularly when the additional modes are of significantly smaller control influences by the actuators; the increased feedback gains might instead amplify various adverse effects of control spillover and system noises.

5.3 Design of Modal Dashpot MD1

The modal dashpot MD1 was designed for SCOLE for quick suppression of the excessive vibrations excited by the rapid BPB LOS pointing slew maneuver. It is composed of two parts. Part 1 is for applying forces at the Reflector mass center in the two transverse directions using a feedback of linear velocities at the Reflector end of the beam. Part 2 is for applying moments also at the Reflector about the three body axes but using a feedback of angular velocities instead.

The location of these actuators are the same as specified by Taylor in Ref. 1 for the control forces and moments at the Reflector. The sensors were located where the "outputs" of Dr. Joshi's modal data set D3D585 had been calculated. Some of the control inputs (u_i) and observation outputs (y_j) were relabeled for technical convenience. Sensors 1 to 8 are not really co-located with the correspopnding actuators, but note that their RMS values of modal observation influences (Table 5-2) exhibit **virtually the same patterns** as those of modal control influences (Table 5-1).

5.3.1 Part 1: Linear Velocity Feedback Force Control

Two force actuators (or equivalently, a single force actuator capable of delivering separate forces in two independent axes) are assumed to be placed at the center of the Reflector. The force inputs* u_7 and u_8 (in the x and y directions, respectively) are each limited to 800 lb as specified. Two linear velocity sensors (or equivalently a single velocity sensors capable of measuring the rate of linear displacements in two independent axes) are assumed to be located at the Reflector end of the mast beam. The sensor outputs** y_{15} and y_{16} (in the x and y directions, respectively) represent the time rate of deflection of the Mast beam at the Reflector end relative to the Shuttle end. Note that these sensors are only **approximately co-located** with actuators: they are apart by 18.75 ft and 32.5 ft in x and y directions, respectively, whereas the beam is 130 ft long.

The design problem is thus to determine a 2x2 gain matrix G_{LVR} for the following linear velocity feedback control law

$$\begin{bmatrix} u_7 \\ u_8 \end{bmatrix} = -G_{LVR} \begin{bmatrix} y_{15} \\ y_{16} \end{bmatrix} \tag{5-1}$$

The foregoing analysis of the control influences has suggested that only Modes 1 and 2 be selected as the "modeled modes" for this part of design. Accordingly, the control and observation influence matrices $\Phi_M{}^T B_F$ and $C_V \Phi_M$ on the two modeled modes to be used in the modal dashpot design equation (4-8) have the following numerical values:

$$\Phi_M^T B_F = \begin{bmatrix} .19875923E+01 & .62669927E-01 \\ .14599262E+00 & -.20186396E+01 \end{bmatrix} \tag{5-2a}$$

$$C_V \Phi_M = \begin{bmatrix} .18012760E+00 & .21140305E-01 \\ .55188192E-04 & -.18927317E+00 \end{bmatrix} \tag{5-2b}$$

Before solving the corresponding design equation (4-8) for a specific gain matrix, we must specify the desired value for the additional damping matrix Δ_M^*. For technical simplicity, we choose it to be diagonal, so that its diagonal elements† δ_{M1}^* and δ_{M2}^* can be used rather directly for guiding the modal-dashpot design. Since both modes 1 and 2 substantially dominate the vibratory response of the SCOLE configuration to the BPB pointing maneuver, we wish to augment each with active damping as close to 70.7% †† of critical damping as

---

* These correspond to $u_4 = F_{rx}$ and $u_5 = F_{ry}$, respectively, in Dr. Joshi's notation.

** These are indirectly equal to the derivatives of the deflections $y_7 = \xi_x$ and $y_8 = \xi_y$ in Dr. Joshi's notation.

† These terms represent the additional damping coefficients in the corresponding decoupled equations of motion; see Eqs. (4-14)-(4-15). In multivariable root-locus analysis, these values also represent the "rate of departure" from the open-loop poles when the feedback loops are closed.

†† 70.7% is an optimal value in the sense that the second-order system corresponding to the single mode will neither be too sluggish nor have a large overshoot.

possible. Let us attempt a theoretical 2% settling time of 3 seconds for Mode 2 in estimating the desirable additional damping coefficient δ_2^*. The corresponding time constant is 3/4 sec; thus by definition

$$\bar{\zeta}_2 \omega_2 = 4/3$$

where $\bar{\zeta}_2$ denotes the closed-loop damping ratio desirable of Mode 2. Substituting in the natural frequency $\omega_2 = 1.97024$ rad/sec yields

$$\bar{\zeta}_2 = 0.6767,$$

which is acceptably close to the optimal value. Whence, the closed-loop damping coefficient desirable of Mode 2 is given by

$$\bar{\delta}_2 = 2\ \bar{\zeta}_2\ \omega_2 = 8/3.$$

Since an inherent damping of 0.3% has been specified in the data set "D3D585" for each mode, the desirable additional damping coefficient# desirable of Mode 2 is

$$\delta_2^* = \bar{\delta}_2 - 2\ \zeta_2\ \omega_2 = 8/3 - 2 \times 0.003 \times 1.97024 = 2.6548$$

Next, we choose the additional damping desirable of Mode 1 to be 60%, i.e., $\zeta_1^* = 0.6$, since Mode 1 has a smaller magnitude of vibration than Mode 2.

In summary, the desired damping coefficients as in Eqs. (4-14)-(4-15) for the two modeled modes are then readily given as

$$\delta_{M1}^* = \delta_1^* = 2\ \zeta_1^*\ \omega_1 = 2 \times 0.6 \times 1.7470 = 2.0964 \qquad (5\text{-}3a)$$

$$\delta_{M2}^* = \delta_2^* = 2.6548. \qquad (5\text{-}3b)$$

Now the feedback gain matrix G_{LVR} is readily obtained from solving (4-8) as

$$G_{LVR} = \begin{bmatrix} .58420630E+01 & .43392044E+00 \\ .42038249E+00 & .69796355E+01 \end{bmatrix} \qquad (5\text{-}4)$$

5.3.2 Part 2: Angular Velocity Feedback Moment Control

Three torquers (or equivalently, a single torquer capable of delivering separate touques about three independent axes) are assumed to be located on the Reflector. The torque inputs* u_4, u_5, and u_6 (about the x, y, and z axes, respectively) are each limited to 10,000 lb-ft as specified. Three angular velocity sensors (or equivalently a single sensor capable of measuring separately the rate of rotations about three different axes) are assumed to be located at the Reflector end. The sensor outputs** y_{10}, y_{11}, and y_{12} (about the x, y, and z axes, respectively) represent the time rate of rotations of the

---

The corresponding additional damping ratio ζ_2^* for Mode 2 is 0.6737. A few slightly modified values were also tried when the design of this part was repeated (see Section 6.2).

* These correspond to Dr. Joshi's $u_6 = T_{rx}$, $u_7 = T_{ry}$, and $u_8 = T_{rz}$, respectively.

** These correspond to Dr. Joshi's $y_{12} = \dot{\phi}_r$, $y_{13} = \dot{\theta}_r$, and $y_{14} = \dot{\psi}_r$, respectively.

Reflector end of the mast due to bending and torsion. Again, these sensors are **only approximately co-located** with the actuators. Note that the Reflector itself is a rigid body.

The design problem is to find a 3x3 gain matrix G_{AVR} for the following angular velocity feedback control law

$$\begin{bmatrix} u_4 \\ u_5 \\ u_6 \end{bmatrix} = -G_{AVR} \begin{bmatrix} y_{10} \\ y_{11} \\ y_{12} \end{bmatrix} \tag{5-5}$$

Similarly, as suggested by the previous analysis on control influences, we choose Modes 3, 4, and 5 to be the "modeled modes" for this part of the design. Accordingly, the specific control and observation influence matrices are given by

$$\Phi_M^T B_F = \begin{bmatrix} .10761780E-01 & -.18101653E-01 & -.18012847E-01 \\ .37541741E-01 & .22172032E-01 & .45802862E-04 \\ -.31739483E-01 & .54643290E-01 & .81303515E-03 \end{bmatrix} \tag{5-6a}$$

$$C_V \Phi_M = \begin{bmatrix} .10592386E-02 & .35194610E-02 & -.30149737E-02 \\ -.17367745E-02 & .21135667E-02 & .52175940E-02 \\ -.52450669E-02 & .13325330E-04 & .23641118E-03 \end{bmatrix} \tag{5-6b}$$

Since the vibratory responses of Modes 3, 4, and 5 are much smaller in magnitude than those of Modes 1 and 2, it is reasonable to augment them with only a relatively small amount of active damping. We chose rather arbitrarily 3% of critical damping for each. The diagonal elements of the desired additional damping matrix Δ_M are then given as follows:

$$\delta_{M1}^* = \delta_3^* = 2 \times 0.03 \times \omega_3 = 0.3065 \tag{5-7a}$$

$$\delta_{M2}^* = \delta_4^* = 2 \times 0.03 \times \omega_4 = 0.4470 \tag{5-7b}$$

$$\delta_{M3}^* = \delta_5^* = 2 \times 0.03 \times \omega_4 = 0.7742 \tag{5-7c}$$

Substituting (5-5)-(5-7) in Eq. (4-8) and solving the resulting equation, we get the following gain matrix

$$G_{AVR} = \begin{bmatrix} .24172707E+04 & .16653096E+03 & .45158162E+03 \\ .15734103E+03 & .21781213E+04 & -.72768193E+03 \\ .13433660E+04 & -.22055215E+04 & .42951681E+04 \end{bmatrix} \tag{5-8}$$

6. PERFORMANCE OF VIBRATION CONTROL DESIGNS ON SCOLE

To evaluate the vibration control performance of the modal dashpot design MD1, we incorporate the two feedback laws (5-1) and (5-5) into the same SCOLE flexible-body dynamic model as was used in simulating its vibratory responses to the BPB pointing maneuver. As stated in the beginning of Section 3, the undeformed SCOLE configuration was assumed to have been aligned with the specific attitude of zero LOS error. Thus, the velocity-sensor outputs would contain only the flexible-body rates*, just as desired for feedback control of the excited vibrations. Recall that the model is of the "full order" in the sense that it includes all the ten modes as provided in the data set D3D585. In order that the control moments and forces do not exceed their specified limits, the computer program also simulates the saturation of the actuators at their respective limits. For example, if at any time the feedback control input, say, u_8 would command the actuator to exert more than 800 lb force to the Reflector, the actual force applied would be only 800 lb maximum.

The feedback control consisting of the two parts of modal dashpot MD1 is turned on **right after** the completion of the BPB pointing maneuver. Thus the terminal state of the SCOLE vibrations (i.e., the LOS error, the deflection and its rate of change, the angular displacement and its rate, modal displacements and velocities,...) at the end of the maneuver become the **initial conditions** of the feedback controlled system. The vibration control is applied for five seconds, which is about the same duration as of the pointing maneuver. We intentionally use such a rather "long" period in order to check if instability in the closed-loop system might start to develop after the excessive vibrations has been rapidly forcefully suppressed. Various versions of the modal dashpot design MD1 (each with a slightly different value for the additional damping coefficient δ_2*) were evaluated. Reported below are two representative cases.

6.1 Simulation Results of Modal Dashpot Design MD1

The specific values of the gain matrices G_{LVR} given by (5-4) and G_{AVR} given by (5-8) were incorporated with the control laws (5-1) and (5-5) respectively in the full-order dynamic simulation. The simulation results are summarized by time-history plots in Fig. 6-1.

The history of the applied moments and forces (Fig. 6-1a) shows that the applied moment about each axis never exceeded the limit of 10,000 lb-ft, nor did the applied force in each direction exceed the limit of 800 lb. Large moments and forces were needed only during the early portion of the control period, but did not exceed the limits because of "saturation". All the applied forces and moments quickly reduced to minimum automatically because the sensed rates of vibrations rapidly became insignificant.

Fig. 6-1b shows that the LOS error was rapidly subdued to 11.79° from 71.43° where the pointing maneuver ended. Note that the initial LOS error continued to rise to 85.29° (or 115.13° = 180° - 64.87° if not taking the principal

---

* If the configuration had not been so aligned, then rigid-body rate would also be present and some filtering or signal processing might be required. Alternatively, one could use relative sensors instead of inertially referenced sensors.

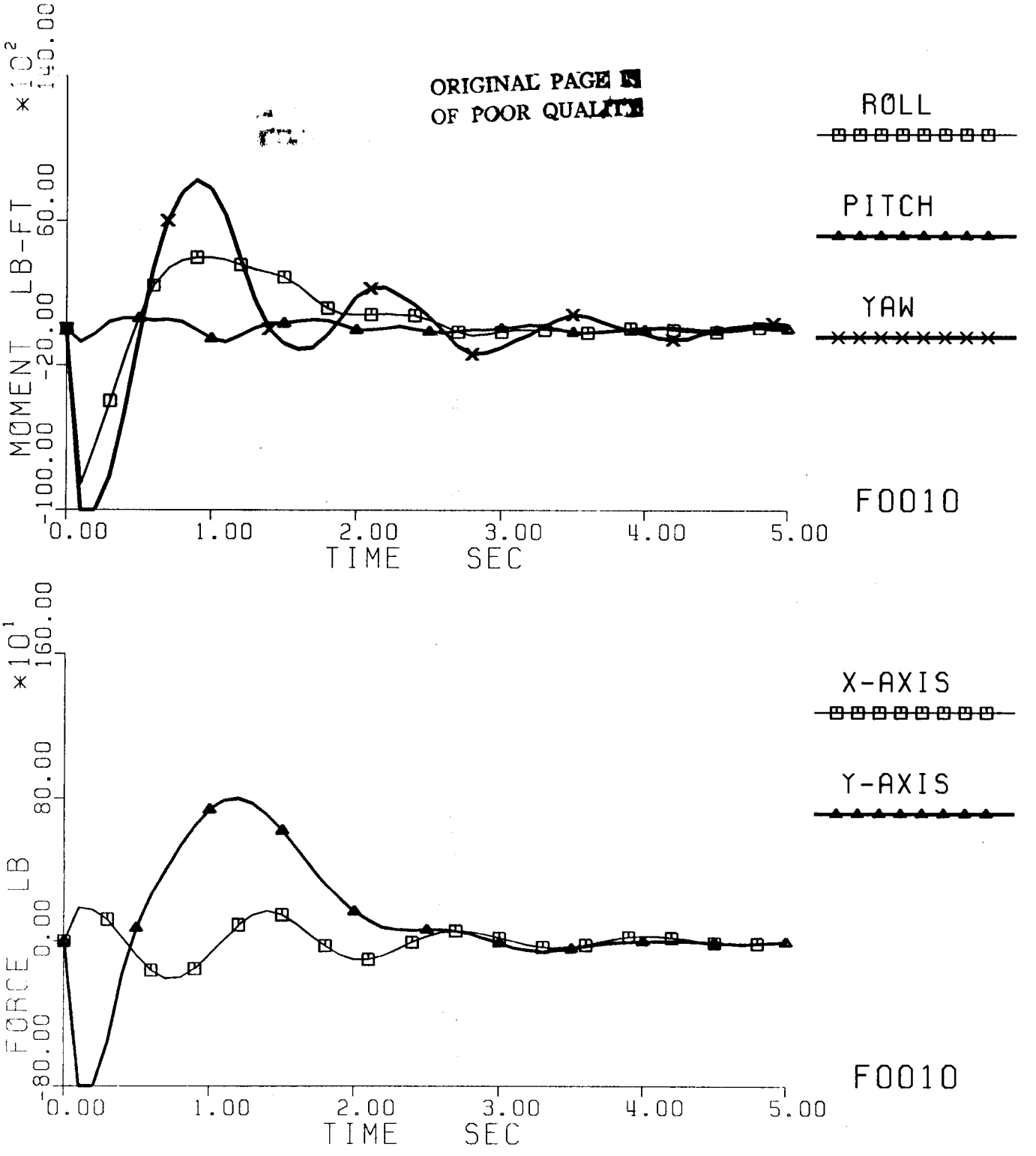

Fig. 6-1 Simulation results of vibration control design MD1;
a. Histories of applied moments and forces at the Reflector.

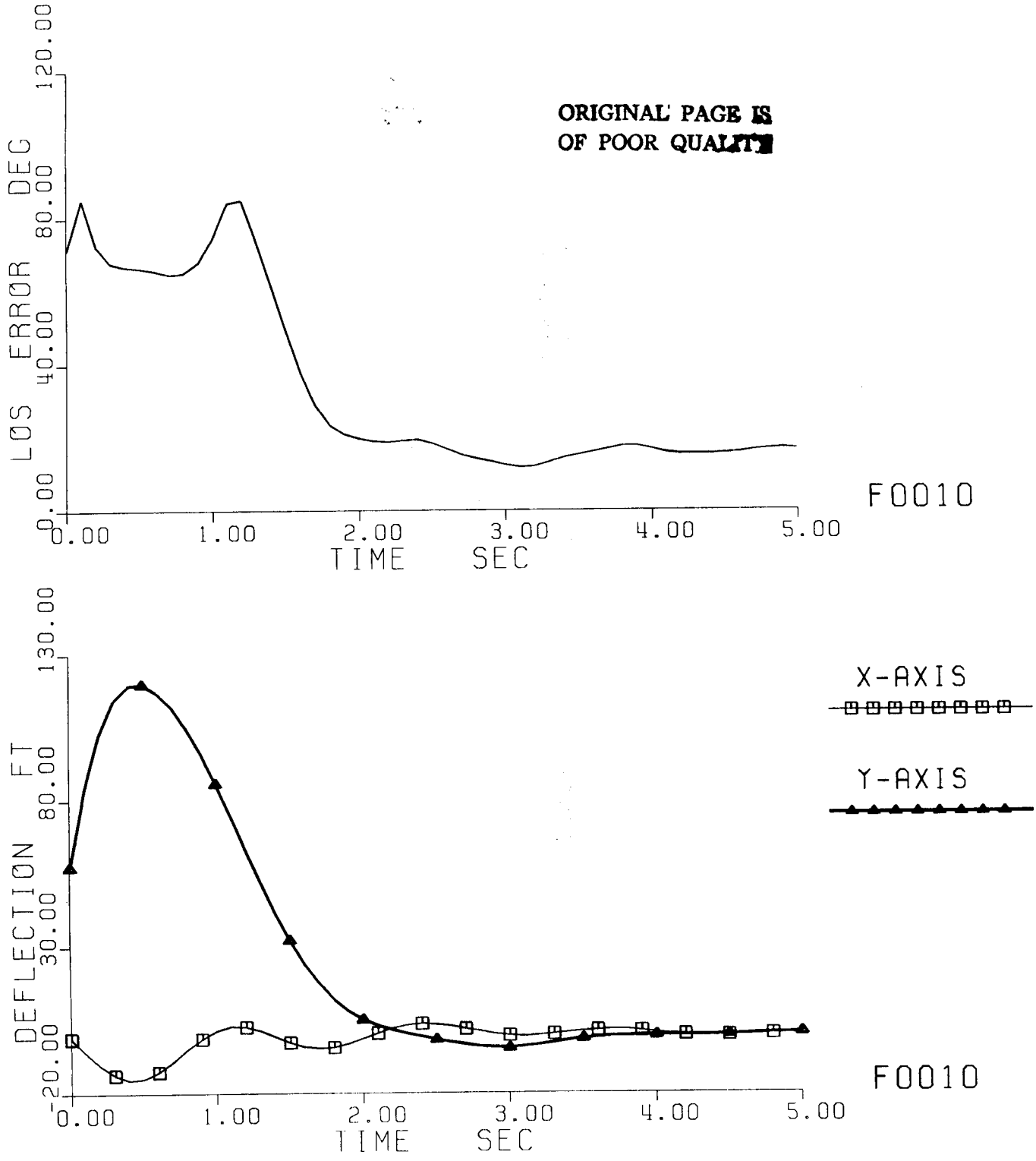

Fig. 6-1 Simulation results of vibration control design MD1;
b. Histories of line-of-sight error and Mast tip deflection.

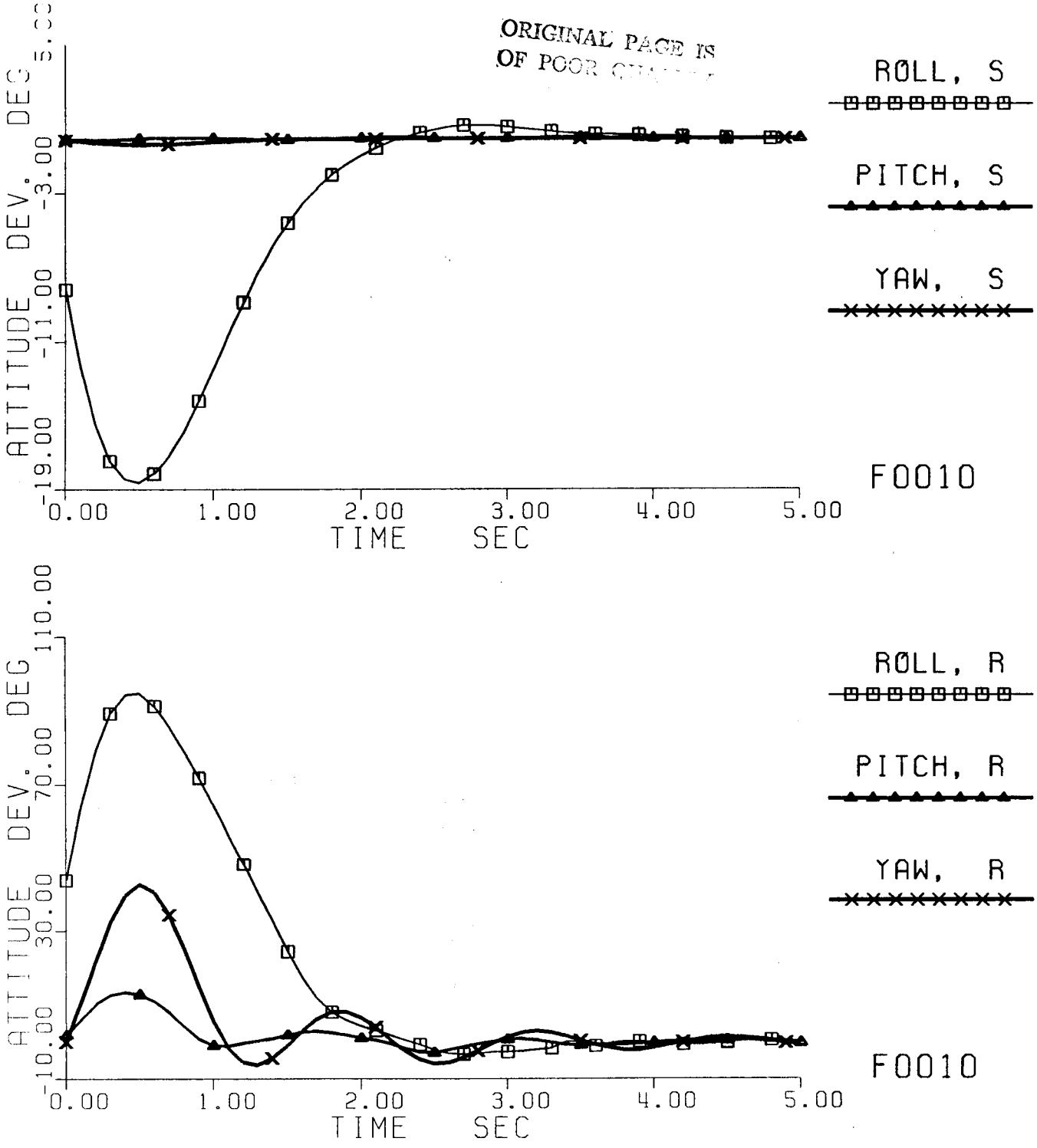

Fig. 6-1 Simulation results of vibration control design MD1;
c. Histories of attitude deviations at Shuttle (S) and Reflector (R) ends

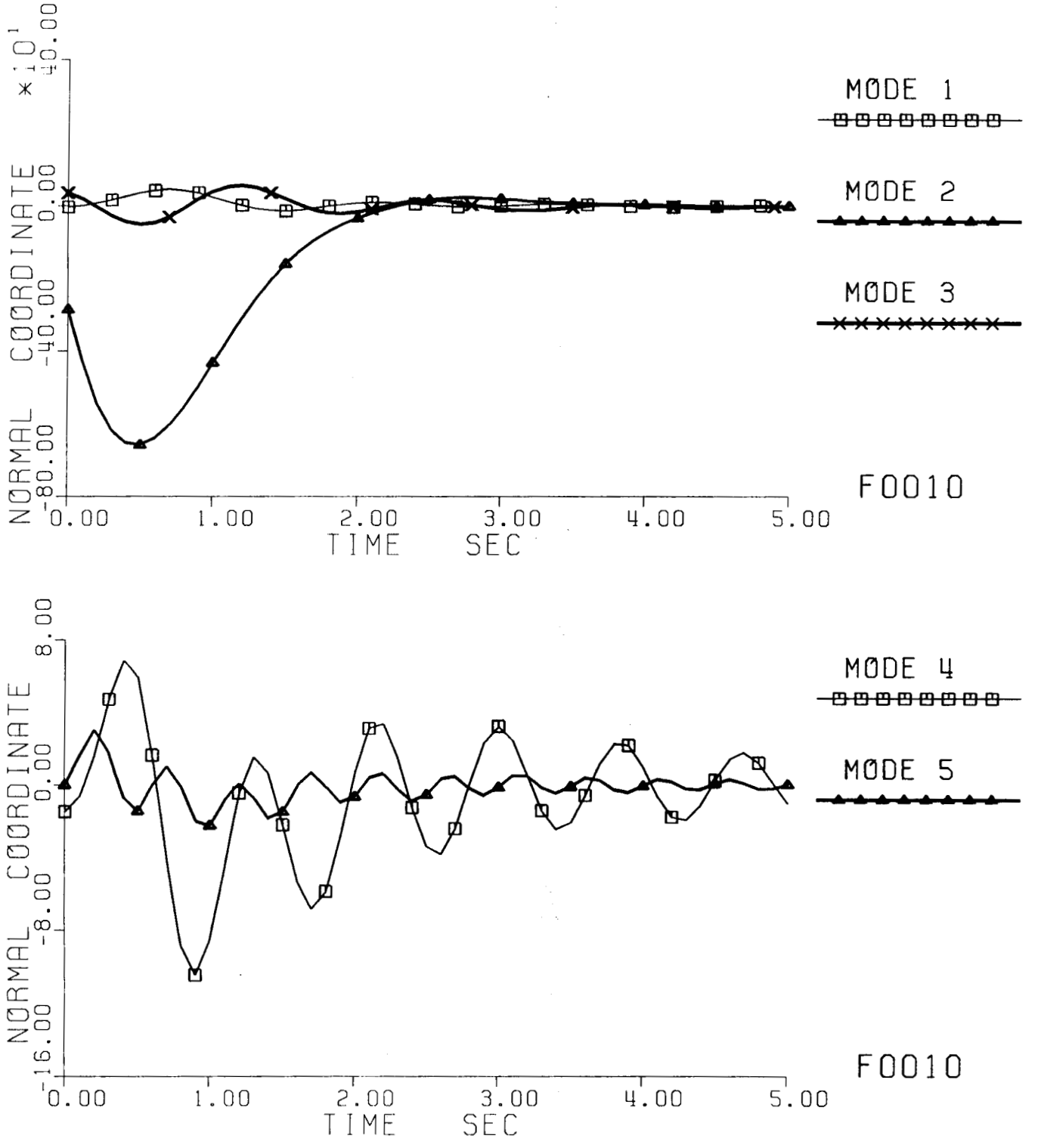

Fig. 6-1 Simulation results of vibration control design MD1;
d. Histories of normal coordinates of the 10 modes.

value of the arcsine function) because of its large rate of change at the very instant of switching from pointing maneuver to vibration control. Nevertheless, the LOS error was suppressed down within **18.46° after only 2.5 sec** of active vibration control and remained below 17.54° thereafter. Moreover, it was even reduced to 11.79° in 3.1 sec.

The bending of the mast beam was very rapidly suppressed to virtually null. Observe in particular that even the y-directionally deflection at the Reflector end (i.e., y_{14}) continued to increase to 119.7 ft (again because of the large "initial" rate of change), it was suppressed **down into the band of ±5 ft in only 2 sec**, and into the band of ±0.5 ft in 4.2 sec. It is interesting to notice that it took less than 2.9 sec* to settle within 2.4 ft, 2% of the peak value. Recall that a 2% settling time of 3 sec for Mode 2 was used in the design.

Fig. 6-1c shows the rapid reduction of the initially large deviations in the Shuttle and Reflector attitude angles to zero in a very short time. The last peak diviation of the Reflector roll, pitch and yaw attitude angles is **only 0.460°, 0.546° and 1.360°**, respectively.

Fig. 6-1d shows that the large-magnitude vibrations of first five modes all were rapidly suppressed to virtually zero in a very short time. Note in particular that this vibration control was **very effective** for **quick** reduction of the **excessively large magnitude** of Mode 2. Observe, on the other hand, that Mode 5, the secondary candidate, was reduced only in a moderate rate by a moderate amount, but recall that it was not really significant at first place with respect to excitation by the BPB maneuver nor its contribution to the LOS error. Mode 5 did not need much active control anyway, and hence only a very small additional damping was designed for it.

The vibrations in other modes (i.e., Modes 6 to 10) remained virtually in the same insignificant levels as before, and hence their plots are omitted. Still their magnitudes were more or less decreased with time because of some concomitant additional damping as a side benefit of spillover.**

6.2 Simulation Results of A Modified Version of MD1A

We also tried a few other versions of the modal dashpot design MD1 by varying the additional damping coefficient δ_2* desired of Mode 2. Because of the saturation of the actuators at the imposed limits, it is reasonable to consider some smaller feedback gains. The following is a typical case.

---

* The peak occurred at t = 0.5 sec whereas the deflection was -2.24 ft at t = 3.4 sec.

** In the standard LQG design, one will generally try hard to reduce spillover because it has been well known to degrade performance and even to introduce closed-loop instability. With a modal-dashpot design, **spillover can be beneficial instead**, in leaking some active damping forces to unmodeled modes. Such is particularly the case when the design is not carefully focussed. The side benefit in our design was **intentionally minimized** because we tried to maximize our effort on the most important modes and matched them with most influential control actuators to minimize the leak.

This version, let us call it MD1A, is almost the same as before, except that the additional damping ratio ζ_2^* desired of Mode 2 was arbitrarily set equal to that of Mode 1; namely,

$$\zeta_2^* = \zeta_1^* = 0.60.$$

Therefore,

$$\delta_2^* = 2\ \zeta_2^*\ \omega_2 = 2 \times 0.6 \times 1.97024 = 2.36429 \qquad (6\text{-}1)$$

Mode 2 would then have a theoretical 2%-settling time of 3.38 sec.

Using the new value for δ_2^* in (5-3b), and repeating Part 1 of the modal dashpot design, the following new value of the feedback gain matrix was readily obtained.

$$G_{LVR} = \begin{bmatrix} .58420557E+01 & .45784262E+00 \\ .42061494E+00 & .62209375E+01 \end{bmatrix} \qquad (6\text{-}2)$$

The same simulation was then repeated with these new values. Results are summarized by the plots in Fig. 6-2. The applied moments and forces shown in Fig. 6-2a are virtually the same as before (Fig. 6-1a) with only some invisible differences. Some meaningful differences do exist in the histories of LOS error and beam deflection.

Observe that the LOS error (in Fig. 6-2b) quickly reduced to about 9.57° from the same initial value (71.43°). Similarly, due to large initial rate of change at the end of the pointing maneuver, the LOS error also continued to rise to 85.61° (or 180° - 64.81° = 115.19° if not taking the principal value of the arcsine). The large LOS error was suppressed **down to the level of 16.66° in 1.8 sec**, and remained under it thereafter. Moreover, it was reduced to 9.57° also 3.1 sec after the vibration control began.

The bending of the Mast was also suppressed down very rapidly. Though it continued to increase to 120.28 ft, the y-directionally deflection at the Reflector end (i.e., y_{14}) was suppressed **down into the band of ±7.35 ft in less than 1.8 sec.**, and into the band of ±0.75 ft in 3.7 sec. It took less than 3 sec for the large deflection to settle down to the band of 2% of the peak*, i.e., ±2.4 ft. Recall that 3.38 sec is the theoretical 2%-settling time used for Mode 2 in this modified design.

The histories of attitude changes (Fig. 6-2c) and modal responses (Fig. 6-2d) are again virtually the same as before (compared to Figs. 6-1c and 6-1d, respectively) with only some invisible or insignificant differences. The last peak deviation of the Reflector roll, pitch, and yaw attitude angles **is only 0.714°. 0.582°, and 1.399°**, respectively.

---

* The peak occurred at t = 0.5 sec., whereas the deflection was only -1.95 ft at t = 3.5 sec.

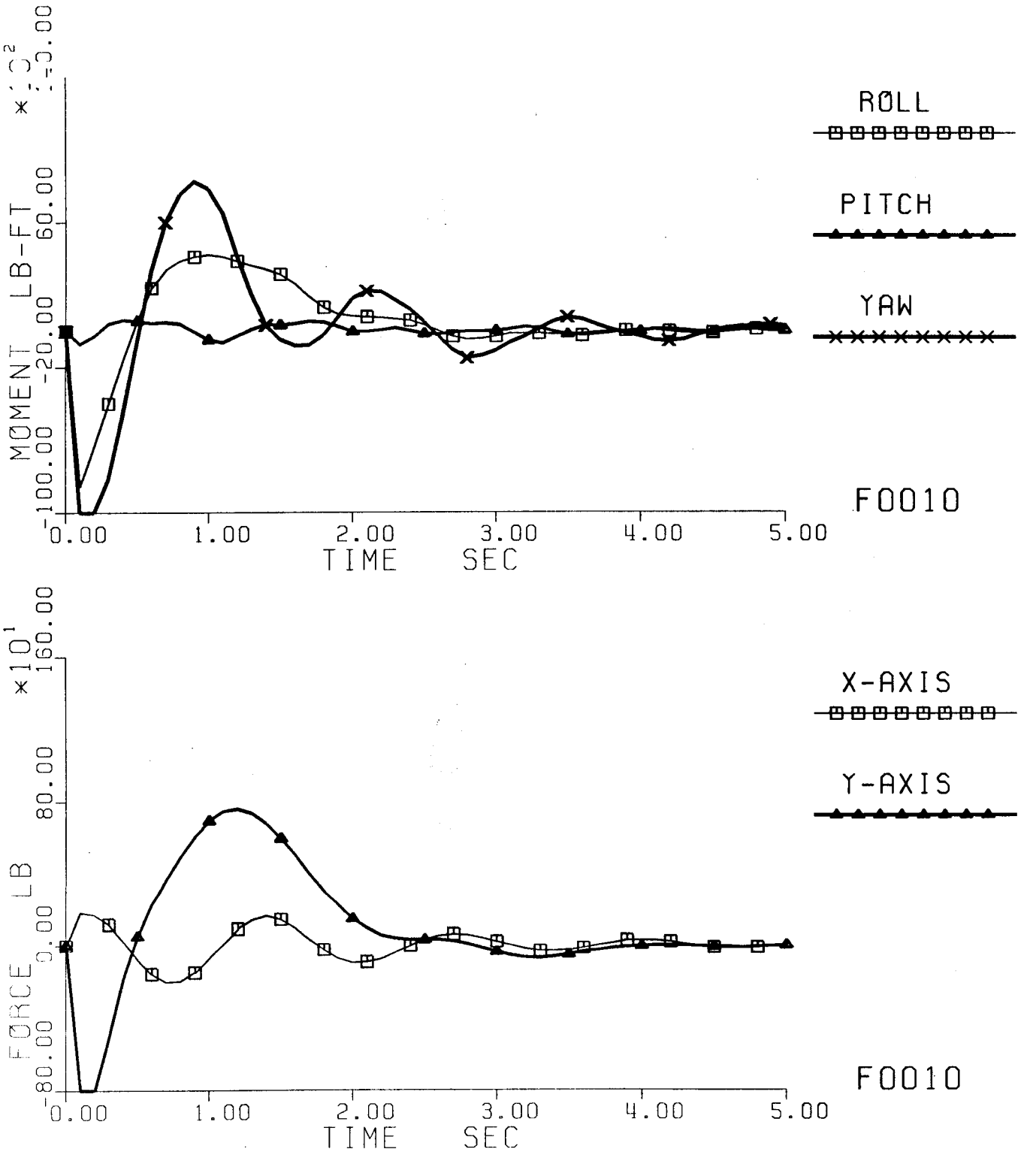

Fig. 6-2 Simulation results of vibration control design MD1A;
a. Histories of applied moments and forces at the Reflector.

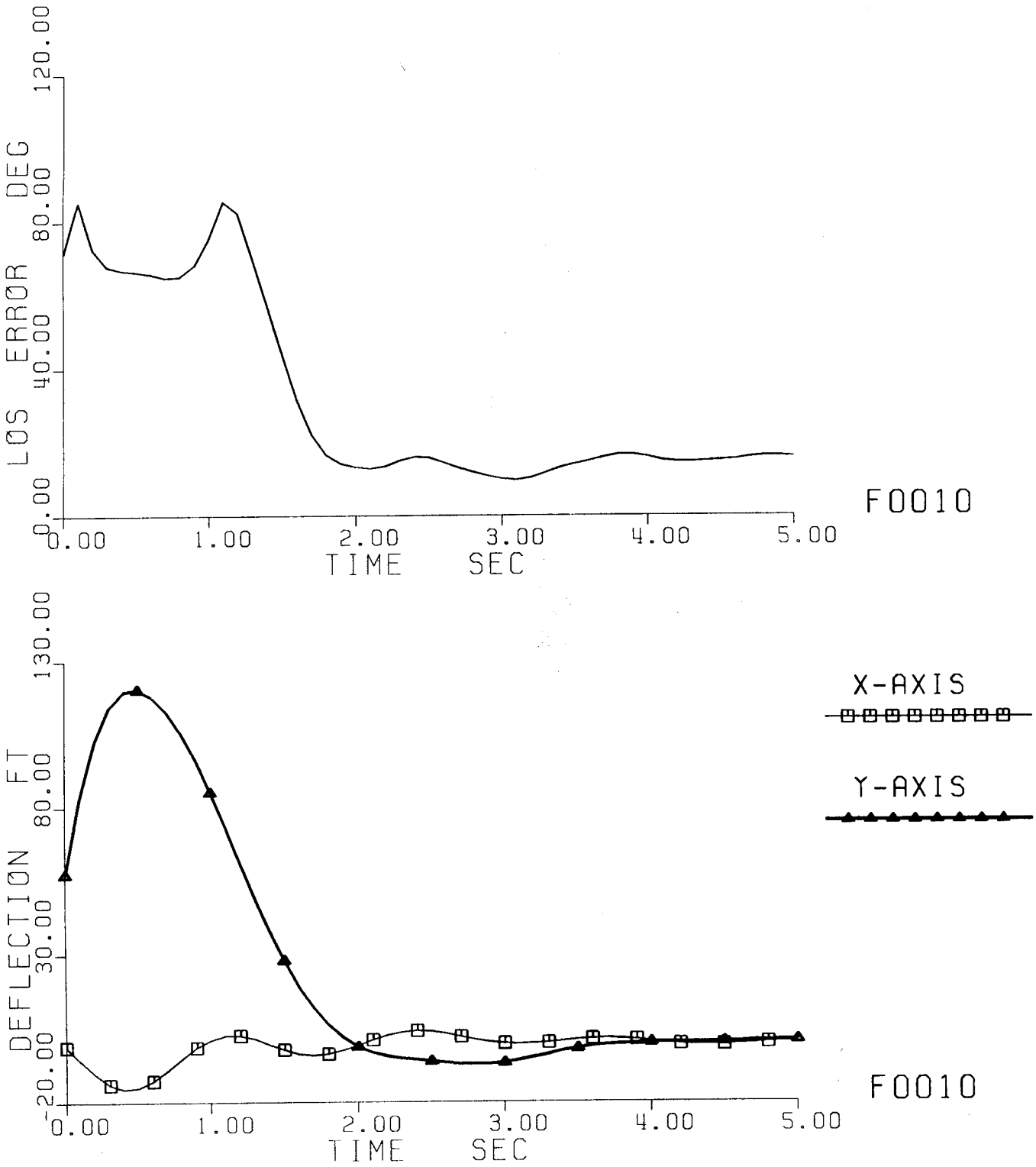

Fig. 6-2 Simulation results of vibration control design MD1A;
b. Histories of line-of-sight error and Mast tip deflection.

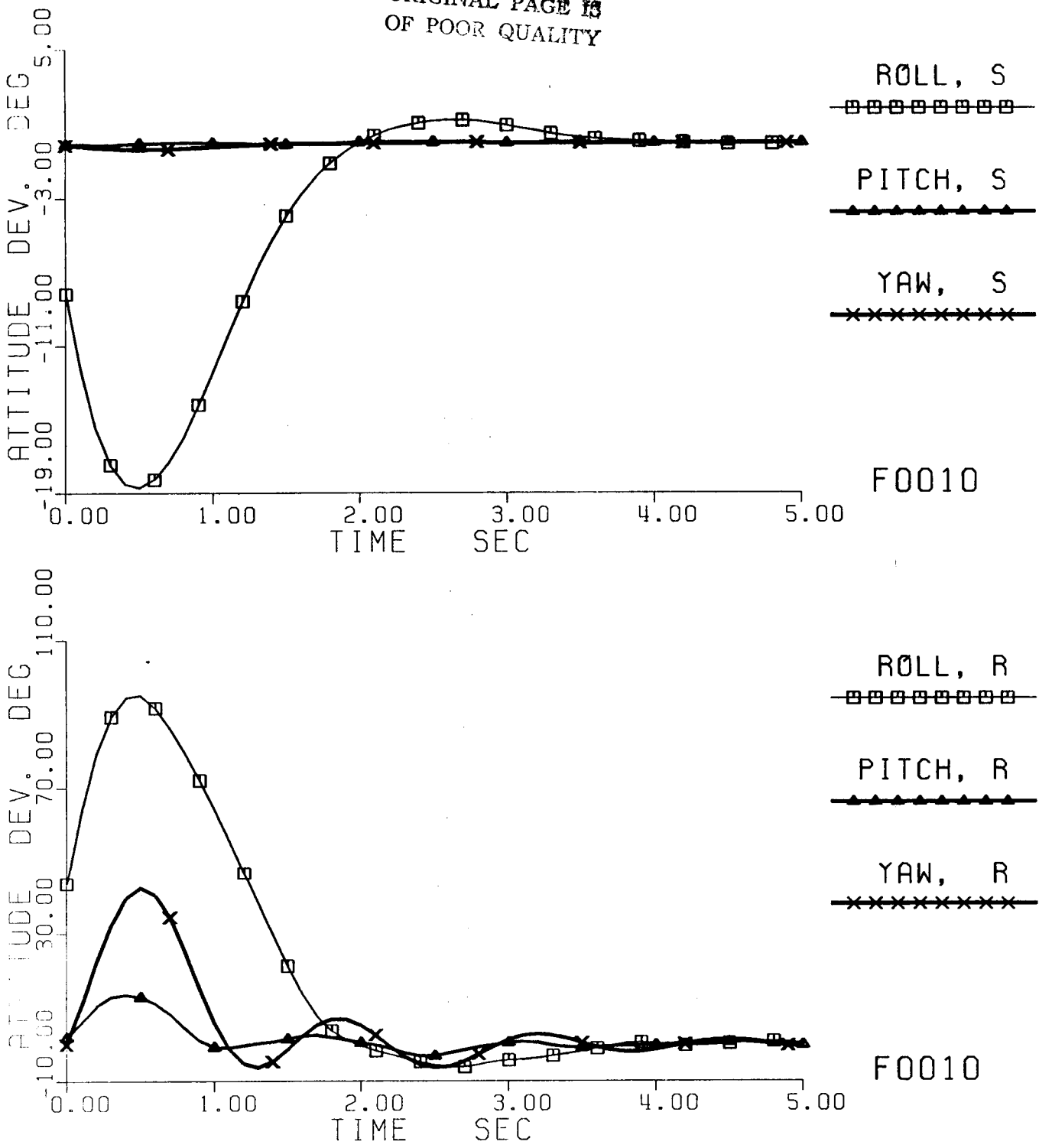

Fig. 6-2 Simulation results of vibration control design MD1A;
c. Histories of attitude deviations at Shuttle (S) and Reflector (R) ends

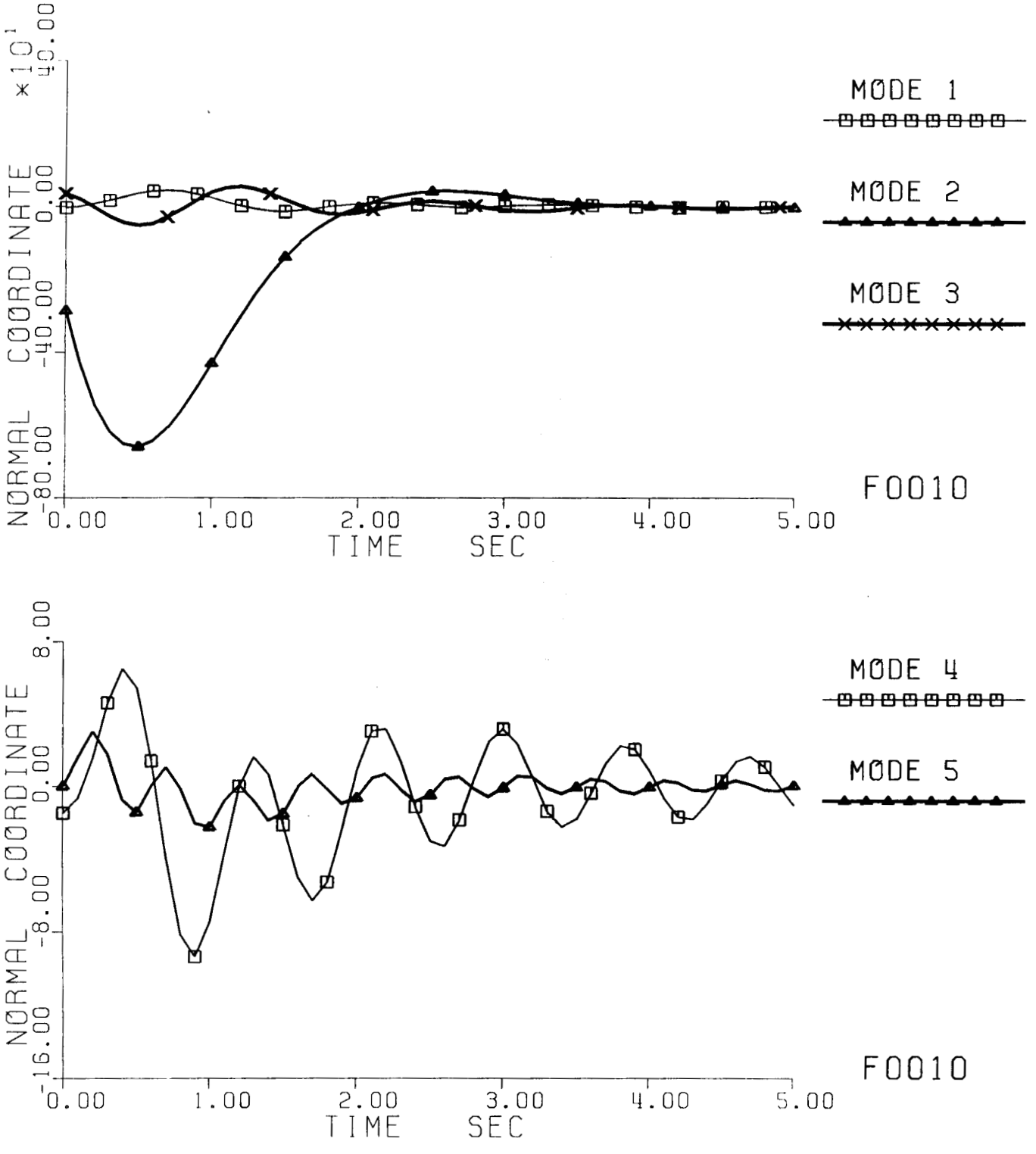

Fig. 6-2 Simulation results of vibration control design MD1A;
d. Histories of normal coordinates of the 10 modes.

6.3 Comments

6.3.1 The modal dashpot designs of vibration control **met the vibration control design challenges fairly well** and are effective and fast in suppressing excessive vibrations. Excited by BPB type rapid pointing slew maneuver, the flexible mast beam deflected between +114 ft and -113 ft, but such an excessive vibration was then quickly suppressed down to less than 0.75 ft in less than 3.7 sec after a modal-dashpot vibration control was turned on. The roll vibration of the Reflector between -86.96° and +88.35° during the maneuver was also quickly suppressed down to less than 0.72°. The large LOS error of 89.8° (or 133.3° if not taking the principal value of the arcsine) was also reduced quickly to less than 17.54°.

6.3.2 The original version of the modal dashpot design MD1 performed slightly better than the modified version MD1A in suppressing the deflection of the Mast beam and all the attitude deviations, but not so well in reducing the LOS error. The modified version used a slightly smaller additional damping ratio for Mode 2 in the design, i.e.,

$$\zeta_2^* = 0.60 \quad \text{instead of} \quad \zeta_2^* = 0.6737.$$

6.3.3 When a velocity feedback control, whether it is of the modal-dashpot type or not, is not properly designed, even feedback gains of an intermediate magnitude can cause severe interactions between modeled and unmodeled (or, equivelently, between "controlled" and "uncontrolled") modes, and hence badly degrade the desired performance of active damping augmentation [24]. The results of these two versions have shown, on the other hand, that if modal dashpots are properly designed, both the modal interactions and the performance degradation are not problems.

Thus, some of the additional damping can be as high as the optimal value 0.707 if necessary, hence can have high feedback gains, to be really effective in quick suppression of vibrations. In other words, **not all velocity output feedback vibration controllers are of low authority, low performance !**

6.3.4 Now, not having to worry about the spillover and modal interaction problems, the feedback gains of properly designed modal dashpots ideally can be as high as the designer wishes. High gains can be as desirable for flexible-body vibration control as they have traditionally been for effective control of rigid bodies.

High gains are desirable for generating comparable negative feedback to offset the vibrations. Theoretically, the higher the better. For example, the version MD1 has a higher gain (because of higher ζ_2^*) than the version MD1A, the deflection and attitude deviations can be continuously suppressed down to smaller values (e.g., ±0.5 ft vs ±0.75 ft, in deflection; 0.46° vs 0.714° in Reflector roll angle,...).

The size of the feedback gains for a properly designed modal-dashpot vibration control is virtually limited only by the force and torque capability of the actuators. Since the vibrations were initially very large, the high gains resulted in requiring larger forces and torques than their limits. The simulated saturation thus restrict the applied force/torques to the limits. Therefore, there are no needs to be concerned with high gains as much as before, even the actuators may saturate at their force/torque limits.

6.3.5 Recall that the badly excited modes, i.e., Modes 2 and 1, were **made most strongly controllable and obserable** by carefully matching them with actuators and sensors with the strongest influences. Recall also they were strongly controlled by selecting them as modeled modes in the Part 1 design of the modal dashpots and by **adding to them the highest additional damping ratios.** The results of Sections 6.1 and 6.2 show that the resulting modal-dashpot designs are **very effective for fast suppression of large vibrations.** The results also show that **spillover is minimum** and that the unmodeled modes receive some small concomitant additional damping because of spillover.

6.3.6 Unlike all other vibrations (deflections, attitude deviations and modal responses), the LOS error was not reduced to a smaller value by the version MD1 than by the version MD1A. Also, the LOS error was not continuously reduced to near zero as were all other vibrations, although the reduction from its excessively high peak was quite substantial. **Nonlinear properties** of large Euler attitude angles, and the **truncated forces and moments** from the saturated actuators (due to high feedback gains) likely are the causes. We have no clear explanations at the present time. Nevertheless, observe Figs. 3-1c, 6-1c and 6-2c that the Reflector continued to have sufficiently large pitch and yaw ratations during the initial phase of the vibration control, in addition to the main (and larger) roll rotations.

6.3.7 Figs. 6-1 and 6-2 show that after the excessive vibrations have all been suppressed down to sufficiently low levels, the **time rates of change naturally start to become much less significant,** and the modal-dashpot vibration control also starts to become less effecitve. Unless the feedback gains are increased thereafter, the vibrations may not continue to be reduced to the desired precision in a reasonably short time. One way to achieve the desired precision is to start to increase the modal-dashpot gains progressively after the vibrations become sufficiently small, e.g., after 2 seconds of the initial vibration control.

Another way is to **switch to some form of "modern control"** for completing the vibration suppression and precision pointing. When all the displacements and rates of change have become reasonably small, the whole dynamic system becomes legitimately linear, and the LOS error expression legitimately linearizable. The condition is **very suitable** for application of the modern optimal state-feedback control technique.

Modern control using standard Linear-Quadratic-Gaussian (LQG) optimal state regulators and optimal state estimators has traditionally performed very well in precision pointing and attitude control of rigid-body systems, even using small signals. For application to a flexible-body system, the modern control must be very carefully designed, however; otherwise the notorious spillover problems may destabilize the system instead!

6.3.8 Several major approaches to extend or adapt the LQG design techniques were proposed during the years of **ACOSS** (Active Control of Space Structures) and **VCOSS** (Vibration Control of Space Structures) programs [38]-[45], [15], [46]-[50]. Either the weighting matrices in the control performance index is modified in some ways [51]-[52], or some positivity requirement is imposed on the design [53], or some pre-design compensation of the actuator/sensor influences is made [35]-[36]. All were successful to some limited extents in addressing the major challenge of spillover problems, but are not

readily applicable to realistic large flexible space structures.

Formal applications of the robustness theory [54]-[55] were started recently [56]-[59]. The method of **loop transfer recovery (LTR)** was also applied to recover sizable gain and phase margins of LQ regulators. The modification recently proposed by Blellock and Mingori [58] appears to have made the LTR method more directly applicable to LQG controllers designed for large space structures, so far as the uncertainties in the modal frequencies of the plant are concerned. Recent results obtained by Sundararajan, Joshi, and Armstrong [59] are rather encouraging. Based on their interpretation of spillover problems as additive uncertainty [60], [55], they were able to make an innovative application of the LTR method **to overcome spillover problem** with their LQG attitude controllers designed for the Hoop/Column antenna. This approach has a great potential for practical application to realistic large flexible space structures, since it appears to be able to overcome the spillover problem of an unlimited number of unmodeled modes.

Incorporating modal dashpots into a LQG or LQG/LTR design and following a similar sequence of careful pre-design analyses certainly will greatly enhance the stability and performance of the resulting **LQG/MD or LQG/LTR/MD vibration controller.** The two proof-mass actuators placed on the mast beam may be used together with all the force and moment actuators on the Reflector and the Shuttle for such a low-power but high-precision control.

7. CONCLUSIONS

7.1 The two-stage approach is a feasible and promising one for rapid slewing and precision pointing/retargeting of large flexible space systems and, in particular, the orbital SCOLE configuration. It is **capable of rapidly slewing the line-of-sight and settling the excited vibrations in a minimum time.** The resulting control design, in general, will consist of the following three parts in cascade:

Stage 1: a bang-bang type rapid slew maneuver based on the rigid-body dynamics for pointing/retargeting in a minimum time; if excessive vibrations may be excited, using smaller forces and moments should be considered.

Stage 2, Part 1: a high-power modal-dashpot design of velocity output feedback control based on the flexible-body dynamics for fast and effective reduction of large excited vibrations to a small magnitude;

Stage 2, Part 2: a LQG/LTR design of optimal state feedback control augmented with a broad-band low-power modal-dashpot design of velocity output feedback control, also based on flexible-body dynamics, for (i) achieving the specified pointing accuracy in a short time and (ii) maintaining the precision and closed-loop system stability. The LQG/LTR design may be incorporated or integrated with an appropriate modal-dashpot design.

7.2 Not all bang-bang (BB) type of time-minimized slew maneuvers will excite large structural vibrations. When large forces are used up to their extremes (for example, 800 lb on the Reflector) to complete the specified slew angle (20°) of the rigidized configuration in the shortest time, the excited vibrations can be excessively large in magnitude (e.g., a 114-ft peak deflection of the 130-ft Mast beam), even only moderated maneuvers of the bang-pause-bang (BPB) type is used instead. On the other hand, when properly selected small forces, e.g., 25 lb, of the kind of **vernier RCS thrusters onboard the Space Shuttle**, are used, **even BB-type maneuvers will excite very little vibrations** (e.g., 0.3 ft peak deflection of the Mast beam).

If the excited vibrations are excessive, a **"high-power" modal-dashpot design** of velocity output feedback control can be used in the first part of the Stage 2 to suppress the vibration down to a reasonable small magnitude **quickly and effectively.** If the excited vibrations are relatively small, or have already been suppressed to a small magnitude, **some modified form of linear-quadratic (LQ) optimal state feedback control augmented with a "low-power" design of modal dashpots** can be used in the Stage 2 to achieve the desired pointing precision.

7.2.1 The vibration modes of the SCOLE configuration were excessively excited when an 800-lb force was applied on the Reflector in the y direction during a BB type slew maneuver. When the best Stage-1 design, i.e., the BPB roll-axis slew having the best LOS pointing accuracy with a minimized slew time (4.89 sec) and the least sensitivity to nonzero products of interia) was applied to the SCOLE flexible-body dynamics, the Reflector end of the mast vibrated between +114 ft and -113 ft, the Reflector rolled

between -86.96° and +88.35°, and the line of sight jittered between 89.8° (or 133.3° if not taking on the principal value of the sine function) and 14.7°.

Our carefully designed modal-dashpot type of velocity output feedback control was **able to suppress the excessive vibratiions quickly and effectively:** the Reflector end deflection down to ±5 ft in 2 sec, and to ±0.5 ft in 4.2 sec; Reflector roll to ±3.48° in 7.1 sec, and to ±0.54° in 4.4 sec; and the LOS error down to 11.79° in 3.1 sec. In other words, after only about 2 to 3 seconds of applying the "high-power" modal dashpots, the vibrations were reduced to a region where some form of linear-quadratic optimal "state" feedback control (properly augmented with "low-power" modal dashpots) would be effective in futher reducing the vibrations and LOS errors to the desired precision.

7.2.2 The large magnitude of the force, i.e., **800 lb,** applied on the Reflector was **responsible for the excessive excitation of vibrations** in the SCOLE configuration. Whether bang-bang type time-optimal slew maneuvers would excite excessive vibrations or not depends on the allowable maximum magnitude of the applied forces. When the limit of the force was decreased to only one tenth (i.e., 80 lb) but the pointing slew maneuver was still performed in a similar time-optimal bang-bang manner for the same 20° angle, the excited vibrations were significantly decreased. The maximum LOS error was 24.7°, comparable to the specified initial value (20°) due to the initial misaligment of the SCOLE configuration. The maximum tip deflection (20.6 ft) of the mast beam was also quite reasonable compared to the length of the Mast (130 ft). When no additional forces were applied, however, the vibrations excited by the applied moments alone **increased, instead.**

We found that if the applied force on the Reflector was about 25 lb, i.e., in the range of the **vernier RCS thrusters used on the Space Shuttle,** the corresponding time-minimized bang-bang pointing slew maneuver would excited **very little vibrations** in the SCOLE configuration. The Reflector end of the mast vibrated only between +0.25 ft and -0.30 ft, the Rellector rolled only between +0.16° and -0.30°, and the LOS error was at most 0.51°. If the BB slew maneuver was followed immediately by some form of linear-quadratic optimal "state" feedback control (properly augmented with "low-power" modal dashpots), such small vibrations and LOS errors would be easily reduced to the desired precision.

7.2.3 During Stage 1, the BB maneuver using a 25 lb force on the Reflector required 10.96 seconds to complete the 20° slew while the BPB amneuver using a 800 lb force on the Reflector required only 4.89 seconds. A "high-power" modal-dashpot design of velocity output feedback control required additional 2.5 to 3 seconds to bring the excessive vibrations excited by the 800-lb maneuver down to the same order of magnitude as the vibrations excited by the 25-lb maneuver. Therefore, the **total time required for both Stage 1 (slew) and Stage 2 (stabilization and precision pointing)** is likely to be **around 10 and 12 seconds,** respectively, for the two cases.

The two stages of the 800-lb BPB maneuver will probably require the least total time, but the excessive vibrations during the maneuver are impractical and undesirable.

The 80-lb BB maneuver requires a similar high-power design of modal-dashpots for quick and effective suppression of the moderately large vibrations to the same order of magnitude as the case of 25-lb maneuver. The total time required for the two stages is likely to be **also around 12 seconds or a little less.**

7.3 Although modal-dashpot type of velocity output feedback control can be designed as a usual diffuse (or "broad-band") low-power (or "low-authority") control, the simulation results of our careful designs have shown that modal dashpots can also be a concentrated high-power ("high-authority") control for fast and effective suppression of large vibrations. **Careful pre-design analyses made it possible to do so for SCOLE.**

7.3.1 Our pre-design analysis on the vibration modes of the SCOLE configuration shows that **modes 2,3,4,1,5** are the five **most important** modes requiring for vibration control and LOS error reduction, with mode 2 needing active control the most.

7.3.2 Our Pre-design analysis on the modal control influences of the actuators shows that: **two force actuators on the Reflector** in x and y directions, respectively, are most effective for controlling modes 1 and 2; **three moment actuators also on the Reflector** about the x, y, and z (i.e., roll, pitch, and yaw) axes, respectively, are most appropriate for controlling modes 3, 4, and 5.

7.3.3 For quick effective suppression of the excessive vibrations in the SCOLE configuration excited by the time-minimized BPB slew maneuver, it is more appropriate to design the modal dashpots into separate parts than to lumping up all the 5 most important modes to be controlled by all the five actuators together. **High gains** not only **do not create spillover and interaction problems as uaual** but rather make the resulting modal dashpots truly powerful and effective for quick suppression of excessive vibrations.

7.4 In general, modal dashpots when properly and carefully designed, can add desirable amount of active damping to modeled (or "controlled") modes. Unmodeled modes can also receive some concomitant active damping, as a **benefit of spillover** to complement their inherent damping.

8. RECOMMENDATIONS

We recommend that:

1. the two-stage approach be accepted as a promising one, and included in Part Two of the Design Challenge, for validation using the hardware SCOLE laboratory facility and for comparison with other approaches, and

2. theoretical and simulation studies on the two-stage approach be continued using the mathematical models of both the orbital and the laboratory SCOLE configurations for further development of the technology.

8.1 Careful scientific studies have been successfully conducted on the two-stage approach to rapid pointing and vibration control of the flexible orbital SCOLE configuration, and the results have been very encouraging. Now that the physical SCOLE labortory facility is operational, we recommend that the design techniques developed and the technical knowledge gained on the two-stage approach be translated to the tethered laboratory SCOLE configuration and be tested and validated by the experimental apparatus. Specifically:

(1) Design a rapid time-minimize bang-pause-bang line-of-sight pointing slew maneuver (Stage 1), and a fast effective modal-dashpot type of vibration controller (Stage 2), using the mathematical model of the tethered configuration and the actuators and sensors actually available on the laboratory article. Test the designs on the SCOLE facility in real time.

(2) Then, conduct a comprehensive sequence of experimental evaluations similar to Steps (a) through (e) below.

8.2 To further develop the technology associated with the promising pratical two-stage approach and to gain additional technical knowledge, we recommend that studies be conducted on the use of **MD-augmented LQG/LTR design** of vibration control for attaining the specified LOS pointing accuracy. We also recommend that the **limit on the applied force at the Reflector** of the orbital SCOLE configuration be lowered by one order of magnitude from 800 lb to between 100 and 200 lb, or alternately between 20 and 30 lb, in each direction.

Specifically, we recommend that:

(1) a series of design, simulation, study and evaluation be carried out on two representative cases,

(2) the total time required from the beginning of the LOS pointing slew maneuver to the end of stabilization with the desired 0.02° precision be determined for each case, and

(3) a trade-off study be conducted.

Case 1. Limit set at 150 lb*

(a) Use a Stage 1 design similar to the one described in Section 3.2.2 for the time-minimized pointing slew maneuver. Simulate such a BB slew maneuver on the 3-dimensional nonlinear **rigid body** dynamics of the SCOLE configuration first; evaluate the LOS accuracy, and assess the effects of nonzero products of inertia during the rapid maneuver; compare the results with BPB slew maueuver with the 800-lb limit.

Then simulate this slew maneuver on the **flexible-body** dynamics of the configuration as if it were a time-varying disturbance, and analyze the vibrations thus excited.

(b) Design a similar high-power modal-dashpot type of velocity output feedback control (following the same design proceedure as in Section 5). Such a vibration control design is to be used, as the first part of Stage 2 for suppressing the (moderately) excited vibrations quickly and effectively to some desirable low levels.

(c) Design a "low-power" modal dashpot (MD) type of velocity output feedback control first. Augment the SCOLE configuration with the resulting modal dashpot design. Then design a LQG/LTR type of optimal state feedback control. Such a **LQG/LTR/MD control design** is to be used as the second part of Stage 2 for continuing on suppressing the vibrations quickly to the desired LOS pointing accuracy of 0.02°. All force and moment actuators, including the two proof-mass actuators, are to be used in both the MD and the LQG/LTR/MD designs.

(d) Simulate the entire Stage 2 design on the SCOLE flexible-body dynamics and evaluate the vibration control performance numerically.

(e) Integrate the Stage-1 and Stage-2 designs (for a continuous operation of both pointing slew and vibration control), simulate their application on the coupled SCOLE dynamics (i.e., flexible-body dynamics kinematically coupled with rigid-body dynamics); evaluate the **total** LOS pointing and vibration control performance and determine the **total** time required for achieving the desired precision.

Case 2. Limit set at 25 lb

Use the same Stage 1 design as described in Section 3.2.3, instead of Section 3.2.2, for the time-minimized pointing slew maneuver. Conduct all the corresponding sequence of design, simulation, and evaluation as Case 1 except step (b).

---

* In the laboratory SCOLE configuration, the equivalent torque the thrusters on the Reflector can generate is about two times the torque producible by the CMG on the Shuttle. For the same ratio, the applied force on the Reflector of the orbital SCOLE configuration is approximately 160 lb.

REFERENCES

[1] L.W. Taylor, Jr., and A.V. Balakrishnan, "A Mathematical Problem and A Spacecraft Control Laboratory Experiment (SCOLE) Used to Evaluate Control Laws for Flexible Spacecraft... NASA/IEEE Design Challenge," presented at NASA/ACC Workshop on Identification and Control of Flexible Space Structures, San Diego, CA, June 4-6, 1984;
also in Proceedings of SCOLE Workshop--1984, NASA Langley Research Center, Dec., 1984, pp. 1-27.

[2] J.G. Lin and L.W. Taylor, Jr., "Time-Optimal Bang-Bang Slew of Rigidized SCOLE Configuration," Proceedings of Workshop on Indentification and Control of Flexible Space Structures, San Diego, CA, June 1984 (JPL Publication 85-29, April 1, 1985), Vol. I, pp. 383-399.

[3] J.G. Lin, "Rapid Single-Axis Torque-Bounded Slewing of SCOLE Configuration," paper presented at SCOLE Workshop, NASA Langley Research Center, Hampton, VA, DEC. 6-7, 1984.

[4] J.G. Lin, "Rapid Torque-Bounded Line-of-Sight Pointing of SCOLE with a Designer's Choice of Initial Alignment," paper presented at SCOLE Workshop, NASA Langley Research Center, Hampton, VA, DEC. 6-7, 1984.

[5] J.G. Lin, "Rapid Torque-Limited Line-of-Sight Pointing of SCOLE (Spacecraft Control Laboratory Experiment) Configuration," Paper 86-1991, AIAA Guidance, Navigation and Control Conference, Williamsburg, VA, August 1986, pp. 106-114.

[6] L.S. Pontryagin et al, The Mathematical Theory of Optimal Processes, New York: John Wiley, 1962.

[7] G. Leitmann, An Intruduction to Optimal Control, New York: McGraw-Hill, 1966.

[8] M.J. Balas, "Active Control of Flexible Systems," J. Optimization Theory and Applications, Vol. 25, No. 3, pp. 415-436, July 1978.

[9] D.C. Herrick, "An Experimental Investigation of Modern Modal Control," presented at 17th Aerospace Sciences Mtg, New Orleans, AIAA Paper No. 79-0199, Jan. 1979.

[10] J.R. Canavin, "The Control of Spacecraft Vibrations Using Multivariable Output Feedback," Paper 78-1419, AIAA/AAS Conference, Los Angeles, CA, Aug. 1978.

[11] "Passive and Active Suppression of Vibration Response in Precision Structures -- State-of-the-Art Assessment, Volume 2: Technical Analysis," Report No. R-1138, C.S. Draper Lab., Cambridge, MA, Feb. 1978.

[12] J.R. Canavin, "Control Technology for Large Space Structures," Paper 78-1691, presented at AIAA Conf. Large Space Platforms: Future Needs and Capabilities, Los Angeles, CA, Sept. 1978.

[13] J.N. Aubrun, "Theory of the Control of Structures by Low-Authority Controllers," J. Guidance and Control, Vol. 3, No.5, Sept-Oct 1980, pp.444-451;
also Paper 78-1689 presented at AIAA Conf. Large Space Platforms: Future Needs and Capabilities, Los Angeles, CA, Sept. 1978.

[14] J.G. Lin, D.R. Hegg, Y.H. Lin, and J.E. Keat, "Output Feedback Control of Large Space Structures: An Investigation of Four Design Methods," Proc. 2nd VPI&SU/AIAA Symp. Dynamics and Control of Large Flexible Spacecraft,

June 1979, pp. 1-18.

[15] J.G. Lin, Y.H. Lin, D.R. Hegg, T.L. Johnson, and J.E. Keat, "Actively Controlled Structures Theory-- Interim Technical Report, Volume 1: Theory of Design Methods," Report No., R-1249, C.S. Draper Laboratory, Cambridge, MA, Apr. 1979;
also Raeport No. RADC-TR-79-268,Vol. I, Rome Air Force Development Center, Griffiss AFB, NY, Nov. 1979.

[16] L.E. Elliott, D.L. Mingori, and R.P. Iwens, "Performance of Robust Output Feedback Controller for Flexible Spacecraft," Proceedings 2nd VPI&SU/AIAA Symp. Dynamics and Control of Large Flexible Spacecraft, June 1979, pp. 409-420.

[17] S.M. Joshi and N.J. Groom, "Modal Damping Enhancement in Large Space Structures Using AMCD's," AIAA J. Guidance and Control, Vol.3, No.5, pp.477-479, Sept-Oct 1980.

[18] S.M. Joshi, "An Asymptotically Stable Damping Enhancement Controller for Large Space Structures," paper No. AIAA-81-0455, AIAA 2nd Conf. on Large Space Platforms: "Toward Permanent Manned Occupancy in Space", San Diego, Calif., Feb. 1981.

[19] M.J. Balas, "Direct Velocity Feedback Control of Large Space Structures," AIAA J. Guidance and Control, Vol.2, No.3, pp.252-253, May-June 1979.

[20] J.G. Lin, "Closed-loop Asymptotic Stability and Robustness Conditions for Large-Scale Systems with Reduced-Order Controllers," Proc. 20th IEEE Conf. Decision and Control, Dec. 1981, pp. 1497-1502.

[21] J.G. Lin, Y.H. Lin, and R.B. Preston, "Stability Augmentation for Large Space Structures by Modal Dashpots and Modal Springs," Proc. 3rd VIP&SU/AIAA Dynamics and Control of Large Flexible Spacecraft, June 1981, pp. 393-408.

[22] J.G. Lin, "General Conditions on Reduced-Order Control for Ensuring Full-Order Closed-Loop Asymptotic Stability," Proceedings of NCKU/AAS Intl Symposium on Engineering Sciences and Mechanics, Taiwan, Taiwan, Dec. 29-31, 1981, pp. 1003-1030.

[23] J.G. Lin, "Closed-Loop Stability and Robustness Conditions for Large Space Systems with Reduced-Order controller," Section 3 in **Active Control of Space Structures--Final Report**, Report No. R-1454, C.S. Draper Lab., Cambridge, MA, Feb. 1981;
and in **ACOSS Six (Active Control of Space Structures)**, Final Technical Report No. RADC-TR-81-289, Rome Air Force Development Center, Griffiss AFB, NY, October 1981.

[24] J.G. Lin and W.J. Jasper, "Interaction Problems in Active Damping Augmentation for Large Flexible Space Structures," paper presented at Symposium on Advances and Trends in Structures and Dynamics, Washington, D.C., Oct. 22-25, 1984.

[25] D.K. Robertson, "Three-Dimensional Vibration Analysis of a Uniform Beam With Offset Inertial Masses at the Ends," NASA Technical Memo. 86393, NASA Langley Research Center, Sept. 1985.

[26] S.M. Joshi, "A Modal Model for SCOLE Structural Dynamics," paper presented at SCOLE Workshop, NASA Langley Research Center, Dec. 6-7, 1984.

[27] NASA Office of Aeronautics and Space Technology Notice, "Control of Flexi-

ble Structures (COFS) Technology Program," Feb. 7, 1986; Update, April 24, 1986.

[28] "Space Construction Experiment Definition Study (SCEDS) part II Final Report," Report No. GDC-ASP-82-004, General Dynamics Convair Div., April 1982.

[29] "Space Construction Experiment Definition Study (SCEDS) part I Final Report," Report No. CSDL-R-1583, C.S. Draper Lab., Aug. 1981

[30] J.A. Roebuck, Jr., "Shuttle Considerations for Design of Large Space Structures," NASA Contractor Report 160861, NASA Johnson Space Center, Houston, TX, Nov. 1980;
also SSD80-0183, Rockwell International Corp; Downey, CA.

[31] G.H. Golub and C.F. Van Loan, Matrix Computations, Baltimore: Johns Hopkins Univ. Press, 1983.

[32] G.H. Golub and W. Kahan, "Calculating the singular Values and Pseudo-Inverse of a Matrix," SIAM J. Numerical Analysis, Vol. 2, pp.205-224, 1965.

[33] T. Henderson, "Active Control of Space Structures (ACOSS) Model 2," Technical Report No. C-5437, C.S. Draper Laboratory, Cambridge, MA, Sept. 1981.

[34] R.R. Strunce, D.R. Hegg, J.G. Lin, and T.C. Henderson, "Actively Controlled Structures Theory, Final Report," Report No. R-1338, Vol. 2 of 2, C.S. Draper Lab., Cambridge, MA, Dec. 1979; alsko, "ACOSS Four (Active Control of Space Structures) Theory Appendix," Final Technical Report RADC-TR-80-78, Vol II (of two), Rome Air Force Development Center, Griffiss AFB, NY, April 1980.

[35] J.G. Lin, "Three Steps to Alleviate Control and Observation Spillover Problems of Large Space Structures," Proc. 19th IEEE Decision and Control conf., Dec. 1980, pp. 438-444.

[36] J.G. Lin, "Reduction of Control and Observation Spillover in Vibration Control of large Space Structures," Paper No. 79-1763 presented at AIAA Guidance and Control Conf., Boulder, CO, Aug. 1979;
also Section 2 in **Actively Controlled Structures Theory, Final Report**, Report No. R-1338, Vol. 1 of 2, C.S. Draper Lab., Cambridge, MA, Dec. 1979,
and in **ACOSS Four (Active Control of Space Structures) Theory**, Final Technical Report No. RADC-TR-80-78, Vol I (of two), Rome Air Force Development Center, Griffiss AFB, NY, April 1980.

[37] S.M. Joshi, "Robustness Properties of Collocated Controllers for Flexible Spacecraft," J. Guidance, Control, and Dynamics, Vol. 9, No. 1, January-February 1986, pp. 85-91.

[38] J.R. Sesak, "ACOSS One (Active Control of Space Structures) Phase I," Report No. RADC-TR-80-79, Rome Air Development Center, Griffiss AFB, NY, Mar. 1980 (General Dynamics Convair Division: contractor).

[39] J. R. Sesak, "ACOSS Seven (Active Control of Space Structures) Final Technical Report," Report No. RADC-TR-81-241, Rome Air Development Center, Griffiss AFB, NY, Sept.1981 (General Dynamics Convair Division: contractor).

[40] M.G. Lyons, J.N. Aubrun, G. Margulies, N.K. Gupta, et al, "ACOSS Three (Active Control of Space Structures) Phase I," Report No. RADC-TR-80-131, Rome Air Development Center, Griffiss AFB, NY, May 1980 (Lockheed Missiles & Space Company: contractor).

[41] J. N. Aubrun, J. A. Breakwell, N. K. Gupta, M. G. Lyons and G. Margulies,

"ACOSS Five (Active Control of Space Structures) Phase 1A," Report No. RADC-TR-82-21, Rome Air Development Center, Griffiss AFB, NY, Mar. 1982 (Lockheed Missiles & Space Company: contractor).

[42] J.N. Auburn, "ACOSS Twelve (Active Control of Space Structures)," Report No. RADC-TR-82-320, Rome Air Development Center, Griffiss AFB, NY, Dec. 1982 (Lockheed Missiles & Space Company: contractor)

[43] R.P. Iwens, R.J. Benhabib, and F.C. Tung, "ACOSS Eight (Active Control of Space Structures), Phase II," Report No. RADC-TR-81-242, Rome Air Development Center, Griffiss AFB, NY, Sept. 1981 (TRW: contractor).

[44] "Vibration Control of Space Structures VCOSS-A; High and Low Authority Implementation," AFWAL-TR-83-3074, Flight Dynamics Laboratory, Air Force Wright Aeronautical Laboratories, Wright-Patterson AFB, Ohio, July 1983 (Lockheed Missiles & Space Company: contractor).

[45] L. Brady, G. Franco, L. Keranen, J. Kern, R. Neiswander and F. Tung, "Vibration Control of Space Structures, VCOSS B: Momentum Exchange and Truss Dampening," Report No. AFWAL-TR-83-3075, Flight Dynamics Laboratory, Air Force Wright Aeronautical Laboratories, Wright-Patterson AFB, Ohio, July 1983 (TRW Space and Technology Group: contractor).

[46] R.R. Strunce, D.R. Hegg, J.G. Lin, and T.C. Henderson, **ACOSS Four (Active Control of Space Structures) Theory**, Final Technical Report, No. RADC-TR-89-78, Vol I, Apr. 1980 (C.S. Draper Laboratory: contractor).

[47] R.R. Strunce, J.G. Lin, D.R. Hegg, R.K. Pearson, L.P. Govignon and T.C. Henderson, "ACOSS Six (Active Control of Space Structures) Interim Report," Report No. RADC-TR-80-377, Rome Air Development Center, Griffiss AFB, NY, Jan. 1981 (C.S. Draper Laboratory: contractor).

[48] R.R. Strunce, J.G. Lin, D.R. Hegg, E. Fogel, J.D. Turner, R.K. Pearson, G. J. Kissel, H. M. Chun and N. H. McClamroch, "ACOSS Six (Active Control of Space Structures) Final Technical Report," Report No. RADC-TR-81-289, Rome Air Development Center, Griffiss AFB, NY, Oct. 1981 (C.S. Draper Laboratory: contractor).

[49] J.G. Lin, G.J. Kissel, D.R. Hegg, R.K. Pearson, J.D. Turner, H.M. Chun, and E. Fogel, **ACOSS Eleven (Active Control of Space Structures)-- Interim Report, Volume II**, Report No. RADC-TR-82-131-VOL-2, May 1982 (C.S. Draper Laboratory: contractor).

[50] R.R. Strunce, E. Fogel, D.R. Hegg, J.G. Lin, J.D. Turner, and H.M. Chun, "ACOSS-11 (Active Control of Space Structures) Volume 2 Interim Report," Report No. RADC-TR-82-295-VOL-2, Rome Air Development Center, Griffiss AFB, NY, Nov. 1982 (C.S. Draper Laboratory: contractor).

[51] N.K. Gupta, "Frequency-Shaped Cost Functionals:Extension of Linear-Quadratic-Gaussian Design Methods," J. Guid. Contr., Vol. 3, No. 6, pp. 529-535, Nov.-Dec. 1980.

[52] J.R. Sesak, P.W. Likins and T. Coradetti, "Flexible Spacecraft Control by Model Error Sensitivity Suppression," The J. Astronautical Sciences, Vol. 27, No.2, pp.131-156, April-June, 1979.

[53] R.J. Benhabib, R.P. Iwens and R.L. Jackson, "Stability of Distributed Control for Large Flexible Spacecraft Structures Using Positivity Concepts," AIAA Guidance and Control Conference, Boulder, CO, Aug. 1979.

[54] J.C. Doyle and G. Stein, "Multivariable Feedback Design Concepts for a

Classical/Modern Synthesis," IEEE Trans. on Automatic Control, Vol. AC-26, No.1, pp.4-16, Feb 1981.

[55] N.A. Lehtomaki, N.R. Sandell, Jr., and M. Athans, "Robustness Results in Linear-Quadratic Gaussian Based Multivariable Control Designs," IEEE Trans. Automat. Contr., Vol. AC-26, No. 1, pp. 75-93, Feb. 1981.

[56] R.L. Kosut, H. Salzwedel, and A. Emami-Naeini, "Robust Control of Flexible Spacecraft," AIAA J. Guidance, Control, and Dynamics, Vol. 6, No.2, pp. 104-111, March-April 1983.

[57] N. Sundararajan, S.M. Joshi and E.S. Armstrong, "Robust Controller Synthesis for a Large Flexible Space Antenna," Proc. 23rd Conf. Decision Contr., 1984, pp. 202-208.

[58] P.A. Blelloch and D.L. Mingori, "Modified LTR Robust Control for Flexible Structures," Paper 86-2051, AIAA Guidance, Navigation and Control Conference, August 1986, Williamsburg, VA, pp. 314-318.

[59] N. Sundararajan, S.M. Joshi, E.S. Armstrong, "Attitude Control System Synthesis for the Hoop/Column Antenna Using the LQG/LTR Method," Paper 86-2139, AIAA Guidance, Navigation and Control Conference, August 1986, Williamsburg, VA, pp. 469-478.

[60] J.B. Cruz, Jr., J.S. Freudenberg, and D.P. Looze, "A Relationship Between Sensitivity and Stability of Multivariable Feedback Systems," IEEE Trans. Automat. Contr. Vol. AC-26, No.1, pp.66-74, Feb. 1981.

NASA National Aeronautics and Space Administration

Report Documentation Page

1. Report No.	2. Government Accession No.	3. Recipient's Catalog No.
NASA CR-178392		

4. Title and Subtitle

Control Design Challenges of Large Space Systems and Spacecraft Control Laboratory Experiment (SCOLE)

5. Report Date

October 1987

6. Performing Organization Code

7. Author(s)

Jiguan Gene Lin

8. Performing Organization Report No.

10. Work Unit No.

506-46-11-01

9. Performing Organization Name and Address

Control Research Corp.
6 Churchill Lane
Lexington, MA 02173-5821

11. Contract or Grant No.

NAS1-18185

13. Type of Report and Period Covered

Contractor Report

12. Sponsoring Agency Name and Address

National Aeronautics and Space Administration
Langley Research Center
Hampton, VA 23665-5225

14. Sponsoring Agency Code

15. Supplementary Notes

Langley Technical Monitor: Suresh M. Joshi
Final Report

16. Abstract

The principal objective of this research was to investigate if the structural vibrations excited by bang-bang (BB) type time-optimal slew maneuvers could be quickly suppressed via "modal-dashpot" design of velocity output feedback control. Simulation studies were conducted, and modal dashpots were designed for the SCOLE flexible-body dynamics. A two-stage approach was proposed for rapid slewing and precision pointing/retargeting of large, flexible space systems: (Stage 1) slew the whole system like a rigid body in a minimum time under specified limits on the control moments and forces, and (Stage 2) damp out the excited structural vibrations afterwards. This approach was found to be a promising one. "High-power" modal/dashpots can suppress very large vibrations quickly and effectively, and can add desirable amount of active damping to modeled modes. Unmodeled modes can also receive some concomitant active damping, as a benefit of spillover.

The results also show that not all BB type rapid pointing maneuvers will excite large structural vibrations. When properly selected small forces (e.g., vernier thrusters) are used to complete the specified slew maneuver in the shortest time, even BB-type maneuvers will excite only small vibrations (e.g., 0.3 ft. peak deflection for a 130 ft. beam).

17. Key Words (Suggested by Author(s))	18. Distribution Statement
vibration control, modal dashpots, velocity feedback, active damping, SCOLE, large space structures, space mast Shuttle-attached payload, beam bending, rapid pointing, slew, retargeting, time-optimal maneuver, bang-bang control	Unclassified-Unlimited Subject Category 18

19. Security Classif. (of this report)	20. Security Classif. (of this page)	21. No. of pages	22. Price
Unclassified	Unclassified	71	A04